PARAMETRIC INSTABILITIES IN INHOMOGENOUS PLASMAS

Iain M. Begg

A Thesis Submitted for the Degree of PhD
at the
University of St Andrews

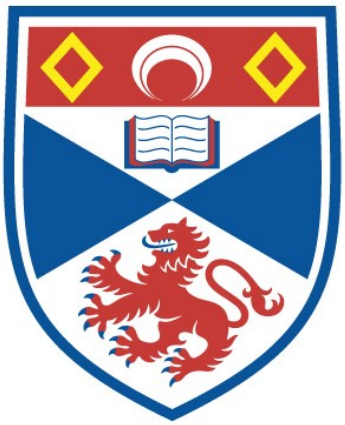

1976

PARAMETRIC INSTABILITIES

IN

INHOMOGENEOUS PLASMAS

IAIN M. BEGG

Thesis submitted for the Degree of Doctor of Philosophy of the University of St. Andrews.

March 1976

Th 8920

ABSTRACT

This thesis will deal with certain problems of parametric instabilities in the inhomogeneous plasma. A large amplitude, 'pump' wave can deposit some of its energy into the plasma through resonance with two lower frequency waves (which may be damped). This type of process is a parametric decay of the pump wave and has applications in many fields. We consider, predominantly, that of laser fusion, in which the pump wave is electromagnetic and incident on the plasma. The objective is to deposit as much energy as possible within the plasma. Instabilities reducing this energy input are therefore of importance and it is, mostly, to these that this thesis will turn. They are mostly scattering processes in which one of the decay modes is electromagnetic. We examine the stimulated Brillouin backscattering process (the other decay mode being an ion accoustic wave) from a reference frame in which the plasma is streaming outwards. It is found that,if this velocity is near the sound velocity, the ion acoustic wave has a frequency Doppler -shifted to zero, the electromagnetic waves then having equal frequencies. In such a situation, any reflection of the pump wave at the critical surface will enhance the initial level of the backscattered wave. We find that, allowing for this, there is considerable enhancement of backscatter from the plasma, with consequent energy loss to the pump. Since the effect is noticeably unaffected by 'off-resonance' situations, it is felt that this process could mount a barrier to possible applications. We next consider the stimulated Compton scattering process, where the pump is scattered off the 'bare' or thermal electrons in the plasma. It is found that this rather weak instability occurs predominantly only when electron plasma waves are heavily dampled. Substantial reflection only occurs for high pump powers. Whilst there is little loss to the pump energy, there is substantial perturbation to the background distribution function. However, at the high powers involved filamentation and modulation

of the pump can occur with a resulting enhancement of the scattering. Finally, we consider the effect on the decay instability (photon → plasmon + phonon) of the presence of substantial filamentation of the critical surface. It is found that the growth rate is substantially reduced.

TO MY PARENTS

ACKNOWLEDGEMENTS

First and foremost, I should like to thank my supervisor, Dr. R.A. Cairns, for his support, encouragement and friendship at all stages in this work and without whose guidance it would not have been completed. I should also like to thank Mr. John Henderson and the Advisory Service of the Computing Laboratory for their assistance in sorting out the many computing difficulties which arose in the calculations. Finally, my thanks go to Miss Seonaid McCallum for cheerfully typing this thesis. The work was performed under award no. B73/0709 from the Science Research Council.

C O N T E N T S

CHAPTER I

INTRODUCTION

We shall discuss, in this thesis, the problem of parametric instabilities in inhomogeneous plasmas. A convenient definition of these processes, which bears on some of the later work, is the following (1) :- parametric excitation is the amplification of an oscillation due to the periodic modulation of some parameter characterising the oscillation.

It appears that the first systematic investigation of these phenomena was carried out by Lord Rayleigh (2) in 1883, who studied the effects, on a stretched string, of an attached tuning fork vibrating in the direction of the string. The string vibration was noted to be amplified when the tuning fork vibrated at twice the natural frequency of the string. It was explained by saying that the longitudinal vibration of the string, induced by the tuning fork, modulates the string tension and, hence, the transverse oscillation. This oscillation is then described by a Mathieu equation,

$$\frac{\partial^2}{\partial t^2} + \omega_o^2 (1 + \varepsilon \cos 2\omega t)\, u = 0$$

where u is the amplitude and ω_o the natural frequency of the string oscillation and ε is a small parameter. It has solution

$$u = D_1 A(t)\, e^{\mu t} + D_2 B(t)\, e^{-\mu t}$$

where D_1, D_2 are constants, A,B have period π and μ is, usually, complex. It is thus a modulated wave solution.

This same modulation, at twice the natural frequency can be seen in a common example - that of a child on a swing. As the swing passes its lowest point, the child moves up and down, modulating the arc of the swing and, hence, the frequency. The basic principle is that an input (pump) mode couples, by modulating, an idler and signal mode, to use the notation of parametric amplifiers in electrical circuits. In the above cases, both idler and signal modes have the same frequency.

The problem of spatial resonance in fluids affords an example of the situation where idler and signal frequencies are unequal. A long tank is set up such that only a small air gap is present above the water surface. A loud speaker pointing into, and along, this air gap provides the pump driver. Around the acoustic resonance frequency, surface waves of low frequency and long wavelength, are seen to develop. These waves are not limited by small amplitude effects (3,4). Perhaps more dramatic is the production of stationary surface waves in a circular tank through the modulation of internal waves by an applied longitudinal oscillation (5). At higher amplitudes the effect can be quite spectacular.

On a more rigorous basis, much work has been done on mode interaction in fluids (6, 7, 8). For instance, gravity waves, of frequency $\omega \sim \sqrt{gk}$, can only interact in a 4-wave resonance. However, if one allows for surface tension effects, their frequency becomes $\omega \sim \sqrt{gk + \gamma k^3}$ and 3-wave resonance becomes possible. Similarly, the density stratification associated with an oceanic thermocline allows gravity - surface wave interaction. It is interesting to note Hasselman's criterion for this interaction (6) : instability exists only for resonance conditions of the form

$$\omega_o = \omega_1 + \omega_2 \qquad k_o = k_1 + k_2$$

and not for the corresponding conditions containing a minus sign. This is not the case, invariably, in plasmas, especially where interaction occurs in a density profile. Of more direct analogy with plasmas is the work on mode interaction in shear flows (9, 10, 11). In the earliest work it was shown, figure (1),

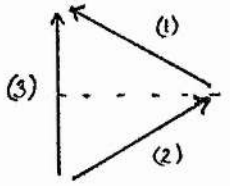

Figure 1 Resonance of obliquely incident waves in a shear flow

that obliquely incident waves of the same frequency, (1) and (2), could interact resonantly with a third wave in the shear flow. Instability occured when the frequency difference, $\Delta\omega$, was such that the critical layers of each wave coalesced into one layer. To second order, the solutions became unbounded in finite time and the problem is analogous, at this level, to the so-called 'explosive instability' in plasmas, which we discuss in the following chapter. It is also worth noting that this non-linear problem shows a preference for three-dimensionality whilst the linear wave propagation is essentially two dimensional. Again this is not necessarily the case in plasmas. As we shall see many interactions can be one-dimensional. The later work (10, 11) treats the study of resonant gravity waves in shear flows and the effects of waves on oceanic currents. This approach uses mode coupling through the fluid equations, an approach which we shall find useful. An alternative technique is the use of an averaged Lagrangian to generate the coupled equations (7) and this has been successfully used for the problem of resonant gravity wave interaction (12).

We now turn our attention to plasmas. Waves in a plasma, be it homogeneous or inhomogeneous, may be considered as an infinite number of oscillators. In the small amplitude approximation, these oscillators are essentially harmonic and independent of one another - the modes associated with them propagating without interaction. If we account for the nonlinear properties of the medium we then describe a coupling between two of these oscillators, to second order in the amplitude. The resulting perturbation, at the sum and difference frequencies of the two oscillators can then drive a third mode, provided, of course, it is in resonance. We shall consider parametric excitation in which a pump wave, of large amplitude, a natural mode of the plasma, drives two other modes, which, together with it, form a resonant triplet. When we come to discuss this interaction, there are some important differences with the foregoing which we must point out. The essence of the parametric instability is that the pump amplitude is taken to be fixed, although in a non-linear analysis this will not be the case. We shall also talk of the pump wave generating, and decaying into, the idler and signal modes. The reason for this descriptive change is easily seen if we consider each wave as a train of quantised particles. The mode coupling can then be represented, diagramatically,as the interaction between these 'particles',

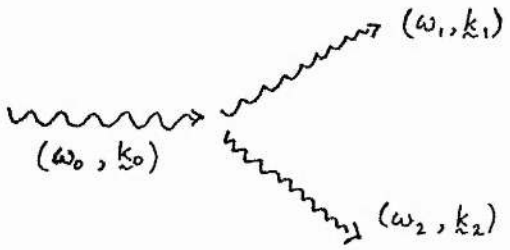

Figure 2 Decay of pump into idler and signal modes

where $(\omega_o, \underline{k}_o)$ represents the incoming pump wave, $(\omega_1, \underline{k}_1)$ the idler and $(\omega_2, \underline{k}_2)$ the signal - the latter being the decay modes. This interaction must

conserve both linear momentum and energy. Since the 'linear momentum' of a wave $(\omega,\underline{k})$ is $\hbar\underline{k}$ and its energy, $\hbar\omega$, we may express these conservation relations in the form of resonance conditions which must be satisfied before mode coupling can occur, i.e.

$$\hat{\omega}_o = \omega_1 + \hat{\omega}_2$$
$$k_o = k_1 + k_2 \qquad \ldots\ldots\ldots (I.1)$$

The pump wave, thus, decays into the two other modes and this type of instability is known as a decay instability. It should be pointed out that this term is used not only to describe the generic instability but also to describe a particular instability, about which we shall have much to say.

The first such example to be discussed in a plasma context was the decay of a longitudinal electron plasma wave (pump) into another plasma wave, of lower frequency, and an ion acoustic wave (13, 14). Since the sound waves were assumed long-lived, the condition $T_e >> T_i$ (electron temperature much greater than the ion one) was required, as otherwise the sound waves were heavily damped. Although this was the first instability of its kind to receive theoretical investigation (and many others soon followed), it was only several years later than experimental verification was found (15). Many other decay instabilities have been found for different wave triplets; Oraevsky (16) has presented a survey of this linear stage of investigation into parametric instabilities. One of the most important aspects of this discussion is the question of transference of energy, into both waves and plasma, which can occur through these decay processes. It is easy to see that, if for some reason, one of the decay waves is damped or transfers its energy to high energy particles, through Landau damping, say, energy is being transferred from the pump wave to the plasma. As we shall see this is an important problem. One interesting application concerns dissipation in collisionless shock waves (17). With the

shock wave, there exists a regular wave train and to explain the observed plasma heating these regular oscillations must be turned into a random set of waves. One such mechanism is the decay instability of one Alfvèn wave, associated with the shock wave, into another of lower frequency plus an acoustic mode.

In the case of thermonuclear fusion, these considerations are of prime importance, where the best possible ion heating is required. In Tokomaks where one confines a low density plasma for a relatively long time, of order a second, in a torus, this can be achieved by choosing a pump wave close to the lower hybrid frequency (17). The situation in laser fusion applications will be discussed more fully.

A significant advance in the theory of parametric instabilities came with the analysis of the case where the pump wave had a frequency close to the plasma frequency, $\omega_{pe} \equiv (\frac{4\pi e^2 n_o}{m_e})^{\frac{1}{2}}$. Such a situation can occur when an electromagnetic wave is incident on the plasma (18, 19, 20). The coupling is again to electron plasma and ion acoustic waves. Because the wavenumber of the pump wave is much smaller than either of the two decay waves, the so-called 'dipole approximation', of setting $k_o=0$, is often applied to this decay. This approximation has the advantage of allowing the study of much larger pump amplitudes. There are, however, two conditions on the validity of the approach (i) that one of the decay modes must have a low frequency i.e. $\omega_2 << \omega_1$, (ii) that the frequency shift should be less than the growth rate (17). However, these restrictions can be avoided by deriving the growth rates from a Maxwell stress tensor approach, when most of the other instabilities of an electromagnetic pump also come out of the analysis (21) It has the drawback of obscuring much of the relevant physics.

Nishikawa (30) analysed the situation of photon → plasmon + phonon decay, which, hereafter, we shall refer to as the decay instability, and included the effects of mode damping. Growth rates and thresholds for instability were calculated and we note, for further reference, that much of the subsequent work has been modelled on this analysis. He also showed that there existed another branch to this instability resulting in a non-oscillatory, growing ion mode - the oscillating - two-stream instability (O.T.S.I.). This exists for pump frequencies below the natural frequency of the plasma wave i.e. $\omega_o < (\omega_{pe}^2 + 3k^2 v_e^2)^{\frac{1}{2}}$, and is essentially a 4-wave process coupling waves of frequencies ω_o, ω_1, $\omega_o - \omega_1$, $\omega_o + \omega_1$. The usual 3-wave process is a limited version of this where the so-called 'off-resonant' contribution at $\omega_o + \omega_1$ has been neglected.

Crucial to the whole concept of these parametric instabilities in inhomogeneous systems is the nature of the growth - whether it be absolute or convective. By these terms we mean :- does some initial disturbance grow as its initial point in space with some growth rate (absolute) or does it grow as it propagates, the final level being determined by its convection out of the region of interest (or the region of greatest interaction)? Physically, we can see the difference in figure (3) where snapshots are shown of a developing pulse at different times.

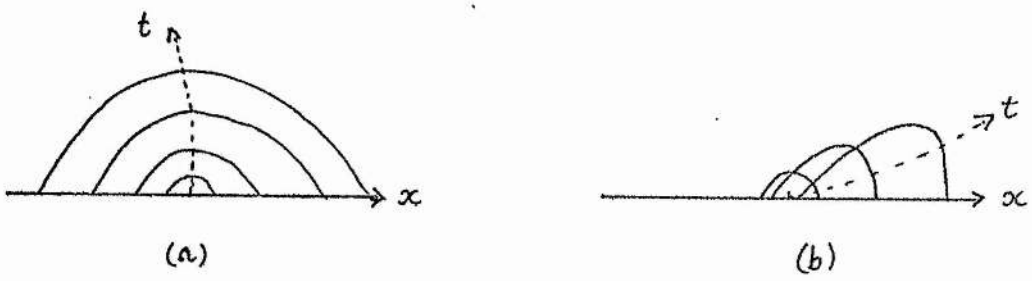

Figure 3 Development of an initial pulse (a) absolutely (b) convectively

As can be seen the absolute pulse spreads as it develops, growth being noticed at all points, whereas the convective pulse propagates along the system such that at any one point the disturbance eventually disappears. In the former, there exists an internal feedback mechanism allowing oscillations to grow in time at a fixed point in space. The latter, however, requires some form of external reflection or feedback to allow temporal growth at a fixed point in space.

This last distinction is a very useful one when we come to discuss the instabilities in more detail. This type of analysis is based on the pioneering work of Sturrock (31) and Briggs (32).

The parametric decays allowing an electromagnetic wave to couple efficiently with two other modes already existent in the plasma will be the main subject of this thesis. We have mentioned two of these already : the decay and the oscillating - two-stream. Both these processes occur near $\omega_{pe} \sim \omega_o$, although the former for $\omega_{pe} < \omega_o$ and the latter, predominantly, for $\omega_o \lesssim (\omega_{pe}^2 + 3k^2 v_e^2)$ i.e. they exist around the surface of reflection for electromagnetic radiation in a plasma (since the dispersion relation for these waves is $\omega_o^2 = \omega_{pe}^2 + k_o^2 c^2$, propagation, for real k_o, is forbidden when $\omega_o < \omega_{pe}$). We call this surface the critical surface. There is a wide range of application for these ideas :- from solid state scattering (17, 35) to pulsars, from perturbation of the ionosphere to thermonuclear fusion through pellet implosion by laser light. For instance, the modification of the ionosphere (34) has, as its main purpose, the 'bending' of radio waves for communication. The modification can last up to several hours. A good opportunity is, thus, afforded for examining the ionospheric properties such as ionised particle temperatures and densities and the effects of the geomagnetic field. It also has the advantage of offering a natural 'plasma laboratory' with a ready, low density, unbounded plasma, upon which experiments can be performed, such as the

examination of mode coupling. Perkins and Kaw (36) have suggested that parametric instabilities, of the above type, could be the cause of observed anomalous effects. More recently, the EISCAT project has been set up, jointly in Europe, to examine these effects in detail (37). The basic theory in this, and the other, applications is similar, although the final results are, obviously, different. They all depend on external, applied, high intensity electromagnetic waves. However, we shall confine ourselves to just one application - that of laser fusion. The results we shall derive will be applied to this special case of interest.

The object, in laser fusion, is to cause a small pellet of material, capable of undergoing nuclear fusion (a deuterium-tritium mixture seems most likely), to implode to a sufficiently large compression and temperature that fusion occurs with the subsequent release of large amounts of energy. the implosion being caused through the energy absorbtion from an incident laser beam. The principle is similar to that used for the implosion of a critical mass in a hydrogen bomb :- spherical heat input causes ablation of material from the core surface; in turn, this causes an inward travelling shock wave (Newton's third law of motion) which brings about the compression and the desired result. However, for fusion, mere compression is not sufficient, heating must be supplied to the particles to overcome their internuclear repulsion.

Let us examine the D-T fusion scheme in more detail. By the above reasoning a temperature of $10^8\ ^oK$ must be obtained before we can ignite the thermonuclear reaction :

$$ {}_1^2D + {}_1^3T \rightarrow {}_2^4He + {}_0^1n + 17.6\ MeV $$

To generate sufficient energy on the macroscopic scale, the plasma must be contained for a time long enough to allow substantial numbers of particles to fuse.

This is expressed by the Lawson criterion :

$$n\tau \sim 10^{14} \text{ s cm}^{-3} \qquad \text{(for DT)}$$

where n is the particle density, τ the confinement time and the calculation assumes no more than one third of the fusion output energy is fed back to sustain the reaction. It has approximately the same value for magnetic confinement devices. The basic principles of the two devices are then easily seen :- the latter is expected to confine a relatively low density plasma ($\sim 10^{14}$ cm^{-3}) for about a second whilst, in the former, it is hoped to confine an extremely dense plasma ($\sim 10^{26}$ cm^{-3}) for a time $\sim 10^{-12}$ s, effectively determined by the inertia of matter. Once fusion has occurred, most of the energy is carried off by neutrons which are absorbed in a lithium blanket (which, incidentially, should generate more tritium by reaction with $^{6}_{3}$Li) raising its temperature, the energy finally being removed by heat exchange.

The main feasibility studies of fusion by implosion were performed by the Lawrence Livermore Laboratory, notably by Nuckolls et al (38) and (39) and also by KMS Fusion Incorporated (40). The principles are neatly explained in the following example. Suppose we have a laser which can produce 10^{6} J of energy : just sufficient to heat a milligram of DT to the ignition temperature of 10^{8} ^{o}K. At normal liquid density this mass would make a sphere of radius $\sim$1mm. The efficiency with which fuel can be burned is determined by the competition between the confinement time, t_c, and the fusion reaction time, t_f. The former is proportional to the radius of the pellet over the thermal velocity of the nuclei and, in this case, is $\sim 2 \times 10^{-10}$ S. The latter, being proportional to inverse density, is $\sim 2 \times 10^{-7}$ S for fuel at liquid density. Thus, only 0.1% of the pellet would burn, recovering $\frac{1}{3}$ of the input energy.

However, if the same pellet were imploded to a tenth of the radius (a thousandth of the volume), $t_c \sim 2 \times 10^{-11}$ S but $t_f \sim 2 \times 10^{-10}$S. Thus, a burn efficiency of 10%, and output of 30 times the input energy, is achieved. It is clear that only by compressing the pellet can it be possible to achieve fusion. Additionally, provided we can compress the pellet in suitable fashion, it is not necessary to raise the whole pellet to the ignition temperature, thus reducing the input energy. Since most of the energy is carried by neutrons (14 Me V) and alpha particles (3.5 Me V) trapping of, at least, some of this within the pellet will be of advantage. In the uncompressed pellet, all this energy is lost but, for a radius .1 mm, the neutron range is only a few times the radius while for the α-particles it is only $\frac{1}{6}$ this distance. These particles thus desposit their energy within the pellet, generating a thermal shock wave - thermonuclear burn front. In this way, the required ignition temperature is reduced by a factor 100. It is because of this fact, that fusion by implosion can be feasible at all - the burn energy gain over ignition energy is not sufficient, by itself, to overcome laserinefficiencies.

In general, we require compression of order 10^4 with a power density of around 10^{19} W/cm^{-2}. This high power is achieved partly by input and partly by self focussing of the laser, by the ablating plasma cloud, onto a diminishing surface. However, getting this compression involves careful calculation. Extensive calculations (38) have shown that a properly chosen laser profile in time can lead to very high compression. The crucial trick is to ensure that material to be compressed is at as low an entropy as possible, so that the thermal pressure is kept to a minimum. A high degree of spherical symmetry is also required. It is worth noting that a constant laser power can achieve compressions only of about 50.

The basic process is the following :- a carefully shaped pulse causes the formation of a plasma cloud and corona around the solid pellet core; the light is absorbed near the critical surface, where $\omega_{pe}(x) = \omega_o$; the temperature gradient is thus set up, generating a pressure gradient and hydrodynamic rarefaction wave; this, in turn, causes an isothermal expansion of plasma and greater absorption; at peak power, shock waves will be formed which propagate inwards. It transpires that the isothermal compression wave propagates just ahead of the temperature front - raw material is thus compressed and heated to ignition temperature. There are several of these waves. Certain undesirable effects can be envisaged at this stage. Because of the high pump powers, electrons and ions can be accelerated by the E-field in opposite directions. When the velocity is high enough unstable plasma waves develop which give rise to turbulence, increasing absorption but producing fast electrons with a long range. This has two effects : they may penetrate deep into the core and preheat this, making compression harder and they may collide less frequently with cold electrons thus reducing heat transfer and implosion efficiency - the process of 'decoupling'.

One obvious requirement is that the critical surface should be as near as possible to the pellet core - since the core is the part where fusion occurs, the less distance the shock waves travel before dissipating themselves, the better. Another is that the absorption process at the critical surface be an efficient one. In the first instance, the larger the frequency and monochromaticity of the laser, these going down as the frequency increases. Thus the two most likely candidates are

(1) 1.06 μm Nd - glass , $\omega_o \sim 1.78 \times 10^{15}\ s^{-1}$, $n_c \sim 10^{21}\ cm^{-3}$

efficiency ~1%, bandwidth at high powers considerable $\sim O(10^{-2}\ \omega_o)$

(2) 10.6 μm CO_2 , $\omega_o \sim 1.78 \times 10^{14}\ s^{-1}$, $n_c \sim 10^{19}\ cm^{-3}$, efficiency 10%
bandwidth $\sim O(10^{-3}\ \omega_o)$

and these aspects do not even cover reliability and the necessity for power output of 10 kJ pulses every 0.02 sec. However, one can argue that these problems are of a predominantly technological nature. Of a more theoretical nature is the question of laser absorption.

Two alarming facts pose the problem. Firstly, (41), from energetic balance, a laser of energy E, coupling with efficiency ε into compression, heating core, producing an output ZE, must exceed a critical value

$$E_c \sim (n/n_o)^{-2}\ \frac{Z^3}{\varepsilon^4} \qquad MJ$$

where n, n_o are the compressed, normal densities, respectively. Z must allow for inefficiencies in the system and will be of order 10. Numerical calculations considering purely hydrodynamic coupling of the hot blow-off plasma to the cold interior, yields efficiencies $\varepsilon \sim 0.1$, $\varepsilon_c \sim 100$ kJ. If the laser-plasma interaction is imperfect then ε will be lower and unreasonable amounts of energy will be required. Secondly, collisional absorption mechanisms cannot account for the dumping of energy :- Nd-glass light is absorbed by collision in 1mm and CO_2 in 100mm. Additionally, the radiation pressure is too small for economical implosion by this mechanism.

We can, however, obtain strong laser-plasma coupling through the sort of parametric coupling processes we have already mentioned. In particular, the three wave coupling process is of considerable interest. It has been pointed out by Kaw and Dawson (42) that certain of these processes can lead to enhanced resistivity in the plasma. In particular, it was hoped that strong absorption might occur for the photon → plasmon + 'phonon' decay of Dubois and Goldman (19). Additionally, the decay, but into a real

phonon, for $T_e > T_i$, has been suggested (42). The OTSI must also be included here, being merely a branch of the decay instability. This is based on the work of many authors and verified experimentally in microwave and atmospheric experiments (47). The enhanced absorption has been noted in simulations (43).

Yet, even if this is the dominant absorption mechanism problems can arise in the underdense plasma corona which can seriously affect the energy reaching the region of projected absorption. The instabilities can be excited through 3-wave coupling to the pump in this region and we shall now list, as far as possible, the instabilities which we can expect, giving a brief description of each one. There are two regions of interest, that near the critical density and the underdense corona.

Defining the field strength parameter, $\eta = v_e/v_o$ (16) where $v_o \equiv eE_o/m\omega_o$, the critical density instabilities are

(i) Decay instability : photon → plasmon + phonon

Convective in the presence of density gradient of scale length L.

Threshold given by

$$\eta^2 \leq \frac{8}{kL}\left(1 + \frac{3T_i}{T_e}\right)\left(\frac{\nu_i}{\omega_i}\right)^{1/2} + 3.2\left(\frac{\nu_i}{\omega_i}\right)\left(\frac{\nu_e}{\omega_{pe}}\right)$$

($\omega_i = kc_s$, ν's are damping rates)

(ii) OTSI : photon → plasmon + non-oscillatory phonon

Absolute with threshold given by

$$\eta^2 \geq \left(1 + \frac{T_i}{T_e}\right)\left(\frac{4\nu_e}{\omega_{pe}} + \frac{8\lambda_D}{L}\right)$$

Optimal growth for $k\lambda_D \ll 1$ and $\omega_{pe} < \omega_o < (\omega_{pe}^2 + 3k^2 v_e^2)^{1/2}$ the latter being difficult to attain.

(iii) Filamentation : density perturbation perpendicular to incident pump wave, whose amplitude undergoes long wavelength modulation. Absolute.

The subcritical density instabilities which may affect the pump penetrating to $\omega_{pe} = \omega_o$, either by scattering or by affecting the coronal properties, are the following. We give estimates for the homogeneous case as absolute instability no longer automatically obtains (see Chapter II, the section on linear theory). They are

(i) Stimulated Raman scattering : photon → photon + plasmon

Occurs only for $n < \frac{1}{4}n_c$ with effective threshold $\sim 10^{13}$ Wcm^{-2} (40) Fastest growth rate of all instabilities $\sim \frac{v_o}{c} \sqrt{(\omega\omega_{pe})}$

(ii) 2-plasmon : photon → plasmon + plasmon

Occurs only at $n = \frac{1}{4}n_c$ with effective threshold 10^{14} Wcm^{-2}
Growth rate $\omega_p \, v_o/c$

(iii) Stimulated Brillouin scattering : photon → photon + phonon

Occurs for $n < n_c$ and threshold $\sim 10^{14}$ Wcm^{-2}
Growth rate $\sim \frac{v_o}{(2cc_s)^{\frac{1}{2}}} \, \omega_{pi}$ (backscatter)

(iv) Quasi-mode scattering : can occur for (i) and (iii) when frequency shift of electrostatic wave exceeds its own eigenfrequency (or pump is sufficiently strong to overcome frequency mismatch). Exist even for conditions under which normal mode does not i.e. $k\lambda_D >> 1$ or $T_i \sim T_e$. Studied by several authors in principle (21, 44, 45, 46).

(v) Induced scattering : resistive scattering off particles themselves i.e. off electrons for $k\lambda_D >> 1$ and ions for $T_i \sim T_e$. Weak instabilitie but growth rate off ions can be near that of (iii) for $k\lambda_D << 1$ (21). No preferred scattering angle up to $\sin^{-1} (k\lambda_D)^{-1}$.

(vi) Modulational : forward scattering with long wavelength scatterer and slow growth rate. Modulation applies to the envelope perturbation of the carrier wave. When this propagates perpendicular to incident wave we get the filamentation instability, causing formation of high density filaments with bunching of pump field in low density regions.

Mention must be made of the experiments performed in connection with this theoretical work. There is no incontrovertible proof that these instabilities are the cause of the observed phenomena, although it is hard to explain the results without recourse to this theory, at least in laser fusion applications. There is well documented evidence of parametric instabilities in microwave and ionspheric experiments giving rise to resonant wave coupling, enhanced heating and anomalous reflectivity (47 - 51). The electromagnetic case has been examined by Franklin et al (15) and good agreement with theoretical thresholds has been obtained, once allowance has been made for density gradients and boundaries (54). In fusion applications, there is scant evidence but there are several convincing experiments. Notably, Yamanaka et al (56) correlated the anomalous absorption, fast ion production and enhanced electron temperature with the decay and O.T.S. instabilities. Bobin et al (57), with pump powers in the range 10^{-1} - 10^{15} Wcm^{-2} give a convincing explanation of Langmuir (i.e. electron plasma) wave coupling to the pump. As far as backscatter is concerned, reflections, typically of order up to 20% have been observed (58 - 61) for powers up to 10^{16} W cm^{-2} (Nd-glass laser). These experiments use a pellet to form the plasma. Experiments with slab geometries generate higher reflectivities, typically of order 50% at 3.10^{14} W cm^{-2} (62). The reflection, in fact, decreases with increasing power due to enhanced absorption and increased damping (63),

as in Figure (4).

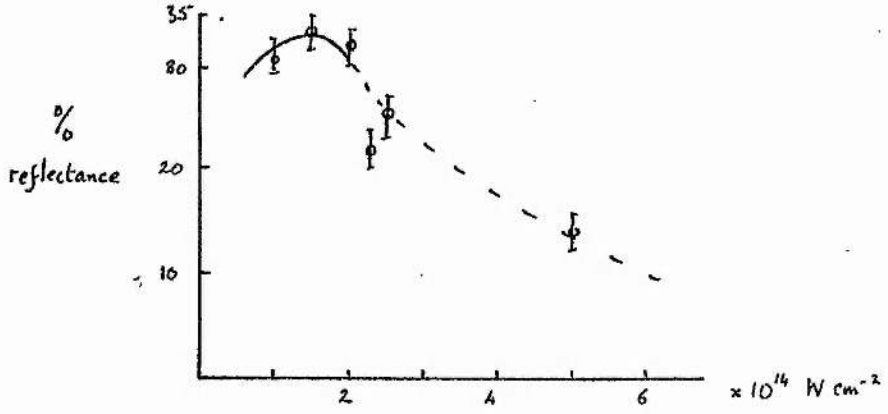

Figure 4 Reflectivity as a function of input power

The reflected pulse shape, in time, shows a plateau followed by a peak, consistent with a saturated reflectivity at high power which increases as the power decreases. There is some evidence that above 10^{15} Wcm^{-2} (CO_2 laser), the reflectivity increases once more (64). As to experiments on laser fusion itself, Nuckolls et al (65) using ½ - 1 TW Nd-glass laser have generated, using glass balloons filled with DT gas, 10^7 14 MeV neutrons, volume compressions $\sim$100, $T_e \sim$ 10-20 ke V and $T_i \sim$ 2 ke V. These are in good agreement with results from their LASNEX simulation code. KMS Fusion Incorporated (66) have obtained neutron yields $\sim 10^7$ and compressions $\sim 10^3$ also using glass balloons. The best results were obtained for gas pressures near 10 atm. and a ratio of radius to shell width of 40:1. It should be noted that the latter group use a two-beam system whilst the former only use a single one. Obviously, there is still a long way to go in this direction but progress is being made.

Returning to the theoretical problems connected with the effects of the instabilities, we note (41) that both the decay and OTS instabilities saturate with the production of a high energy tail to the electron distribution. The oscillations grow until electron trapping occurs at the phase velocity of the fastest growing mode, typically $\sim 10\ v_e$. By considering energy

conservation and the Manley-Rowe relations,

$$\frac{d}{dt}\left[|a_o|^2\ \omega_o + |a_1|^2\ \omega_1 + |a_2|^2\ \omega_2\right] = 0$$

$$\frac{d}{dt}\left[|a_1|^2 - |a_2|^2\right] = 0$$

where a_j is the amplitude of wave, frequency ω_j, with $\omega_o \gtrsim \omega_1 \gg \omega_2$,

We see that, at saturation, $|a_1| = |a_2|$ and the energies in the decay modes are in the ratio $\omega_1:\omega_2$. In other words, most of the energy has been fed into ω_1 mode and little into the low frequency mode from which energy deposition can occur more easily. There are, however, simulation studies (70) which indicate the occurence of ion heating by their interaction with the turbulent plasma generated in the nonlinear stages of these instabilities. Whilst there is evidence of ion heating, the deleterious effects of these instabilities through fast particle generation and through minimal direct heat transfer to particles at the critical surface, indicate that these instabilities may not be the main absorption mechanism.

Whatever energy they may contribute will, undoubtedly, be affected by the subcritical density instabilities, which will tend to reduce, by scattering, the energy reaching the dense regions. From linear theory, the most dangerous is the Raman scattering process. Whilst it has the largest linear growth rate, it is easily saturated at the non-linear level - mostly through the 'modulational' instability. In this, the plasmons cause enhancement of low density fluctuations. When these fluctuations become too large, they stabilise the Raman scatter by destroying the 3-wave resonance conditions, in much the same way as would a regular density gradient. Rosenbluth and Sagdeev (41) estimate the mean free path of back-scatter to be

$$\lambda_{bs} \sim \lambda_o \frac{\omega_{o_2}^2}{\omega_p} (c/v_e)^4$$

λ_o being the pump free-space wavelength, indicating a ratherlow level of saturation of backscatter.

On the other hand, no such mechanism stabilises the Brillouin scatter there being no such process to limit the build-up of ion acoustic fluctuations. We note however, a convection mechanism which will impose a limit on the time for which a substantial reflection will occur (71). The energy and momentum deposition resulting from the reflection of input laser light causes a reflection front to propagate outwards through the underdense plasma at supersonic speeds. The propagation time for this front to exceed the width of the underdense plasma then gives a limit on the time over which substantial reflection can occur. For example, for a DT-plasma, CO_2 laser power of 10^{14} W cm^{-2}, the reflection lasts $\sim$1.3 ns, at least two orders of magnitude greater than the growth rate. These findings compare favourably with computer simulations and recent experiments. We can thus expect substantial levels of scattering. In fact, experimental results indicate a scattering of 10-20% of the incident power through this effect (58 - 61, 63). Theory predicts (72) that even when the mismatch is large we can still obtain both these scattering instabilities (but at increased power densities), so that saturation at an initial power does not prevent scattering at peak power.

It is of obvious interest to reduce the deleterious influence of these instabilities and work has been performed in this direction, by either increasing the threshold or reducing the growth rate. However, with the swelling of the pump mode near the critical surface, we find (136) that the thresholds can actually be reduced. Nuckolls et al (38) have suggested the use of shorter wavelength lasers and of seeding the plasma with high atomic number material to reduce instability. The use of finite pump frequency widths (i.e, we destroy the essential monochromaticity of the laser) has also proved, theoretically,of use in homogeneous plasmas. Valeo

and Oberman (87) consider a random phase in the pump (which is equivalent, in their case, to a Lorentzian distribution in power) and find the growth rate reduced by a factor D/γ_o (D is the diffusion coefficient with which the phase random walks). Thomson et al (88, 136) examine amplitude modulation effects, lifting some of the restrictions of the former authors. Assuming the autocorrelation time (of the amplitude variations) to be short compared to the growth time, they find, for sufficiently large bandwidth, $\Delta\omega$, the precise statistical model is unimportant, the growth rate is reduced by $\gamma_o/\Delta\omega$ and the threshold by $\Delta\omega/\min(\nu_e, \nu_i)$ [decay instability] or $\Delta\omega/\nu_e$ [OTSI], where $\nu_{e,i}$ are the damping rates. It is worth noting that sinusoidal variation of the pump central frequency is not an efficient way of reducing the effects. The calculations, in agreement with simulations (69), exhibit the resonant character of the instabilities. With an initial spread of incident energy, only part will be available (due to frequency mismatch) to drive unstable waves and so the growth rate is diminished. However, in an inhomogeneous plasma this is not the case entirely. Because of the spatial dependence of the resonance region, different triplets of waves may interact at different points on the density profile. To see the effect, consider the wavenumber mismatch

$$K(x) = k_o(x) - k_1(x) - k_2(x)$$

where $k_j(x) = k_j(\omega_j, x)$.

If we assume perfect matching at $x = 0$ and expand this expression in a Taylor Series about this point, then

$$K(\omega, x) = K(\omega_o, x_o) + (\omega - \omega_o)\left(\frac{\partial K}{\partial \omega}\right)_o + (x - x_o)\left(\frac{\partial K}{\partial x}\right)_{x_o} = 0$$

For a finite bandwidth pump, we now have the situation that the mismatch may vanish (to 1^{st} order) when (137)

$$(\omega-\omega_o)\ \frac{\partial K}{\partial \omega_o} + (x - x_o)\ \frac{\partial K}{\partial x_o} = 0$$

We can thus expect resonance at several points in the plasma and the possibility of their maintaining the original instability at its level for a monochromatic pump. As yet, numerical results are inclusive. We point out that this has not been observed before and does not follow any of the modifications to the linear, inhomogeneous theory which we shall discuss in Chapter II. We note, here, anticipating these results that absolute instability is lost in infinite, inhomogeneous plasmas if $K(x) = K' x$ but retained if $K(x) = K''x^2/_2$. It is thus possible, in principle, to retain absolute instability by use of finite bandwidth lasers.

Of the other instabilities little work has been done on the non-linear effects, in inhomogeneous plasmas, of induced Compton scattering, as the linear theory (22) only becomes effective at pump powers where the other instabilities are in their non-linear stage. The filamental instability is saturated when the filaments are fully formed, the ponderomotive force, in the region of enhanced field, then balancing the thermal pressure. We shall discuss both these effects at greater length in subsequent chapters.

So, how do we intend achieving strong coupling of laser light to, and heating of, the plasma? The current answer does not, in fact, involve parametric coupling at all - merely the linear conversion of the laser energy into plasma waves through the process of resonant absorption. When the polarisation of the pump is included, the two components propagate independently, the one perpendicular to the plane of incidence, exhibiting the usual Airy function dependence, while the component in the place of inciden

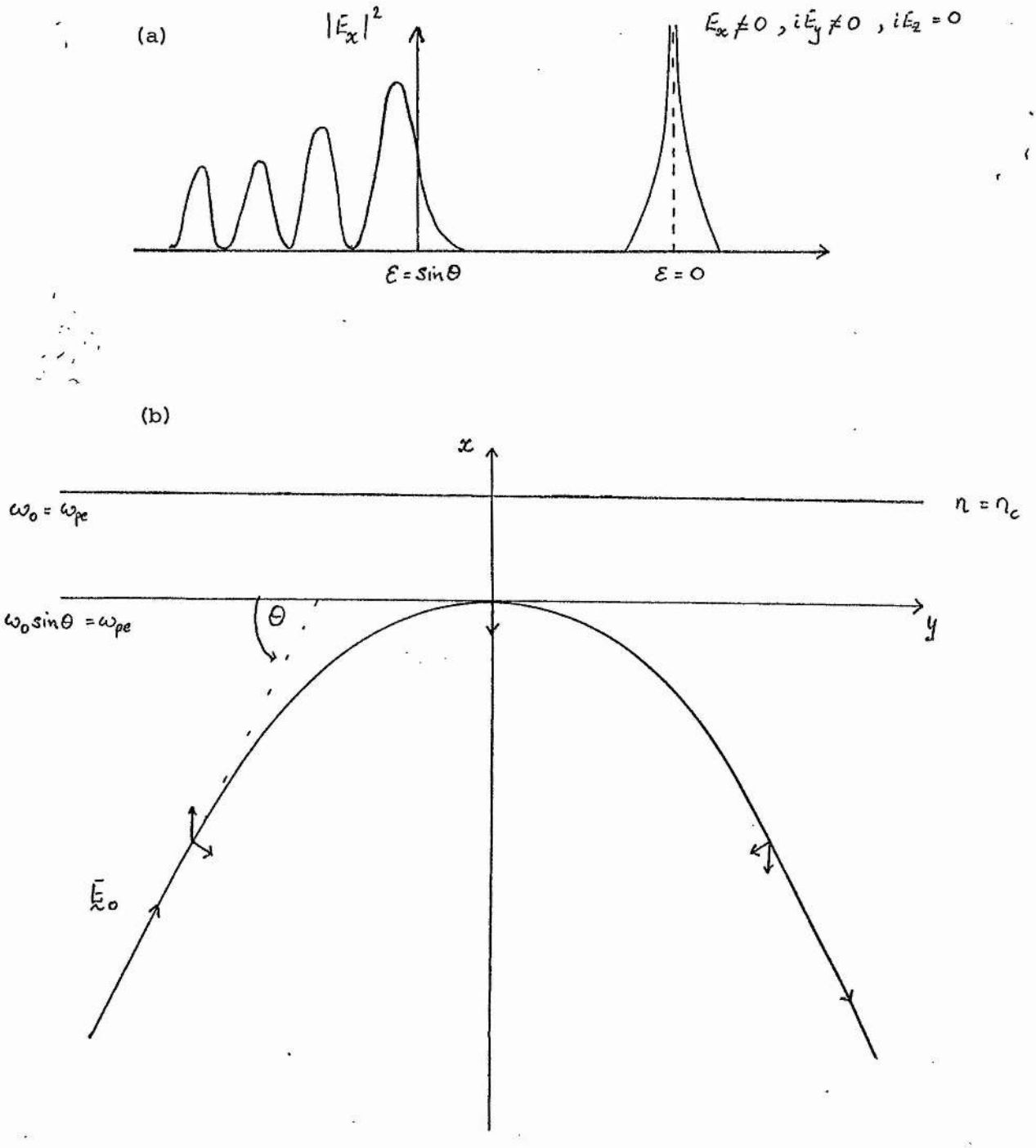

Figure 5 : Oblique incidence of pump wave on critical surface

(a) Amplitude variation

(b) Ray path, showing component along density gradient at reflection surface

$$= 1 - \omega_{pe}^2 / \omega_o^2$$

exhibits a singularity at the critical surface, when incidence is oblique (73).

As can be seen from figure (5.), the energy in the laser field has a non-zero component along the density gradient, at the point of reflection. This component varies with the angle of incidence, θ, for, $\theta \to \pi/2$ corresponds to normal incidence and, as $\theta \to 0$, the point of reflection recedes from the critical surface. A plasma oscillation is driven by E_{ox}, leading to the conversion of electromagnetic to electrostatic energy (74). This linear conversion of oblique electromagnetic waves to plasma waves which are subsequently Landau damped as they propagate outwards, constitutes a strong heating mechanism (75). These calculations have been updated by Forslund et al (76) showing peak enhanced absorption of $\sim$50% for a wide range of electron temperatures. The density profile in such a situation evolves self-consistently towards large light absorption.

At present, then, this seems to be the most likely process by which energy will be absorbed. Certainly, the experiments do indicate substantial absorption, even if at lower powers. Whilst hardly a justification of the fusion scheme, it is, at least, a pointer in the right direction.

Even if this does turn out to be the dominant absorption mechanism, the subcritical density instabilities are still of importance. Consequently, we shall discuss these further, of equal relevance is the perturbation of the critical surface which can result from the filamental instability. The subsequent chapters of this thesis are thus divided in the following manner. In Chapter II we discuss the theoretical approach to the problem of parametric processes in both linear and non-linear regimes. We also summarise the main simulation results as they elucidate some of the more complex effects. In Chapter III, we propose a mechanism whereby we get

considerable enhancement of backscatter from an expanding plasma, through the Stimulated Brillouin Scattering process. Chapter IV deals with the induced scattering off "bare" electrons and ions, examining the perturbation of the background distribution function and the effect of finite bandwidth pump waves. In Chapter V, we examine the effects of a filamented critical surface upon the decay instability and find the growth rate to be reduced. Finally, in Chapter VI, we draw together the various results we have obtained.

CHAPTER II

THE MATHEMATICAL BACKGROUND TO THE STUDY OF PARAMETRIC INSTABILITIES IN PLASMAS

INTRODUCTION

In this chapter, we propose to lay the mathematical background upon which the later work will be based and to summarise, briefly, and collate the enormous quantity of material which has been published on the subject. For the most part, the immediate application was to laser fusion, but, as we have already mentioned, there are several other easily accessible areas of interest. Having first discussed the general formalism of parametric instabilities we shall discuss both the linear and non-linear development of these effects in a variety of pertinent situations, all approximating to our conception of the real one. We shall, as far as possible, attempt to relate the results in physical terms whilst simultaneously explaining the mathematics which will crop up in subsequent chapters.

(i) General Formalism

We assume a constant amplitude pump wave $(\omega_o, \underline{k}_o)$ driving two decay modes $(\omega_1, \underline{k}_1)$ and $(\omega_2, \underline{k}_2)$. In the absence of any mode interaction, each mode satisfies

$$\varepsilon_j(\omega_j, \underline{k}_j)\ A_j = 0 \qquad \ldots\ldots\ (II\text{-}1)$$

where $\varepsilon_j = 0$ is the dispersion relation and A_j the amplitude. This is just the result of a linear perturbation of the plasma. Inclusion of coupling between the modes is analogous to a second order expansion of (II-1). We retain a non-zero right-hand side and replace ω_j, $\underline{k}_j$ by $\omega_j + i\partial/\partial t$, $\underline{k}_j - i\partial/\partial \underline{x}$ to allow for amplitude variations. Physically, this corresponds to the

the inclusion of a non-linear current, $\propto \underline{E}_1, \underline{E}_2 \propto e^{i\underline{k}_o \cdot \underline{x} - i\omega_o t}$ (i.e. which oscillates in phase with the pump) such that the charge density is

$$\rho = \underline{\mu} \cdot \underline{E}_o + V \underline{E}_1 \cdot \underline{E}_2$$

V being a coupling constant, and $\underline{\mu}$ giving rise to the dispersion relation. Using Poisson's equation, $\nabla \cdot \underline{E}_o = -4\pi\rho$, we then obtain, with the above replacements for ω_j, $\underline{k}_j$,

$$\varepsilon(-\omega_o + i\partial/\partial t \, , \, \underline{k}_o - i\partial/\partial \underline{x}) \underline{E}_o = \underline{E}_1 \cdot \underline{E}_2$$

which expands, assuming a slow amplitude variation with respect to the exponential variation, to

$$i \frac{\partial}{\partial \omega} \varepsilon(\omega_o, \underline{k}_o) \frac{\partial \underline{E}_o}{\partial t} - i \frac{\partial \varepsilon(\omega_o, \underline{k}_o)}{\partial \underline{k}_o} \frac{\partial \underline{E}_o}{\partial \underline{x}} = \underline{E}_1 \cdot \underline{E}_2$$

Similar equations can be derived for $\underline{E}_1$ and $\underline{E}_2$. This set of equations may be derived by other methods such as a multiple time-scale perturbation analysis (24) or by using an averaged Lagrangian formulation (77, 78), analogous to Whitham's treatment for fluids (7).

Following Coppi et al (79), we define the amplitudes $A_i = E_i \left| \frac{\partial \varepsilon(\omega_i, k_i)}{\partial \omega_i} \right|^{\frac{1}{2}}$ and sign factors $S_i = \text{sign} \frac{\partial \varepsilon(\omega_i, k_i)}{\partial \omega_i}$. Then, the coupled equations in a homogeneous plasma are, in one dimension,

$$\begin{aligned} i S_o \frac{\partial A_o}{\partial t} &= V_{o12} A_1 A_2 \\ i S_1 \frac{\partial A_1}{\partial t} &= V_{1o2} A_o A_2^* \\ i S_2 \frac{\partial A_2}{\partial t} &= V_{2o1} A_o A_1^* \end{aligned} \qquad \text{(II-2)}$$

where, for a non-dissipative system, the coupling coefficients have the symmetry

$$V_{012} = V_{102}^* = V_{201}^* = V$$

We can then derive the following conservation relations,

$$\partial/\partial t\{\Sigma_j \omega_j S_j |A_j|^2\} = 0 \qquad \ldots.(II-3)$$

$$\partial/\partial t\{\Sigma_j k_j S_j |A_j|^2\} = 0 \qquad \ldots.(II-4)$$

$$\partial/\partial t\{S_o|A_o|^2 + S_1|A_1|^2\} = \partial/\partial t\{S_o|A_o|^2 + S_2|A_2|^2\}$$

$$= \partial/\partial t\{S_1|A_1|^2 - S_2|A_2|^2\} \quad \ldots. (II-5)$$

Equation (II-3) gives energy and (II-4) momentum conservation while equation (II-5) givesthe Manley-Rowe relations. The properties of these equations are then dependent on the values of S_j. For $\omega_o \lesssim \omega_1 \lesssim \omega_2$, there are two combinations:-

(a) $S_o=S_1=S_2$ Since $\omega_o=\omega_1+\omega_2$, either all have the same energy sign or the smallest frequency wave has the opposite sign to the others. In both cases, (II-3) shows that all amplitudes are bounded.

(b) $-S_o=S_1=S_2$ The amplitudes are now unbounded, becoming infinite in a finite time - the so-called 'explosive instability'.

For a dissipative system, there is no energy conservation and the symmetry of the coupling coefficients is destroyed (80). From equation (II-5), and the fact that the energies are proportional to $\omega_i|A_i|^2$ we see that the saturation energies are in the ratio

$$\omega_o : \omega_1 : \omega_2$$

i.e. most of the decay energy goes into the higher frequency decay mode.

In finite regions, with a finite wave packet, we have

$$\frac{\partial A_o}{\partial t} + V_o \frac{\partial A_o}{\partial x} = -i V A_1 A_2 \quad , \text{ etc.} \qquad \text{(II-6)}$$

where V_o is the group velocity of the wave. Solutions of these more difficult equations have been obtained (81, 82, 83)

(ii) Linear Theory

We assume a constant amplitude pump wave and consider the above equations (II-6) when dissipation is included. By suitable normalisation of the wave amplitudes it is always possible to write the equations for the decay waves in the symmetric form

$$\left(\frac{\partial}{\partial t} + \nu_1 + V_1 \frac{\partial}{\partial x}\right) a_1 = \gamma_o a_2$$

$$\left(\frac{\partial}{\partial t} + \nu_2 + V_2 \frac{\partial}{\partial x}\right) a_2 = \gamma_o a_1 \qquad \text{..... (II-7)}$$

where $\nu_{1,2}$ are the damping rates and γ_o the homogeneous growth rate (obtained from the equivalent set to (II-2)). Absolute instability occurs only when $V_1 V_2 < 0$ and when the pump wave exceeds a threshold,

$$\gamma_o^2 > \left(\frac{V_1 V_2}{2}\right)^{\frac{1}{2}} \left(\frac{\nu_1}{V_1} + \frac{\nu_2}{V_2}\right)$$

this condition meaning that energy be pumped into the decay modes faster than it can damp away. Otherwise, only spatial amplification over an initial disturbance is possible.

If we limit the interaction to a finite region in space by allowing only a pump of finite extent (1, 84), absolute instability can still be preserved

but with a reduced growth rate and an additional threshold condition

$$(V_1V_2)^{\frac{1}{2}}/\gamma_o < L < \gamma o/(V_1V_2)^{\frac{1}{2}}K^1$$

where the pump has the form $\exp(-x^2/L^2)$

This is to be expected since the finite pump limits the extent to which a pulse may grow. If $|V_1| = |V_2|$, the growth will remain the same. To see this, consider pulses in the situations shown in figure (6).

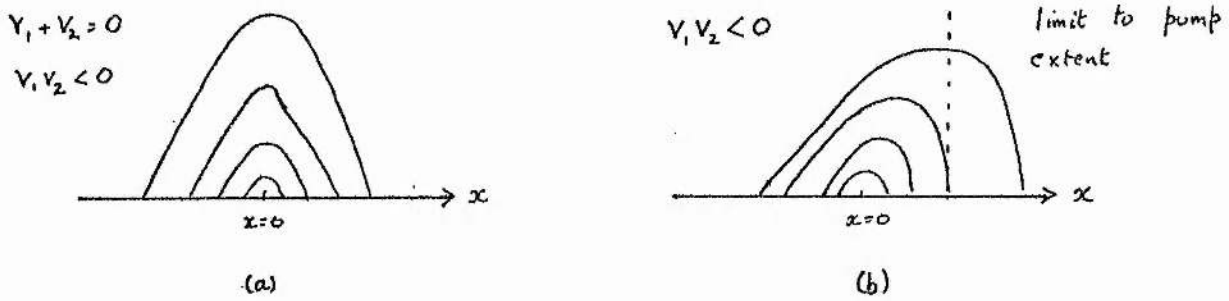

Figure 6 Effect of finite extent pump wave on absolute growth rate

In (a), there is no convection away from x=0 and so the pulse can still grow with its maximum growth rate. However, for (b), there is convection and the amplitudes never attain their full value. A reduced growth rate is measured. If a finite interaction region is applied the growth rate is also reduced as shown.

Inclusion of turbulence (84, 85, 86) indicates the growth rate again to be reduced, as one might expect, extra energy being required to overcome the turbulence during growth. If the turbulence is too strong, the interaction is destroyed and no absolute instability exists. In a similar vein, the effects of an imperfect pump have been examined by several authors (87, 88, 89). Valeo and Oberman (87) examine, for simplicity, the decay instability under the action of a pump wave with a random phase. The growth rate decreases the more pronounced are the random phase displacements.

Thomson and Karush (88) extended these calculations using pump amplitude variation. With several forms to this stochastic driver, the same results were found: that the growth rate diminishes as the frequency width becomes larger. The exact form of the stochastic variation was unimportant for large bandwidths. There is good agreement with simulations (89) indicating the dominant parameter to be the ratio of the resonance width to the driver bandwidth. Physically, this is because when the bandwidth exceeds the resonance width (of order the growth rate) then part of the pump energy becomes ineffective in driving the instability.

Let us now consider the inhomogeneous plasma. Because the wavenumber is now, in general, a function of position, the resonance condition

$$k_o(x) = k_1(x) + k_2(x)$$

is now only satisfied for certain x. There is, then, a mismatch

$$K(x) = k_o(x) - k_1(x) - k_2(x)$$

which will be non-negligible over much of the plasma. This modifies equations (II-7) to,

$$\begin{aligned} (\partial/\partial t + \nu_1 + V_1 \partial/\partial x) a_1 &= \gamma_o a_2 \exp(+ i \int^x K\, dx) \\ (\partial/\partial t + \nu_2 + V_2 \partial/\partial x) a_2 &= \gamma_o a_1 \exp(- i \int^x K\, dx) \end{aligned} \qquad \ldots\ (II-8)$$

The solution here is somewhat more complicated. If we Laplace Transform in time and use the substitution

$$a_j(p,x) = \bar{a}_j(p,x) \exp(\pm \int_o^x dx'\ K/2) \qquad j = 1,2$$

where the plus sign goes with j=1, we generate the following equations -

$$(p + \nu_j + i\frac{K}{2} V_j)\, \bar{a}_j + V_j \frac{\partial \bar{a}_j}{\partial x} = \gamma_o\, \bar{a}_{j'} + \bar{a}_j \quad (0)$$

where $j = 1,2$ and $j' = 2,1$

The usual procedure is then to eliminate $\bar{a}_2$, leaving a second order differential equation for $\bar{a}_1$, which we can solve. In so far as $|\frac{K'}{K}|$ increases without limit, these solutions have the asymptotic solutions, for Re $p > 0$, as $|x| \to \infty$,

$$\bar{a}_1 \sim \exp(-\frac{p + \nu_1}{V_1} x) \qquad \text{or} \qquad \bar{a}_1 \sim \exp(i \int^x K dx' - \frac{p+\nu_2}{V_2}\, x)$$

For temporally growing solutions, there must exist some Re $p>0$ such that there are bounded solutions for large $|x|$. For $V_1V_2>0$ both solutions above are, obviously, unbounded at either $x = \pm \infty$. So, in this instance, no growing solutions are feasible, merely spatial amplification. On the other hand for $V_1V_2<0$ one solution is well behaved at $x = +\infty$ and the other at $x = -\infty$. So, if these solutions can be joined smoothly at $x=0$, where K vanishes, then temporally growing modes can exist.

Rosenbluth (90) and Piliya (91) analysed this situation for an infinite, inhomogeneous plasma in terms of parabolic cylinder functions with the result that if,

(i) $K = K'x$ — no Re $p>0$ existed such that the two asymptotic solutions could be joined at the origin,

(ii) $K = K'' x^2/2$ — there did exist temporally growing solutions.

Since the wavenumber mismatch can be represented, in most cases, by $K=K'x$ this analysis implies that the inclusion of a density gradient immediately converts absolute to convective instability. Whilst this is obviously of advantage in the case of backscatter instabilities, it is also a considerable

nuisance as far as the absorptive instabilities are concerned, limiting, substantially, the energy which can be absorbed. However, this is not the whole story, because it is possible to regain absolute instability in certain circumstances, notably the existence of reflection within, and of some form of finiteness to, the system. We note, however, an elegant treatment of pulse amplification in both space and time (99), which showed the development of an initial disturbance in the case K=K'x. The pulse grows in time but only to oscillate about the level obtained through spatial amplification, these oscillations damping rapidly. This analysis is interesting as it shows a complete solution of these equations.

Let us, now, consider the effect of reflection: in other words, we allow one of the three modes to be reflected back into the interaction region instead of propagating away indefinitely. Physically, we would imagine that waves propagating into regions of higher density would be reflected at their respective critical surfaces and propagate back outwards once more. In two papers, Cairns (93a,93b) discussed just this process and how it can lead to two different absolute instabilities. The analysis concerned primarily, Raman scattering but can be easily modified to other cases. The pump and electron plasma waves are reflected at their respective critical surfaces, $x=x_1$ and $x=x_2$, having first interacted with a backward travelling (i.e. backscattered) electromagnetic wave. At the same point, these reflected waves interact with another electromagnetic wave (now forward travelling) through the same Raman process. By including this additional interaction, i.e. looking at interaction over the whole plasma rather than a smaller resonance region, we again obtain absolute instability with

growth rate

$$p = \frac{\pi}{2|V_1 V_2 K_1|} [\gamma_o^2 + \gamma_1^2] \left[\frac{x_1}{|V_1|} + \frac{x_2}{|V_2|}\right] \quad \ldots.(II-9)$$

where $\gamma_1^2 < \gamma_o^2$, is the growth rate of the reflected wave triplet. The only requirement is that x_1, x_2 be outside the region of strongest interaction. Interestingly, there is only weak dependence on the amplitudes of the reflected waves i.e. as long as there is <u>some</u> reflection and <u>some</u> interaction, then there will be absolute instability. In a later paper (93b), a different mechanism involving reflection returns absolute instability. Here, because of the different rates of variation of the decay wavenumbers we may have backscatter at $x=x_2$ and forward scatter at $x=x_1$, of the same waves. Basically, backscatter occurs at $x=x_2$, the plasma wave propagates to $x=x_1$, where forward scattering occurs with attendant enhancement of the plasma wave. The electromagnetic wave propagates to $x=x_o$ where reflection occurs. It then propagates through x_1 where it is off-resonant, to x_2 where it interacts in the above backscatter, but with an enhanced level. We see that reflection out of the plasma is thus enhanced. The growth rate is

$$p = (\tau_1 + \tau_2)^{-1} \left\{ \frac{\pi\gamma_2^2}{|V_1(x_2)V_2(x_2)K'(x_2)|} + \frac{\pi\gamma_1^2}{|V_1(x_1)V_2(x_2)K'(x_2)|} \right. \quad -\tau_1\nu_1 - \tau_2\nu_2$$

where τ_1 is the time a plasmon takes to travel from x_2 to x_1 and τ_2 the time a photon takes to go from x_1 to x_o and back to x_2. There is a threshold intensity since one must overcome wave damping between points of interaction. In both these instances, the decay can take place over a wide range of frequencies; the only limitation is that decay amplitudes remain of sufficient

size that the two resonance regions and the points of reflection remain separate.

We note, at this stage, the physical importance of these two mechanisms - that the inclusion of some reflection in the system is sufficient to maintain absolute growth of decay instabilities. We shall see that subsequent modifications of the Rosenbluth-Piliya calculations can be explained in terms of this result. It allows a neat description of some of the simulation results which, till now, have had rather bogus explanations.

We now consider the application of some finiteness conditions upon the plasma. Physically, this may have several forms but mathematically we either impose boundary conditions at two finite points, sufficiently far from the interaction region, or we allow a spatial variation in the pump amplitude or both. White et al (84) applied a Gaussian profile $\gamma_o(x)$, $\gamma_o \propto e^{-x^2/L^2}$ but retaining conditions at $x = \pm\infty$. This imposes, for absolute instability,

$$\text{(i)} \quad v_1 v_2 < 0$$

$$\text{(ii)} \quad \gamma_o^2 > \frac{(v_1 v_2)^{\frac{1}{2}}}{2} \left(\frac{\nu_1}{v_1} + \frac{\nu_2}{v_2}\right) \qquad \ldots\ldots \text{(II-10)}$$

$$\text{(iii)} \quad \left(|v_1 v_2|\right)^{\frac{1}{2}} / \gamma_o < L < \gamma_o / K' |v_1 v_2|^{\frac{1}{2}}$$

the lower limit in (iii) requiring γ_o to be finite over a certain region and the upper one requiring a certain gradient in γ_o, since $L = \infty$ corresponds to Rosenbluth's case. Condition (ii) is just the condition for growth in a homogeneous plasma. If we now consider a finite plasma with γ_o constant, then we can also obtain absolute growth if the plasma length, L, satisfies,

$$\frac{\sqrt{|v_1 v_2|}}{\gamma_o} < L < \frac{\alpha \gamma_o}{K' \sqrt{|v_1 v_2|}} \qquad \alpha \text{ constant.}$$

The Rosenbluth-Piliya result is then returned for lengths greater than the upper limit. Since K' is typically proportional to $\frac{1}{L}$, we have the interesting result that absolute growth occurs above a power threshold and independent of inhomogeneity length scale! These calculations were updated by Dubois et al (95, 96) with the result that absolute growth can occur for any plasma length greater than the basic gain length (the lower limit in the above). Essentially, they integrated the first order coupled equations looking for solutions going as $\exp(\delta t)$, adjusting $\mathrm{Im}\delta$ such that the value of the backscattered amplitude was zero at $x = L$; together with a semi-analytic WKB-method generating a dispersion relation which was then solved numerically. As can be seen in figure (7), the solution corresponds to that of Pesme et al up to $L=L_c \equiv \frac{\alpha \gamma_o}{K' \sqrt{|v_1 v_2|}}$ but for $L>L_c$ a whole new family of unstable modes are generated because there is now a frequency shift associated with each unstable mode (a fact excluded by Pesme et al). In other words, the most favourable matching point moves away from x=0 but remaining sufficiently far from the boundary. It appears that $\mathrm{Im}\delta$ is more or less independent of K' but increases almost linearly with L. The condition for absolute instability is,

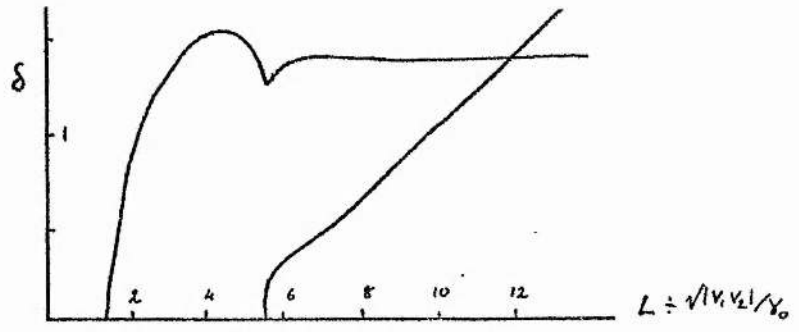

Figure 7 The variation in growth rate as a function of inhomogeneous plasma width (after Dubois, Forslund and Williams, 1975)

therefore, just

$$\lambda \equiv \frac{\gamma_o^2}{K' |v_1 v_2|} > \quad O(1)$$

These results also hold for a spatially varying pump. Physically, there must be a certain distance between the matching and reflection points. Thus, for larger slabs the matching point must move closer to the boundary to preserve absolute instability (as can be seen from that fact that Im δ increases nearly linearly with L), and , hence, Im δ becomes non-zero. This analysis is important in that it extends, considerably, our conception of the solution to the coupled mode equations, both from a numerical and a WKB theoretical approach.

If we now include a level of background turbulence, by writing $K(x) = K'x + \delta K(x)$ and dropping the boundary conditions once more, it is again possible to obtain absolute growth. A Gaussian form of the correlation function of the random part of the wavenumber mismatch is assumed, with RMS amplitude $\Delta \equiv \langle [\delta\kappa(x)]^2 \rangle^{\frac{1}{2}}$. Nicholson and Kauffmann (97) solved the system numerically whilst Yu et al (86) solved it within the WKB approximation, the only difference being the latter dealt with averaged wave amplitudes rather than any one realisation of these amplitudes, as in the former case. The qualitative results were similar.

For finite density gradients, there is a striking variation with the level of turbulence. For low levels, there is only convective instability, as the level increases absolute growth occurs, with rate varying inversely with increasing turbulence till a stage is reached where again only convective growth is possible (here all collective growth is destroyed by the large phase mismatch, due to the strong turbulence). The given

explanation is based on the work of White et al (85):- finite pump extent gives absolute instability by excluding the responses at $x \to \pm\infty$ and hence the destructive interference at x=0. The analogy given is that the medium range turbulence also upsets this destructive interference, allowing the possibility of absolute growth.

However, in the light of recent work by Cairns it would seem reasonable to attach importance to wave reflection rather than destructive interference. Bearing in mind that we only need there to be reflection of waves in the plasma, regardless of the amplitudes (more or less) to regain absolute growth we can explain these findings. For low levels of turbulence, one can assume there to be no reflection whilst in the medium range, reflection occurs at points off the critical surface. The growth rates decrease as this level becomes larger due to γ_1^2, x_1, x_2 becoming smaller in equation (II-9). Finally, for large turbulence levels the phase mismatch destroys the interaction. We feel this to be a clearer explanation.

Of interest, in the steady state is the result (86b) that, for $V_1V_2<0$, the saturation level is enhanced by turbulence - an extension of work by Kauffmann and Cohen (98); when the finite size of the plasma is included there are indications that enhanced saturation levels occur for certain plasma lengths. No calculations have been carried out, to our knowledge, on the case of a finite, turbulent plasma and the possibility of absolute growth.

(iii) Nonlinear Theory

In the non-linear regime, there are several effects which we can include :- such as the action of the decay modes back on the pump, coupling between decay modes, higher order mode couplings, particle trapping and wave breaking. Only the first is usually included in analytic treatments, otherwise the equations become intractable and simulation studies have to be employed. Before we even consider these effects on the parametric instabilities, we must outline the non-linear pump wave optics arising out of the plasma inhomogeneity (99). These studies were motivated by the observation that an enhanced Langmuir wave spectrum, caused by parametric decay of an incident wave and saturated by induced scattering off ions (non-linear Landau damping) could lead to enhanced high frequency electron resistivity (25, 26). The nonlinear propagation of this incident radiation is calculated self-consistently using a generalised non-linear absorptive conductivity. The pump wave , propagating into the density gradient, satisfies

$$\frac{\partial^2 E}{\partial x^2} + \left(1 - \frac{\omega_p^2(x)}{\omega_o^2} + i \frac{4\pi\sigma_T(E\,x)}{\omega_o}\right) E = 0$$

where σ_T is the absorptive part of the transverse conductivity. In a linear density profile, $1 - \omega_p^2/\omega_o^2 = x/L$ and for $\sigma_T = 0$, we observe an Airy behaviour of the pump wave as shown in figure (8).

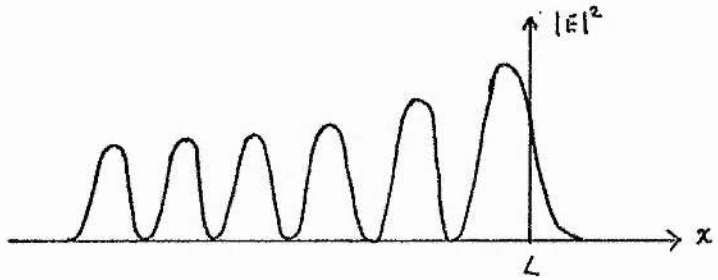

Figure 8 The Airy function behaviour of the incident radiation

It is convenient to work in terms of the vector potentials, $A_{0,1}$, of the pump (0) and backscatter (1) waves. Recalling that

$\nabla \times \underline{v}_j = \frac{e}{im_j} \nabla \times \underline{E}_j = \frac{e\underline{B}}{me}$ for electromagnetic waves, we have from the definitions of $\underline{A}_j$ and $\underline{v}_j$,

$$\underline{v}_j = - \frac{e}{mc} \underline{B}_j \qquad j = 0,1$$

The non-linear terms in equation (II-12) are $(\underline{v}.\nabla)\underline{v}$ and $\underline{v}\times\underline{B}$. For the low frequency response to the high frequency beating force we can use the identity

$$(\underline{v}.\nabla)\underline{v} = (\nabla\times\underline{v}) \times \underline{v} + \nabla(v^2/_2)$$

which, when substituted, with the pressure law, into (II-12) gives

$$\frac{\partial}{\partial t} \underline{v}_\alpha - \frac{\gamma P_{\alpha o}}{n_{\alpha o}} - \frac{e}{m} \underline{E} = -\nabla(\underline{v}_o.\underline{v}_1) = - \frac{e^2}{m^2c^2} \nabla(\underline{A}_o.\underline{A}_1)$$

In (II-11), we linearise with respect to $n_{\alpha o} = n_o$ and $v_{\alpha o} = 0$ (this now only includes up to second order coupling between modes). Elimination of $\frac{\partial v_\alpha}{\partial t}$ gives the separate equations for the electrons and ions

$$\frac{\partial^2 n_e}{\partial t^2} - v_e^2 \nabla^2 n_e + \omega_{pe}^2 (n_e - n_i) = - \frac{e^2}{m^2c^2} \nabla^2 (\underline{A}_o.\underline{A}_1) \qquad \ldots\ (II-13)$$

$$\frac{\partial^2 n_i}{\partial t^2} + \omega_{pi}^2 (n_i - n_e) = 0 \qquad \ldots\ (II-14)$$

where we have neglected the ion response to the beat term, $\underline{v} \times \underline{B}$, due to their heavy mass, and the ion pressure (a valid assumption as long as $T_e >> T_i$, the conditions for the existence the plasma modes, anyway).

Damping of the electron fluctuations can be introduced via $-\gamma_D \underline{v}_e$ in the equation of motion, or $\gamma_D \frac{\partial n_e}{\partial t}$ on the left hand side of (II-13).

The effects of the density fluctuations on the electromagnetic waves are easily derived from Maxwell's equations, e.g. for the scattered wave,

$$\nabla \times \underline{B}_1 = \frac{4\pi}{c} \underline{j} + \frac{1}{c} \frac{\partial \underline{E}_1}{\partial t} = \frac{4\pi}{c} (e n_\alpha \underline{v}_o + e n_{\alpha o} \underline{v}_1) + \frac{1}{c} \frac{\partial \underline{E}_1}{\partial t}$$

where we have used the component of current at the frequency of B_1.

Since $B_1 = \nabla \times \underline{A}_1$, $\underline{v}_o = \frac{e\underline{A}_o}{mc}$ and $\underline{E}_1 = \frac{1}{c} \frac{\partial \underline{A}_1}{\partial t}$, we have

$$\frac{\partial^2 \underline{A}_1}{\partial t^2} - c^2 \nabla^2 \underline{A}_1 + \omega_{pe}^2 \underline{A}_1 = -\omega_{pe}^2 {}^{n_e}/_{n_o} \underline{A}_o$$

A similar equation can be derived for $\underline{A}_o$. Thus, these stimulated scattering processes are described by the following equations, in so far as the effects of electrostatic steepening, higher-order coupling and forward scattering can be ignored :-

$$\frac{\partial^2 \underline{A}_{o,1}}{\partial t^2} - c^2 \nabla^2 \underline{A}_{o,1} + \omega_{pe}^2 \underline{A}_{o,1} = -\omega_{pe}^2 {}^{n_e}/_{n_o} \underline{A}_{1,o}$$

$$\frac{\partial^2 n_e}{\partial t^2} + \gamma_D \frac{\partial n_e}{\partial t} - v_e^2 \nabla^2 n_e + \omega_{pe}^2 (n_e - n_i) = -\frac{e^2}{m^2 c^2} \nabla^2 (\underline{A}_o . \underline{A}_1) \quad \ldots \text{(II-15}$$

$$\frac{\partial^2 n_i}{\partial t^2} + \omega_{pi}^2 (n_i - n_e) = 0$$

Forslund et al (96) have considered solutions to this set of equations in various approximations. The solutions do not account for wave non-linearities (by assumption) but it does indicate regions where they may be of importance, i.e. we can spot regions of particle trapping or wave breaking. The spatial non-linear problem is discussed in the following chapter, so we shall confine ourselves to the temporal one. There are two separate regions (i) the weak coupling limit where the homogeneous growth rate, γ_o, is much less than the uncoupled frequency of the plasma wave, Ω and (ii) the strong coupling limit where $\gamma_o >> \Omega$. In the first instance, the slow amplitude variation approximation is valid i.e. we write amplitudes $\sim a(x,t)e^{i(K x - wt)}$ and neglect the exponentials and $\partial^2 a/\partial \eta^2$, $\eta = x,t$. The equations reduce to the mode coupling equations of Sagdeev and Galeev (13) when $\gamma_D = 0$, with solutions in terms of Jacobi elliptic functions. The behaviour is oscillatory, energy transferring to decay waves, then back to the pump and so on. For a sufficiently large pump strength, the plasma wave will go non-linear giving rise to strong damping e.g. for Brillouin scattering, wave breaking is expected to occur for $\omega_{pe}^2/\omega_o^2 > 4\, c_s/c$ i.e. only in the extremely underdense region. For strong coupling, there is a further classification according to the size of n_e/n_o. For $n_e/n_o < 1$, saturation occurs for $|A_o| \sim |A_1|$, when a standing wave pattern develops in the backscattered wave - wave breaking does not occur before pump depletion. The overall development is then exponential growth to saturation followed by frequency modulation in the electromagnetic waves. However, if $n_e/n_o \gtrsim 1$, at saturation, the theory breaks down but the implied physics is still valid. $n_e/n_o > 1$ implies $v_o/v_e > 1$ so that wave breaking is expected to occur before the above amplitude oscillations. This has been noted in their simulations (96b).

The effects of instabilities near the critical surface have been examined, mostly from the viewpoint of quasi-linear theory and the likely saturation heating. Analogous to the above theory is the work by Thomson et al (69, 100). The theory describes the development of the OTS instability, excluding pump depletion but including decay mode coupling. The plasma heating is calculated through the evolution of the electron distribution function. The results agree with associated computer simulations, showing some heating, fast particle production and a broad spectrum of saturated waves.

The nonlinear calculations which have been done so far and those which will be mentioned in the following chapters present certain problems when one comes to assess the strength and dominance of these interactions. Firstly, the instability calculations assume some initial profile for density, velocity and temperature which are assumed constant over some appropriate time-scale. However, in certain applications, notably laser fusion and pulsars, there is another time-scale present - the hydrodynamic time-scale, over which time these profiles do vary and are altered by the non-linear saturation of the parametric instabilities. Obviously, a closer match of instability behaviour and hydrodynamic calculations is needed. Secondly, there will always be several instabilities taking place simultaneously leading to very different saturation effects. Not only is it necessary to see how the incidence and existence of one instability effects the development of another but also to see how the non-linear stages affect the subsequent generation of further instabilities. These collective effects can lead to absorption, reflection and self-focussing. In Chapter V we go some way to elucidating, analytically one of these hybrid effects.

Nevertheless, one way of examining these effects is through computer simulations, a technique which has been of considerable use in recent years. It is very much a sledge-hammer attack on the problem. By virtue of this technique mirroring the real situation, one must guard against obscuring the physics by making the approach so accurate that one cannot see the results for the pages of output. With this in mind, much constructive work has been done in this line in terms of feasibility of compression and laser fusion and of parametric instabilities in the under-dense plasma. The advantage of this method is that one can obtain long-time solutions of the equations, without having to make any approximations. Saturation effects are readily added, in contrast to theory, so that the non-linear development of the instabilities can be seen. Certain restrictions must, however, be placed on this procedure, in order that one may examine each instability, in turn, before embarking on studies of hybrid effects. Thus, to study the Raman effect we fix the ions whilst for the Brillouin scattering we set a density greater than one quarter the critical density, in the homogeneous case, or a sufficiently large density gradient, in the inhomogeneous case, to discount the Raman effect. Similarly, instabilities excited near the critical surface are eliminated by ensuring the density never approaches close to the critical density.

Forslund, Kindel and Lindman (96) have studied, extensively, the back-scatter processes from homogeneous and inhomogeneous plasmas with bounded or infinite geometries. The simulations fall into two categories :- (i) the weak coupling limit ($\gamma_o < \Omega$) and (ii) the strong coupling limit ($\gamma_o > \Omega$). Since γ_o is a function of pump power, this provides a characterisation of the pump intensity. Considering just the bounded cases, we can note agreement between their results and their non-linear theory, discussed

above, in as far as strongly non-linear effects are neglected. Direct comparison is difficult because a certain amount of particle trapping occurs in the simulations, often making evaluation of reflected powers difficult. In the case of the homogeneous plasma, the effect of random modulation of the pump frequency is of interest. As expected, the reflected power varies inversely with the frequency shift, $\Delta\omega$. What is, perhaps, unexpected is that large values of $\Delta\omega/\gamma_o$ (of order ten) are required for substantial reduction in reflectance. Moving away from the regimes of theory validity, we discuss the cases involving wave breaking and particle trapping. For the stimulated Raman case, a hot electron tail is formed, with velocities $\sim \frac{1}{3}$ c; there is large electron heating through trapping and wave breaking, low reflectance and the ultimate stabilisation occuring through increased Landau damping caused by the hot electrons with the loss eventually balancing the gain through the parametric decay of the pump. The time-scales are, notably, much longer than predicted by theory and than the infinite homogeneous case. In Stimulated Brillouin scattering, no such stabilisation occurs. There is much wave breaking and particle trapping with a corresponding increase in electron and ion heating and deeper pump penetration. Thus, wave breaking now occurs deeper into the plasma and so on. Once breaking has occured one expects an equilibrium of particle energy density and radiation pressure through the Brillouin effect and calculations based on this show low absorption and high reflectance. The most noticable effect is, therefore, a weak absorption but spectacular heating. Of practical interest, are the results allowing for both instabilities to occur in a linear density gradient (as mentioned before the separate processes are examined by suitable manipulation of the ions or density profiles). The Raman backscatter is seen first and

begins to saturate before reflection is increased by the onset of Brillouin scattering. Even at this time there is a noticable high energy blow-off created by the hot electrons through the Raman instability. By the time the ion waves go non-linear, electron heating has caused a reduction in backscatter down to a level ∿10%, with ∿50% transmission. By the end of the run, transmission is down to 40% due to increased electron heating enhancing laser penetration depth. One feature is the shorter time-scales for these Brillouin effects compared to the simulations of just Brillouin scattering. This one can ascribe to the electron heating and, in part, to a different density profile.

Kruer, Estabrook and Thomson (89) have also simulated these instabilities showing in both cases that the reflectance is considerably reduced for $\eta^2 << 1$ (the region of projected applicability for fusion), where $\eta^2 = \frac{E_o^2}{4\pi n_c} kT.$ For the Raman case, they propose a mechanism for reducing the effect of high energy electrons, via effficient coupling through finite amplitude, short wavelength ion fluctuations to slow, damped electron plasma waves, producing less energetic electrons. These ion fluctuations could be produced by counter-streaming between different ion species in the blow-off or steepening of ion waves produced in other decays. Considerable reduction in high energy particle numbers can then be obtained e.g. for Nd-glass laser at power 3.10^{16} W cm^{-2} we achieve reduction by factor ∿8 for $\delta n/n$ ∿ 20%. Lower amplitude fluctuations are required for smaller powers. Additionally, the reflectance from SBS (the most deleterious in this case) can be reduced by introducing a finite bandwidth into the pump by phase modulation. It should be noted that these simulations do apply to the homogeneous case.

Indeed, most parametric instabilities seem to have been studied by computer simulation at one stage or another. One of the aims is to measure the energy deposition efficiency and to elucidate its mechanisms. This illustrates another powerful use of simulations e.g. the resonant absorption already mentioned and the energy deposition from energetic particles. A clearer picture of how the energy can be dumped is now appearing. Even so, because of the complexity of the simulation technique, one is not always wholly sure what physics causes the observed effects. It is thus important to augment some of these simulations with theoretical calculations e.g. the absorption through energetic electrons has been elucidated by Cairns (102).

CHAPTER III

ON THE POSSIBILITY OF ENHANCED BACKSCATTER FROM AN EXPANDING PLASMA

We shall consider the Stimulated Brillouin Scattering process in which an incident electromagnetic wave $(\omega_o, \underline{k}_o)$ decays into a scattered wave (ω_1, k_1) and an ion acoustic wave $(\omega_2, \underline{k}_2)$. For strong interaction we require that energy and momentum be conserved in this process i.e. we require the above wave triplet to satisfy the resonance conditions

$$\omega_o = \omega_1 + \omega_2$$
$$\underline{k}_o = \underline{k}_1 + \underline{k}_2 \qquad \ldots\ldots \text{(III-1)}$$

This limits the interaction to a certain discrete set of wavenumbers (since $\omega_i = \omega_i(\underline{k}_i)$, which, in the presence of a density gradient, limits it further to a finite region in space, the resonance, or interaction, region. We have discussed already the linear evolution of parametric instabilities and the existence of both convective and absolute growth in inhomogeneous plasmas. The non-linear evolution has already been mentioned. The theory deals mainly with the homogeneous case and the steady-state amplitudes are shown as a function of position in Figure 9, as calculated by Forslund et al (96). The theory bears on early work by Tang (33) and has a characteristic parameter, $\beta = \frac{\sqrt{|v_1 v_2|}}{\gamma_o} \frac{\gamma_o}{|v_2|} = \gamma_p T_1$, where γ_p is a damping rate and T_1 a typical time scale. The theory predicts that the limiting value of the reflectivity is given by $R = \frac{V_1 E_1^2}{V_o E_o^2} \equiv \frac{\omega_1}{\omega_o}$. Thus, for Brillouin scattering, where $\omega_1 \sim \omega_o$, we

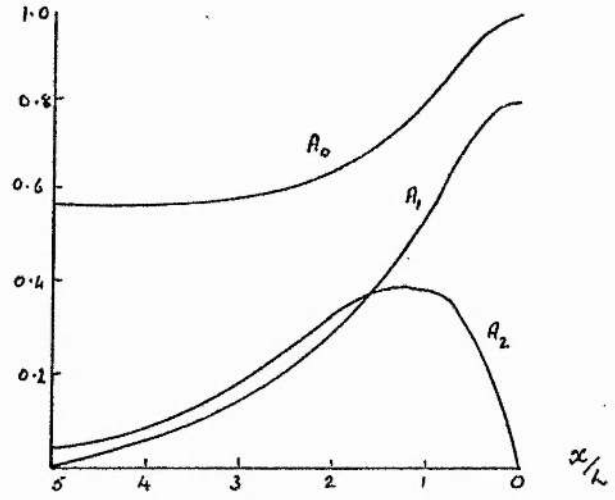

Figure 9 Steady state amplitudes as functions of position with boundary conditions

$A_o(O)=1$, $A_1(L)=10^{-3}$, $A_2(O)=O$, $L=5L_1 = 5\sqrt{|v_1 v_2|}\,/\gamma_o$, $\beta=1$

(after Forslund et al)

expect large values of the reflectance. Figure 9 shows the steady state amplitudes resulting from the integration of the first order coupled equations taking the weak coupling limit, as already mentioned. (This corresponds to the slow amplitude variation approximation applied to equations (II-15)).

We note the pump depletion and large reflection. The backscattered wave has an initial level, as it enters the interaction region, near its thermal level. It should be emphasised that these steady-state amplitudes were calculated for homogeneous plasmas; for comparison with the inhomogeneous case, we must remember several things :- near the critical surface there will be a WKB enhancement of the waves whilst the interaction is now limited to finite spatial extent (<<L). Additionally, different backscattered modes are matched at different densities thus giving rise to a

finite bandwidth in the backscattered spectrum so that the reflectance of each single mode is not expected to be as great as shown in Figure 9. Forslund et al have also integrated the second order coupled equations (II-15) over a large band of modes and found that, whilst, for many modes, saturation due to pump depletion occurs, it does so with small amounts of energy in each mode. For a single mode, there is good agreement with linear theory, including the predicted frequency shift.

Additionally, Liu (45) has considered Brillouin scattering by heavily damped ion waves, where convective loss may be neglected, and in an expanding plasma, with non-uniform expansion velocity. In both cases, conditions for absolute instability are calculated. In either case, only convective amplification exists for backscatter (but absolutely growing modes exist for nearly side- and nearly forward-scattering). The growth rate for sidescatter off a heavily damped ion wave in the inhomogeneous case is the same as that for a homogeneous slab, provided certain threshold conditions are satisfied.

The spatial amplification of two interacting electromagnetic waves of similar powers has been considered by Kauffman and Cohen (98) in the inhomogeneous, non-linear regime. The effects of the plasma wave were included - the analysis was, however, mainly concerned with Raman scattering and required $\omega_o > \omega_1$. This mechanism does give fairly efficient heating of the plasma. Apart from this case, the initial level of one of the electromagnetic waves (the backscatter one) has always been set to its thermal level. We shall show that this does not necessarily have to be the case.

It has been noted (38, 39, 40) that the expansion velocity, of the ablating material forming the plasma corona, is around the sound speed, $c_s = (\frac{kT_e}{M_i})^{\frac{1}{2}}$. Galeev et al (103) have noted that this expansion velocity is likely be non-uniform giving rise to a Doppler-shifted ion sound frequency in the laboratory frame. (We note that inclusion of the flow velocity, not its non-uniformity, gives rise to this shift). One then has, for this frequency,

$$\omega = \frac{kc_s}{(1 + k^2\lambda_D^2)^{\frac{1}{2}}} + \underline{k}.\underline{u} \qquad \ldots\ (III\text{-}2)$$

$\underline{u}$ being the expansion velocity. In general, the x-component of the ion acoustic wave number will be a function of x and of the gradients of u, n, T. These gradients are related by the 1-D equations for continuity and motion, which, for $M_e << M_i$, $T_i < T_e$ and quasineutrality, are

$$M_i n \left(\frac{\partial}{\partial t} + v\frac{\partial}{\partial z}\right)v = -T\frac{\partial n}{\partial z} + n\frac{\partial T}{\partial z} \qquad , T = T_e + T_i$$

$$\frac{\partial n}{\partial t} + \frac{\partial nv}{\partial z} = 0$$

It is usually the case (104) that, because of the rapid electron heat conduction in the plasma, the length scale for temperature variations is considerably greater than either density or velocity variations. Hence, we may safely neglect $\frac{\partial T}{\partial z}$ to find the solutions,

$$n = n_o \exp(-{}^{z}/_{c_t t}) \qquad z > 0$$

$$v = c_T + {}^{z}/_{t}$$

where $c_T^2 = {}^{T}/_{M_i}$, a sound speed

We, thus, have a solution for a plasma expanding from a stationary surface. It is apparent from the form of these solutions that the velocity scale length is greater than the density one and so we shall neglect this also. Indeed, in 3-D we can expect the density gradient to be even longer, due to divergence of the expanding material into an increasing volume.

It, thus, is possible for the ion sound frequency in equation (III-2) to be Döppler-shifted to zero, provided $u \gtrsim c_s$.

The new feature of the work in this chapter is based on just this observation, that, when viewed from the laboratory frame, Stimulated Brillouin scattering can occur, in an expanding plasma, with the pump and backscattered waves interacting resonantly with stationary, zero-frequency ion-sound waves. The resonance conditions, (III-1), imply that

$$\omega_1 = \omega_o \quad , \qquad k_o = - k_1 = \tfrac{1}{2} k_2$$

In this situation, the electromagnetic waves have the same frequency and, as we shall see, the boundary conditions of the problem are drastically altered. We shall consider a system in which there is a stationary density profile, the plasma streaming outwards in the direction of decreasing density - such as might be expected in a plasma produced by ablation from a spherical pellet. For simplicity, we treat the problem in plane geometry and restrict our attention to 1-D scattering, in which all wave vectors are parallel.

Thus, in the rest frame of the plasma,

$$\omega_2 \sim k_2 c_s$$

(assuming $k\lambda_D << 1$) where c_s is the sound speed and so, from (III-1)

$$\omega_1 = \omega_o - k_2 c_s$$

If, however, we consider the same system, but viewed from the laboratory frame, where the plasma has streaming velocity u, then the ion-sound frequency is Döppler -shifted to

$$\omega_2 \sim k_2 (c_s - u)$$

which, as we have already intimated, is zero for $u = c_s$, the pump and backscattered waves then having equal frequencies.

Consider, now, a laser beam incident upon this expanding plasma. This beam travels through the underdense region before reaching the critical surface ($\omega_o = \omega_{pe}$) where strong absorption occurs. In practice, complete absorption would not be expected and a partial reflection of the pump will occur. If the expansion velocity is near c_s, then the incident and this reflected wave (obviously, having the same frequency) can interact resonantly with stationary ion sound waves via the Brillouin scattering which we described above. With our assumption of uniform expansion velocity (at least, over the density scale length), ion sound waves, of wavenumber $2k_o$, will be excited at all points in the plasma. The second feature of this analysis concerns the boundary conditions on the backscattered wave. This wave is none other than the reflected pump wave (by virtue of the fact that $\omega_2 = 0$) and so, its level as it enters the interaction region (now, the whole underdense region) will be some fixed proportion of the pump wave; based on recent experimental findings (58 - 61), as mentioned in Chapter I, we take this to be an energy reflection $\sim$10% and include it in our numerical results. It should be emphasised that, if $\omega_1 \neq \omega_o$, the level

of backscatter at the critical surface is, then, the thermal level of the backscattered mode which would, in general, be several orders of magnitude below the level of the pump mode. Thus, by allowing for the effect of expansion, in this fashion, we can obtain Brillouin scattering in an inhomogeneous geometry with the level of backscatter, at the boundary of the interaction region, several orders of magnitude greater than would normally be expected. In such a plasma, it would seem reasonable that the generation of a backscattered wave of the same frequency as the incoming driver wave would be an important process, the mechanism being simply Brillouin scattering viewed from a reference frame in which the plasma is moving. Even if the expansion velocity is not exactly c_s, $k\lambda_D \gtrsim 1$ or we include $u(x)$, the process can still occur with an off-resonance, stationary ion sound oscillation being driven in the plasma, the results being, as we shall see, fairly insensitive to such variations. In this discussion, we shall follow our published works (105).

For simplicity, we shall now consider these ideas, formally in 1-D, on the assumption (inherent in most calculations in this field) that whilst the full 3-D situation might differ in some detail, the essential features of the simpler 1-D calculations are preserved. We assume a plasma of finite extent, $0 \leq x \leq L$; the pump impinges from $x < 0$; the critical surface ($n=n_c$) is at $x=L$ and there exists a linear density profile of the form $n(x) = n_c\, x/L$. We use the equations of Forslund et al (96) for the amplitudes of the three waves already mentioned (equations (II-15)) and transform them to a reference frame, (x',t'), moving outwards with speed u.

This generates the substitutions

$$\frac{\partial}{\partial t} = \frac{\partial}{\partial t'} + u \frac{\partial}{\partial x'}, \qquad \text{and} \qquad \frac{\partial}{\partial x} = \frac{\partial}{\partial x'}$$

In the stationary state, these equations are (dropping the dashes)

$$((u^2-c^2) \frac{\partial^2}{\partial x^2} + \omega_{pe}^2) A_{o,1} = - \omega_{pe}^2 {}^{n_e}/_{n_o} A_{1,o}$$

$$(u^2-c_s^2)\frac{\partial^2 n_e}{\partial x^2} + u \gamma_D \frac{\partial n_e}{\partial x} + \omega_{pe}^2 (n_e - n_i) = \frac{e^2 n_o}{m_e M_i c^2} \frac{\partial^2}{\partial x^2} (A_o A_1)$$

$$\ddot{y}_2 \frac{\partial^2 n_i}{\partial x^2} + \omega_{pi}^2 (n_i - n_e) = 0$$

where $A_{o,1}$ is the amplitude of the pump (o) or reflected (1) waves and γ_D is a phenomenological damping coefficient (whose values and significance we shall discuss later). There is no coupling term in the ion fluctuation equation because it is assumed that the ions, due to their heavy mass, react only very weakly to the non-linear beat force, $\underline{v} \times \underline{B}$, of the two electromagnetic waves. We now carry out a standard analysis of small amplitude variations over a wavelength on the fluctuations, i.e. we write

$$A_i = \tilde{A}_i \exp (i \int^x k_i(x')dx') + c.c.$$

$$n_j = \tilde{n}_j \exp (i \int^x k_j(x')dx') + c.c.$$

where c.c. represents the complex conjugate. Substituting these into equations (III-3), neglecting second derivatives of the small amplitudes A_i, n_j and recalling that wavenumber matching occurs at all points in the plasma (i.e. $k_o(x) = k_1(x) + k_2(x)$), we can take out the rapid exponential variation. Only terms in which the mismatch, $K = k_o - k_1 - k_2$, is zero

will give a contribution to the coupled terms and so, we obtain

$$\alpha_{o,1} \frac{\partial k_{o,1}}{\partial x} + 2k_{o,1} \frac{\partial \alpha_{o,1}}{\partial x} = -\frac{\omega_{pe}^2}{c^2} \frac{\tilde{n}_e}{n_o} \alpha_{1,o} \quad \text{.... (III-4)}$$

$$k_2 u \gamma_D \frac{\tilde{n}_e}{n_o} + 2k_2(u^2 - c_s^2) \frac{\partial}{\partial x} \frac{\tilde{n}_e}{n_o} = (k_o - k_1)^2 \alpha_o \alpha_1 \quad \text{.... (III-5)}$$

where $\alpha_{o,1} = e \tilde{A}_{o,1} / (m_e M_i c^4)^{\frac{1}{2}}$ and we have neglected u with respect to c (a valid assumption since u is expected to be around the ion sound speed). Recalling that $u \tilde{\sim} c_s$, we see that the group velocity of the ion sound waves is zero and equation (III-5) may be written, dropping the tildes,

$$n_e/n_o = \frac{2k_o c^2}{u\gamma_D} \alpha_o \alpha_1 \quad \text{.... (III-6)}$$

These non-propagating ion-sound waves are assumed to be driven (by the beat disturbance at $(\omega_o - \omega_1, k_o + k_1)$) up to a level at which the input driver energy is balanced by the energy lost through the damping of the ion sound waves. This 'saturation' occurs in a time, τ, short compared with the duration of the laser pulse, t_p. After this time, the density fluctuations, and hence the other two amplitudes, are stationary, the system then satisfying equations (III-4) and (III-6).

It is of interest to estimate this growth time. We expect the sound waves to be driven, in time, according to

$$\frac{\partial n_e}{\partial t} + \nu_{k_2} n_e = n_o A$$

where ν_{k_2} is the kinetic damping rate of ion accoustic waves at wavenumber k_2, as calculated by Fried and Gould (106) (a phenomenological damping rate is not used here) and $A \propto \alpha_o \alpha_1$. We may take A to be constant, provided $\tau << T$, the characteristic time for variations in A. This restriction is none other than $\tau << t_p$, which is just that required above. The equation has solution

$$n_e/n_o = \frac{A}{\nu_{k_2}} \quad (1 - \exp(-\nu_{k_2} t)$$

i.e. n_e/n_o is within 6% of saturation in 3 e-folds. Thus, for $\nu_{k_2}^{-1} = \nu_{2k_o}^{-1} = 0.127$ ns we have near saturation in under 0.5 ns. Whilst this growth time is smaller than those usually quoted for Brillouin scattering, it is still small compared with typical times for pump variation, at least for fusion applications. The reason for this discrepancy is that, here, we consider the driving up of ion sound waves by already existing pump and reflected waves, rather than the simultaneous growth of ion sound and reflected waves. We also note the temporal limitation of Brillouin scattering as proposed by Kruer et al (71), the reflection persisting strongly over a time $t_r \sim L/(\mu V_o)$ where $\mu^2 = m_e/M_i$. In our problem at a power density of CO_2 - laser light of 10^{14} W cm^{-2}, $t_r \sim 0.3$ ns. This would seem to place a limitation on this theory until we recall that our reflected light is merely the reflected pump wave and not an independently generated reflected wave as required by their theory. In other words, since theirs is a convective saturation and we have essentially neglected convective loss by our coordinate transformation, we shall assume that this mechanism does not constitute a serious limitation to the succeeding calculations.

Substituting (III-6) into (III-4) gives the coupled differential equations for α_o and α_1 ,

$$2k_o^{\frac{1}{2}} \frac{d}{dx} (k_o^{\frac{1}{2}}\alpha_o) = -\frac{\omega_{pe}^2}{c^2} \frac{2k_o c^2}{u\gamma_D} \alpha_o \alpha_1^2 \quad \text{.... (III-7)}$$

$$2k_1^{\frac{1}{2}} \frac{d}{dx} (k_1^{\frac{1}{2}}\alpha_1) = -\frac{\omega_{pe}^2}{c^2} \frac{2k_o c^2}{u\gamma_D} \alpha_o^2 \alpha_1$$

which have the 'constant of motion' ,

$$(k_o^{\frac{1}{2}} \alpha_o)^2 - (k_1^{\frac{1}{2}}\alpha_1^2)^2 = K_o^2 c_1^2 \quad \text{.... (III-8)}$$

where $K_o = k_o(0) = |k_1(0)| = \omega_{o/c}$. This result in (III-7) gives the solution for α_o (or α_1) to be

$$(k_o^{\frac{1}{2}} \alpha_o)^2 = k_o^2 c_1^2 \left[1 - \frac{\alpha_o^2(o) - c_1^2}{\alpha_o^2(o)} \exp\left\{-2c_1^2 \int_o^x \frac{\omega_{pe}^2}{k_o u\gamma_D} dx'\right\}\right]^{-1}$$

$$= k_o^2 c_1^2 \left[1 - \frac{\alpha_o^2(o) - c_1^2}{\alpha_o^2(o)} \exp\left\{-\frac{2c_1^2 \omega_o^2 L}{K_o u\gamma_D} \left[2\frac{x}{L}\left(1-\frac{x}{L}\right)^{\frac{1}{2}} + \frac{4}{3}\left(1-\frac{x}{L}\right)^{\frac{3}{2}} - \frac{4}{3}\right]\right\}\right]$$

.... (III-9)

in the density profile $n(x) = n_c\, x/_L$

These solutions, equations (III-8) and (III-9), are finite for $0 \le x \le L$. The standard WKB amplification, as the pump wave nears the critical surface will be exhibited by $\alpha_o\left[\propto \frac{1}{k_o^{\frac{1}{2}}} \propto \frac{1}{(1-x/L)^{\frac{1}{2}}}\right]$. However, by dealing with the amplitudes in the form $(k^{\frac{1}{2}}\alpha)$, we exclude this effect and leave monotonic functions. These functions represent decaying amplitudes with increasing distance into the plasma. Bearing in mind that the group velocities of the

two waves have opposite sign, the solutions show a pump wave moving into the plasma losing energy and, simultaneously, a reflected wave moving out from the critical surface gaining energy. We note, in passing, that this effect depends on the fact that u>0 implies that the pump wave, in the plasma rest frame, has the highest frequency and so drives the other modes.

Let us now examine the properties of these solutions. We consider 10.6 μm CO_2 -laser light as the pump wave [bearing in mind that similar results are obtained for a 1.06 μm Nd-glass laser by increasing the power by a factor 10] and take the following parameter values :-

(i) $u = c_s = 10^8$ cm/s (expected in a typical fusion plasma with $T_e = 10^{8}$°K)

(ii) $L = 300\ K_o^{-1}$ (Brueckner and Jorna (40) mention that the plasma corona surrounding the pellet is of approximately the same dimensions as the initial pellet diameter. This value corresponds to a depth (and diameter) of 0.5 mm)

(iii) $\gamma_D/\omega_o = 0.4075$ (this phenomenological damping coefficient is designed to reproduce, in our fluid model, the kinetic damping results of Fried and Gould (106), ω_{k2}, - a more complete derivation follows later, but we note $\gamma_D = 2^{M_i}/_{M_e}\ \omega_{k_2}$

Incorporating the density profile already mentioned, these solutions are shown in figure 10 The pump mode has a depleted energy at the critical surface whilst the backscattered mode has an enhanced energy as it propagates out of the system at x = 0. We note the relatively large value of mode (1) at x = L which, as has been explained above arises from the partial reflection

of the pump wave. The level of reflection is essentially a parameter of the problem and is taken to be a fixed proportion of the pump wave

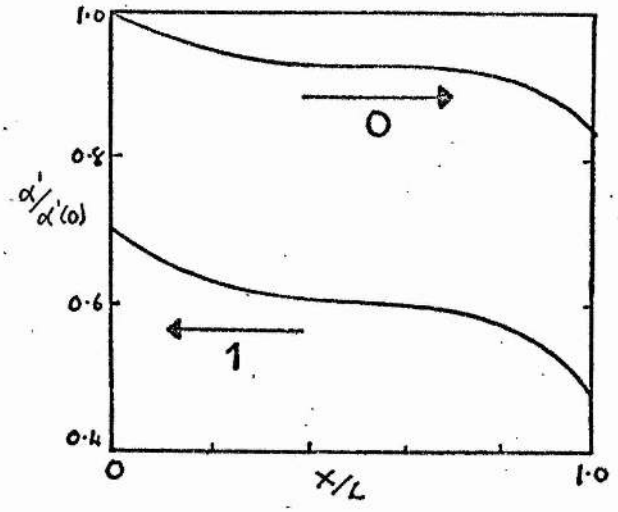

Figure 10 Wave amplitude as a function of distance to the critical surface 20% reflection of pump at x=L. Input power density $= 10^{15}$ W cm^{-2} $\alpha' = k^{\frac{1}{2}}\alpha$

amplitude. The resonant interaction occurs between the pump wave, the reflected wave (which, by the time it leaves the plasma, will normally be measured as the backscattered wave) and stationary ion sound fluctuations and will occur, with near maximum efficiency, at all points on the plasma, thus increasing the level of the reflected (or backscatter) wave. In other words, a strong enhancement of backscatter out of the plasma is obtained by this interaction. We note that, if the plasma were at rest, the pump and backscattered waves (the two electromagnetic modes interacting in Brillouin Scattering) would not have the same frequency and this mechanism would not be feasible - the level of backscatter at the critical surface then being the thermal level of the wave (ω_1, k_1).

We now define the reflection coefficient at x = 0 i.e. that seen by an observer outside the plasma, to be

$$R_o = \left(\frac{(k_1^{\frac{1}{2}}\alpha_1)^2}{(k_o^{\frac{1}{2}}\alpha_o)^2} \right)_{x=0}$$

and that at x = L i.e. the partial reflection of the pump wave at the critical surface, to be

$$R_c = \left(\frac{(k_1^{\frac{1}{2}}\alpha_1)^2}{(k_o^{\frac{1}{2}}\alpha_o)^2} \right)_{x=L}$$

From (III-9) they are related by

$$R_o = R_c \exp\left(2c_1^2 \int_o^L \frac{\omega_{pe}^2}{k_o n \gamma_D}\, dx'\right) = R_c \exp\left(\frac{8}{3} \frac{(1-R_o)A_o^2 L\omega_o^2}{K_o u\, \gamma_D}\right)$$

where $A_o = A_o(o)$. In figure 11, we plot the extent of backscatter as a function of incident power, for partial reflections of 10% and 20% at the critical surface. For low powers, the backscatter is due, almost entirely, to this partial reflection at x = L. However, around 10^{14} W cm^{-2}, there is an increase in backscatter as the effect described above begins to manifest itself. The range of pump powers over which it becomes dominant is relatively small. Thus, in the range 10^{15} - 10^{16} W cm^{-2}, the effect is marked, increasing rapidly,

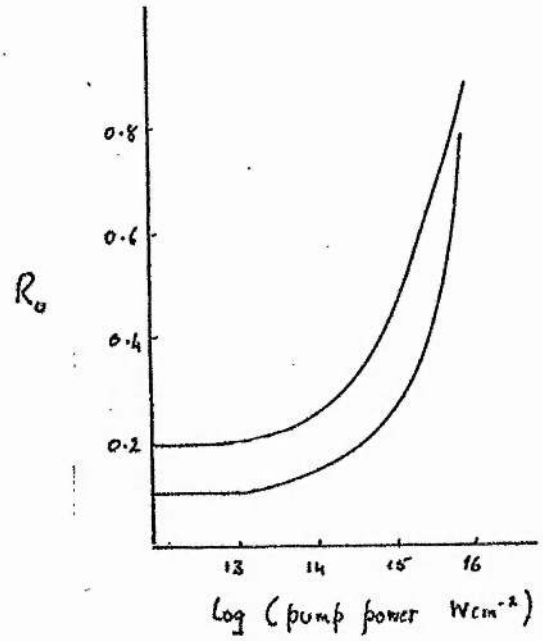

Figure 10 Enhancement of backscatter

and gives cause for concern as these are just the sort of pump powers which are expected in laser fusion applications. Correspondingly, with this large increase in backscatter, there is a large depletion in the pump energy actually reaching the critical surface and this is shown in figure 12.

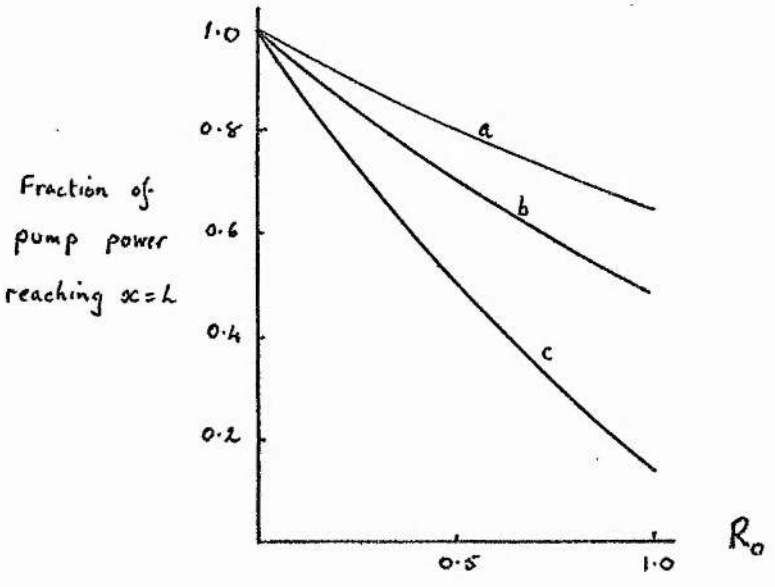

Figure 12 Power reaching the critical surface as a pencentage of incident power for input powers (W cm^{-2}) a, 5 x 10^{14} - b, 10^{15}; c 10^{16})

In the worst case, a staggering 80% of the input power never reaches the critical surface. However, other factors are likely to reduce this. From (III-10) it is clear that the effect is strongly dependent on L, the slab width, and this dependence is shown in figure 13.

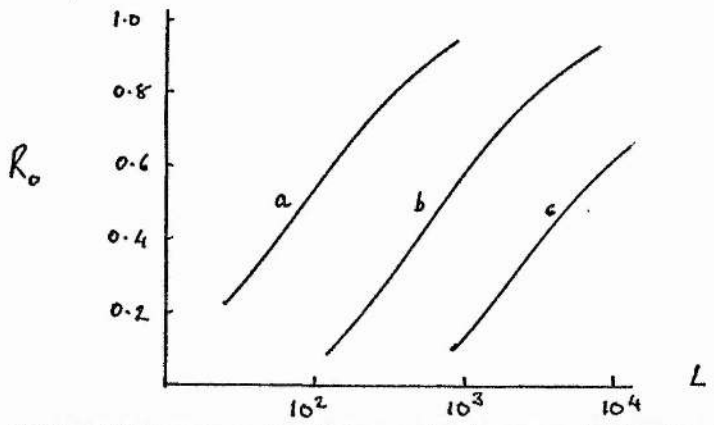

Figure 13 Reflection as a function of plasma width for $R_c = 0.1$ and input power densities (W cm^{-2}): a, 10^{16}; b, 10^{15}, c, 5×10^{14}

At this point, in part because decreased damping will also reduce the reflection, a few words need to be said about the choice of γ_D and its relation to ν_{k_2}. As we mentioned above, γ_D models, in the fluid approximation, the kinetic damping rate, ν_{k_2}, of ion acoustic modes, at least in the linear approximation. Let us consider their relationship. Fourier-Laplace transform the electrostatic equations in (III-3) and eliminate n_i to give

$$\varepsilon(\omega,k)\ n_e = 0$$

where

$$\varepsilon(\omega,k) = -\omega^2 + i\omega\,\gamma_D + k^2 v_e^2 + \omega_{pe}^2\,\frac{\omega_{pe}^2 - \omega_{pi}^2}{\omega_{pi}^2 - \omega^2} = 0 \qquad \ldots\ (III\text{-}11)$$

which has the zero-order ($\gamma_D = 0$) solution for $\omega << \omega_{pi} << \omega_{pe}$,

$$\omega_r = k c_s \quad , \quad c_s = \frac{\sqrt{kT_e}}{M_i}$$

Writing $\omega = \omega_r + i\nu$, assuming $\nu \ll \omega_r \ll \omega_{pe}$, we have, rearranging (III-11)

$$[\omega_r^2 + 2.\nu\omega_r][\omega_{pe}^2 + k^2 v_e^2] - \omega_{pi}^2 k^2 v_e^2 + i\gamma\nu(\omega_{pi}^2 - \omega^2) = 0$$

i.e. $$\nu = \frac{\gamma_D}{2} [\omega_{pi}^2 - \omega^2] \Big/ [\omega_{pe}^2 + k^2 v_e^2]$$

$$\approx \frac{\gamma_D}{2} [\frac{\omega_{pi}^2}{\omega_{pe}^2} - \frac{\omega_r^2}{\omega_{pe}^2}]$$

$$\approx \frac{\gamma_D}{2} \frac{m_e}{M_i}$$

or $$\gamma_D = 2 \frac{M_i}{m_e} \nu_{k_2}$$

We have also calculated ν_{k_2} for a DT plasma with $T_e = 10 T_i = 10$keV from the formula (106)

$$k^2 + \sum_j K_j^2 [1 + \zeta_j Z(\zeta_j)] = 0$$

where $Z(\zeta_j)$ is the plasma dispersion (or Fried-Conte) function

$Z(\zeta_j) = \int dz \frac{e^{-z^2}}{z - \zeta_j}$, ζ_j a phase speed, $= \frac{(\omega_o - \omega_1) + i\gamma}{\sqrt{2}\, k v_j}$, v_j the thermal velocity and $K_j = \frac{1}{\lambda_{D_j}}$ of the j^{th} species. This gave an average linear damping rate $\omega_{k2}/\omega_2 \sim 0.006$ which gives $\gamma_D/\omega_o = 0.4075$. To examine the effect of non-linear damping we plot, in figure 14, R_o as a function of L treating ν_{k2}/ω_2 as a parameter. As expected, anomalous damping is seen to decrease the backscatter.

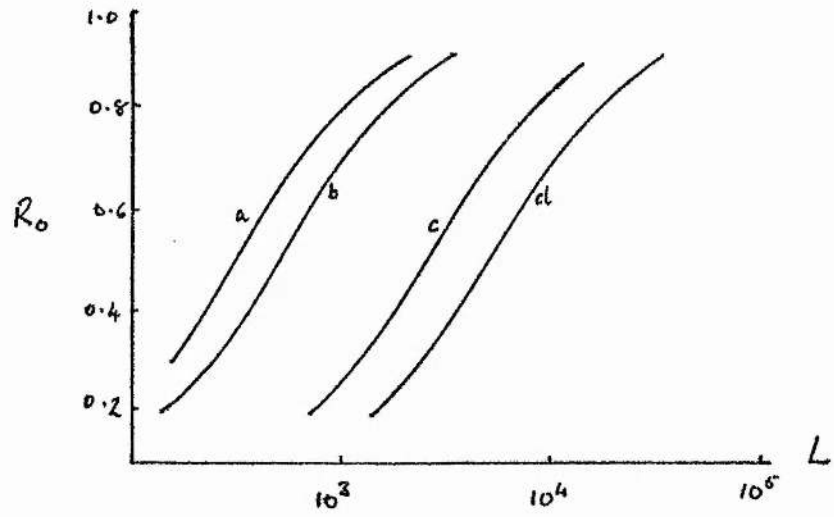

Figure 14 Reflection as a function of slab width with parameters $R_c = 0.1$, incident power density 10^{15} W cm^{-2} and non-linear damping rates a, 0.006; b, 0.01; c, 0.05; d, 0.1

The results quoted so far have been dependent on $u=c_s$. In practice, one would expect this not to be exactly true and that there might be some velocity discord. In such a case, we replace $\frac{1}{u\gamma_D}$ in (III-6) by the broader resonance function $\frac{1}{|\varepsilon|}$ where $|\varepsilon| = [k^2(c_s^2-u^2)^2 + \gamma_D^2 u^2]^{\frac{1}{2}}$.

Because of the definition of γ_D, we note, in most cases, that $u\gamma_D >> k \times (c_s^2 - u^2)$ so that $\frac{1}{|\varepsilon|} \sim \frac{1}{u\gamma_D}$ and the effect of an off-peak expansion velocity is expected to be small. In fact, to reduce the backscatter, in the case of linear damping, by a factor 10, we require $[(c_s^2-u^2)/c_s^2]^{\frac{1}{2}} \sim 10$. At higher damping rates, the effect will be smaller still. Using this argument, we can see that no strong limitation to the theory is provided by different wavenumber ion sound waves. More precisely, the ion sound frequency, in plasma rest frame, is given by

$$\omega_2 = \frac{kc_s}{(1 + k^2\lambda_D{}^2)^{\frac{1}{2}}}$$

Thus, for short wavelength waves; there is no serious shortcoming as their effect may be accomodated in a modified sound speed $c_s' = c_{s/(1+k^2\lambda_D{}^2)^{\frac{1}{2}}}$ For instance, only for $k\lambda_D > 10$ do we obtain a reduction in backscatter by factor 10, by which stage, other effects could well have altered the physics.

We can thus see that our mechanism for enhanced backscatter, from an expanding plasma, is relatively insensitive to several 'off-resonance' situations. Since this mechanism involves the initial generation of backscatter by reflection of the pump wave at the critical surface and its subsequent enhancement by interaction with incoming pump and stationary ion sound waves, the reduction in energy available at the critical surface could be severe and provide a possible barrier to laser fusion applications.

CHAPTER IV

THE INDUCED SCATTERING PROCESSES

We shall examine, in detail, the problem of induced scattering off unshielded particles in the plasma. Till now, we have considered the problem of scattering of incident electromagnetic radiation by collective oscillations in the plasma, these oscillations being normal modes of the plasma. However, the resonance conditions (III-1) can be satisfied by a (ω_2,k_2) which does not correspond to a normal mode, when $\omega_2 = k_2 v_e$ or $\omega_2 = k_2 v_i$. This means that the incident wave is scattered by a quasi-wave resonant with the thermal particles. Alternatively, we can view the situation as the decay of a pump wave into a scattered wave, the excess energy and momentum being carried off by particles resonant with the beat disturbance of these two waves. It is analogous to the non-linear Landau damping mentioned earlier in connection with the work of Dubois and Goldman (19) where incident radiation decays into a plasma wave, the excess energy and momentum being carried by particles. Because (ω_2,k_2) is not a normal mode of the system, we would not expect scattering off such a mode to occur preferentially. Hence, this type of scattering would be most easily realised when the normal mode is heavily damped i.e. for electron plasma waves, $k\lambda_D >> 1$. By virtue of its analogy with other branches of physics, this process is often referred to as Stimulated Compton Scattering. Induced scattering off ions will occur for $T_e \lesssim T_i$.

The early work on this type is predominantly experimental, concerned mainly with the problem of heating a plasma. As we mentioned earlier this did not give rise to heating sufficient for fusion purposes, but nevertheless, useful results were obtained. Not surprisingly, the heating rate was

found to be proportional to the beam intensity (107, 108). Heating explicitly through Compton scattering was studied by Martineau and Pepin (109). The effect of the instability on the pump has been investigated for Nd-glass lasers e.g. forward scattering (or transmission) (110, 111) with the results that short wavelength radiation was absorbed while longer wavelengths were intensified, there was no strong angle dependence and the transmitted intensity had a large red shift. Similar experiments have been performed by Burnett, Kerr and Offenberger (112) using CO_2 - laser light. Here, a smaller shift in wavelength was noted and it was estimated that only $\sim\frac{1}{40}$ of the electrons participated in the scattering. Electron temperatures were 10 - 100 eV and power densities 5×10^{10} - 10^{12} W cm^{-2} were used. The theory behind these experiments has been set out using the methods of Tsytsovich (23) - considering photon scattering off electrons. Babuel - Peyrissac (113) explain the results of Decroisette et al (111) whilst Offenberger and Burnett (114) explain their own results.

Of special interest to laser fusion is the possibility of plasma heating by two opposing laser beams of different frequencies (98, 115). Kauffman and Cohen, and Kazabov et al (116) performed just this experiment, but with equal beam frequencies, finding substantial heating but also the amplification of the weaker beam through this instability. The consequences, as far as laser fusion are concerned, were explained by Kraysuk et al (117) who analysed the coupling to generate an equation set similar to (III-7) for the two electromagnetic waves. For the same parameter values as we used but with an Nd-glass laser, they found high levels of reflectance i.e. at 10^{16} W cm^{-2} (10^{15} W cm^{-2} for CO_2-laser), $R_c = 0.1$, $L = 300$, a reflectance of 30% was obtained. This is a substantial effect. Saturation effects were not included. Vinogradov et al (118) extended the calculations

in this direction by calculating the gain and using this to find the saturated reflected flux (at which time exponential has given way to linear growth), with the result that, at a power flux of 10^{16} W cm^{-2}, a saturated reflectance of $<10^{-4}$ is expected (a level certainly tolerable in laser fusion schemes). This work, however, is based on the example of scattering from a sinusoidal lattice and does not include any reflection from the critical surface, thus, not invalidating (117). A similar analysis by Albritton (119), for a Nd-glass laser, shows fairly substantial reflectance, even with the low gain of this scattering process, from a homogeneous plasma. This result echoes both those of Kraysuk et al and of Vinogradov et al, for the saturated reflectivity. It would seem that his analysis, based on the kinetic theory approach to an electron-photon gas derived by Dreicer (120), bears out both sets of previous results.

The effect has also been examined in the more easily realisable mode coupling approach (44, 46, 121, 122). Particular attention has been paid to the type of scattering involved. In the homogeneous case, the condition for substantial gain in the backscattered direction is (127) $\gamma L/c > 1$ whilst for sidescatter it is only $2 \frac{\omega_o}{\omega_p} \frac{\gamma L}{c} > 1$, where γ is the Compton scatter growth rate. Simulations were performed for this latter case with scattering of order 10% at saturation. The effect on the background electron distribution function, f_{e_o}, shows considerable broadening as the main body of electrons are heated. It is expected that sidescatter should affect, predominantly, this part of f_{e_o} as scattering is occuring partly into regions of equal density. For backscatter, the waves propagate outwards, generating a tail of fast electrons. Lin and Dawson (44) also carried out simulations for this process and compared it to the modified Raman instability (essentially, quasi-mode scattering where the pump power is strong enough to

overcome the frequency mismatch). They discovered substantial pump depletion and modification of the background electron distribution function with quasi-linear flattening due to the formation of a high energy tail, in the region $0.8 < v/v_p < 4.4$ whilst for the modified Raman case tail formation occured for $v/v_p \sim 6$.

We intend to discuss these results further for the inhomogeneous case and show that whilst reflection is still relatively small, there is considerable modification to f_{e_o} in the range of pump powers of interest for laser fusion. Other effects are considered such as finite bandwidth pump waves and distortion of the pump partial continuity. The corresponding induced scattering off ions is also considered.

We shall follow, in our derivation, the mode coupling approach adopted by Lin and Dawson (44). One piece of their analysis deserves mention. They derive the equation for the growth rate, γ, of the scattered mode $(a+i\gamma, k_1)$,

$$\gamma = -\frac{k_2^2 v_o^2}{8a} \operatorname{Im} \frac{X_e(1 + X_i)}{1 + X_e + X_i} \qquad \ldots\ (IV\text{-}1)$$

where $v_o = \frac{eE_o}{m\omega_o}$, the oscillatory velocity of an electron in the incident pump field. They then solve, for $X_i = 0$,

$$\gamma \operatorname{Im}\left(1 + \frac{1}{X_e}\right) = -\frac{k_2^2 v_o^2}{8a} \qquad \ldots.(IV\text{-}2)$$

where in both cases, $X_\alpha = X_\alpha(\omega_2, k_2)$, the particle susceptibility and the electrostatic mode is (ω_2, k_2), to obtain values of γ. We derived (IV-1) in a slightly different way and solved it to generate their results which could not be obtained from (IV-2). This does not, however, constitute any overall fault in their work.

We shall consider the action of an incident electromagnetic wave on a finite, inhomogeneous slab of plasma, with this mode being given by -

$$E_o = E_o \cos(\omega_o t - k_o x)\, \hat{\underline{y}} = \tfrac{1}{2} E_o \left[e^{i(\omega_o t - k_o x)} + \text{c.c.}\right] \hat{\underline{y}}$$

(ω_o, k_o) is a normal mode of the system (i.e. $\omega_o^2 = \omega_{pe}^2 + k^2c^2$). We shall allow velocity components in three directions but variation in only one spatial component, x. Let there also be present a backscattered wave

$$E_1 = E_1\, e^{i(\omega_1 t + k_1 x)}\, \hat{\underline{y}}$$

and consider the longitudinal plasma oscillation driven by the $\underline{v} \times \underline{B}$ force arising from these two modes. The component of interest, from our mode coupling approach, is the one

$$\underline{v} \times \underline{B} = \frac{eE_o E_1 k_2}{2m\,\omega_o a}\, e^{i(\omega_2 t - k_2 x)}\, \hat{\underline{x}} \qquad \ldots\ (\text{IV-3})$$

where $a^2 = \omega_{pe}^2 + k_1^2 c^2$ and equations (III-1) are satisfied by the wave triplet (ω_o, k_o), (ω_1, k_1) and (ω_2, k_2). Plasma oscillations are thus driven. If (ω_2, k_2) is a normal mode of the system (i.e. $\varepsilon(\omega_2, k_2) = 0$) then a collective plasma oscillation is excited (e.g. the Raman backscatter when (ω_2, k_2) corresponds to an electron plasma wave). Suppose this not to be the case, $\varepsilon(\omega_2, k_2) \neq 0$, but that $\omega_2 = k_2 v_e$ (v_e being the electron thermal velocity) then the non-linear beat force interacts with the particles resonant with the beat wave (IV-3). To realise this mode, we require the electron plasma wave to be damped (i.e. $k\lambda_D \gg 1$ or $\omega_o \gg \omega_{pe}$). In other words, the greatest interaction will occur for $v/v_e \sim 1$, the interacting particles then lying on the steepest slope of the distribution function. This process is known as stimulated Compton scattering.

One may still use our fluid approach with the particle perturbation,

$$\delta N_e = \delta n_e\, e^{i\omega_2 t - ik_2 x}\, \hat{\underline{x}}$$

From Maxwell's equations,

$$\nabla \times \underline{B} = \frac{1}{c} \frac{\partial \underline{E}}{\partial t} + \frac{4\pi}{c} \underline{j} \qquad \text{and} \qquad \nabla \times \underline{E} = - \frac{1}{c} \frac{\partial \underline{B}}{\partial t}$$

we get, in 1-D,

$$\frac{1}{c^2} \frac{\partial^2 E_1}{\partial t^2} - \frac{\partial^2 E_1}{\partial x^2} = - \frac{4\pi}{c^2} \frac{\partial j}{\partial t} = i \frac{4\pi}{c^2} \omega_1 j_1 \qquad \ldots \text{(IV-4)}$$

where j_1 is the current component at frequency ω_1. It arises from the backscattered field E_1 and from the coupling of the pump and density perturbation at frequency ω_1, and taking the form

$$j_1 = e\, n_o v_1 + e\, \delta n_e\, v_o$$

Now, $\frac{dv_o}{dt} = \frac{e}{m} E_o$ and so the component of v_o going as $\exp(i\omega_o t - ik_o x)$ is

$$v_o = - \tfrac{1}{2} \frac{ie}{m\omega_o} E_o\, e^{i\omega_o t - ik_o x}$$

Similarly, $v_1 = \frac{ie}{m\omega_1} E_1\, e^{i\omega_1 t + ik_1 x}$

and (IV-4) becomes

$$\frac{\partial^2 E_1}{\partial t^2} - c^2 \frac{\partial^2 E_1}{\partial x^2} + \omega_{pe}^2 E_1 = - \frac{4\pi e^2 \omega_2}{2m\omega_o} \delta n_e^*\, E_o \qquad \ldots \text{(IV-5)}$$

Finally, writing $E_1 = E_1(x,t)\, e^{+i(\omega_1 t + \int^x k_1 dx')}$ and taking out the exponential variation, we have

$$- 2i\omega_1 \frac{\partial E_1}{\partial t} - 2ikc^2 \frac{\partial E_1}{\partial x} - i E_1 c^2 \frac{\partial k_1}{\partial x} = - \frac{4\pi e^2}{2m\omega_o} E_o\, \delta n_e^*$$

$$\text{i.e.} \quad \omega_1 \frac{\partial E_1}{\partial t} + k_1^{\frac{1}{2}} c^2 \frac{\partial}{\partial x} (k_1^{\frac{1}{2}} E_1) = - i \frac{4\pi e^2 \omega_1}{4m\omega_o} E_o\, \delta n_e^*$$

We need another relation between δn_e and E_1. This we may derive, in lowest order, from the Vlasov equation, including the non-linear driving term. The magnitude of the beat force at (ω_2, k_2) is, as above,

$$- \frac{ie\, E_o E_1}{m\omega_o\, a}\, k_2$$

The Vlasov equation is then

$$\frac{\partial f_e}{\partial t} + v \frac{f_e}{\partial x} + \frac{e}{m}(E_s + F_{NL}) \frac{\partial f_{e_o}}{\partial v_x} = 0 \qquad \ldots\ (IV\text{-}6)$$

where E_s satisfies Poisson's equation, $-ik_2 E_s = 4\pi e(\delta n_i - \delta n_e)$ and $F_{NL} = - \frac{ieE_o E_1}{m\omega_o\, a} k_2$ is the non linear beat force. If we assume the perturbation, f_e, varies as $\exp(i\omega_2 t - ik_2 x)$ then (IV-5) gives

$$f_e = \frac{e(E_s + F_{NL})}{im(\omega_2 - k_2 v_x)} \frac{\partial f_{e_o}}{\partial v_x}$$

and so

$$\delta n_e = N_o \int f_e\, dv_x = \frac{(E_s + F_{NL})}{i4\pi e}\, k_2\, X_e \qquad \ldots\ (IV\text{-}7)$$

where $X_e = X_e(\omega_2, k_2) = \frac{\omega_{pe}^2}{k_2^2} \int dv_x \frac{k_2\, \partial f_{e_o}/\partial v_x}{(\omega_2 - k_2 v_x)}$ is the electron susceptibility.

The ion motion due to the beat force is assumed to be negligible, due to the heavy ion mass. The corresponding expression for the ion density perturbation is then

$$\delta n_i = - \frac{k_2 X_i E_s}{i4\pi e}$$

where X_i is the ion susceptibility. Substitution of these expressions into Poisson's equation yields the self-consistent space-charge field,

$$E_s = - \frac{F_{NL} X_e}{(1 + X_e + X_i)}$$

which, upon insertion into (IV-7) and using the expression for F, gives the electron density perturbation,

$$\delta_{n_e} = - \frac{k_2^2 E_o E_1}{8\pi m \omega_o a} \quad \frac{X_e(1 + X_i)}{1 + X_e + X_i}$$

Thus, we have, in (IV-5) and taking real parts,

$$a_1 \frac{\partial E_1}{\partial t} + k_1^{\frac{1}{2}} c^2 \frac{\partial}{\partial x} (k_1^{\frac{1}{2}} E_1) = - \frac{k_2^2 v_o^2}{8} \text{ Im } \frac{X_e(1 + X_i)}{1 + X_e + X_i} \quad E_1 \quad \ldots\ldots \text{(IV-8)}$$

This equation now determines the spatial and temporal evolution of the backscattered mode. We must determine whether the resulting instability results in absolute (i.e. simultaneous spatial and temporal gain at all resonance points) or merely convective (i.e. spatial gain limited by convection out of the appropriate resonance region) amplification. For two reasons one would expect this instability to be of the latter rather than the former type. Firstly, the plasma disturbance is <u>driven</u> by the electromagnetic modes. Since it is not a normal mode of the system, the resulting perturbation energy is easily diffused away onto other particles. Secondly, to generate absolute instability in a finite inhomogeneous slab, one requires reflection or some internal feedback mechanism of the electromagnetic modes (93, 94, 95) - a process which we find unlikely in the present situation.

However, let us treat (IV-8) in the usual way. Rewriting in terms of $\alpha_1 \equiv k_1^{\frac{1}{2}} E_1$,

$$\omega_1 \frac{\partial \alpha_1}{\partial t} + k_1 c^2 \frac{\partial \alpha_1}{\partial x} = - \frac{k_2^2 v_o^2}{8} \text{ Im } \frac{X_e(1 + X_i)}{1 + X_e + X_i} \quad \alpha_1$$

and Laplace transforming the equation by $\alpha_1(x,p) = \int dt\, e^{-pt}\, \alpha_1,(x,t)$, we can solve the resulting O.D.E. for

$$\alpha_1(x,p) = \alpha_1(0,p) \exp\left(px + \int^x \mu(x')\,dx'\right)$$

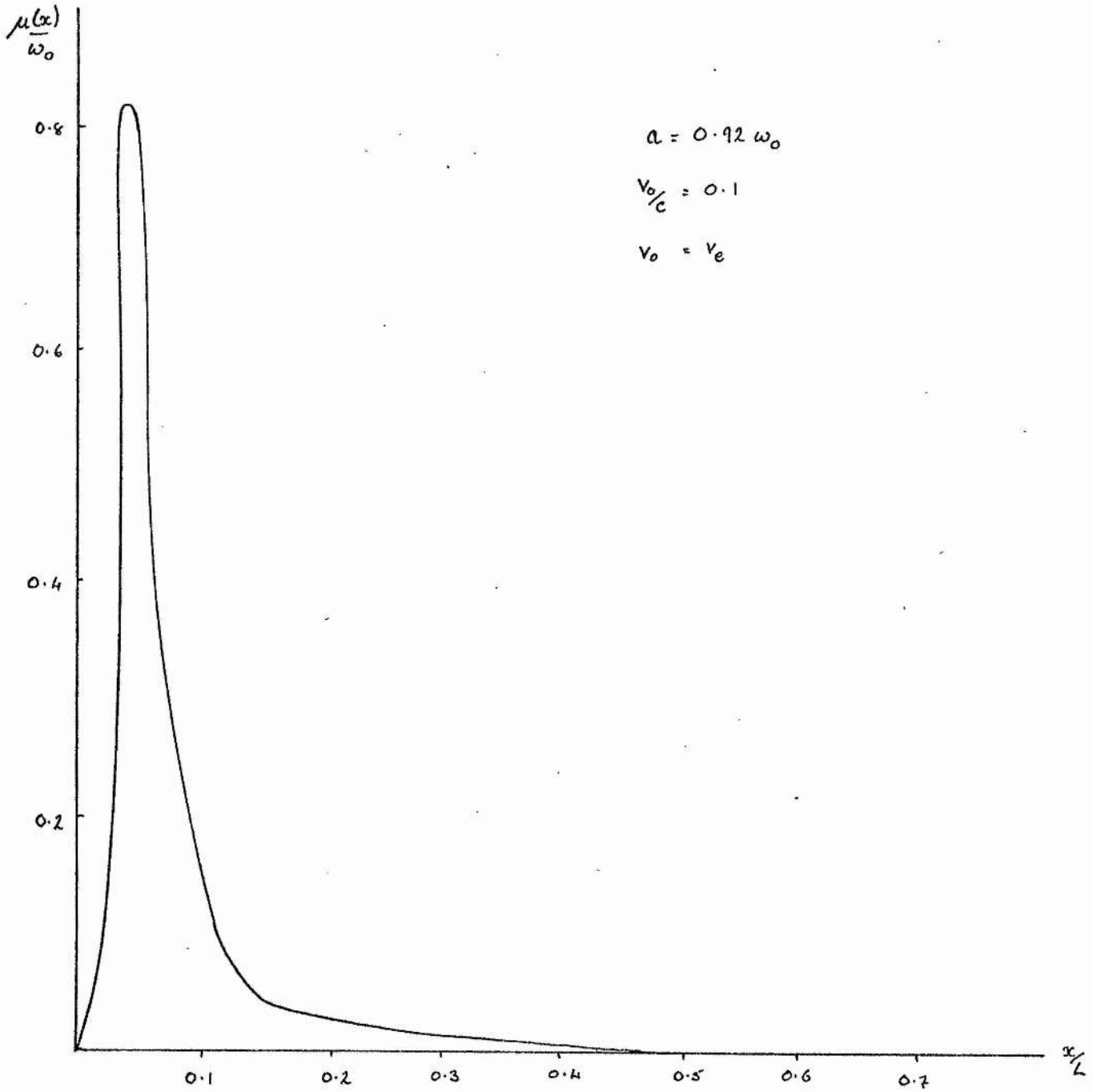

Figure 14 : Absolute or convective gain :- $\int_o^x \mu(x')dx' \to \infty$ required for former case

where $\mu(x') = -\frac{k_2^2 v_o^2}{8c^2}\ \mathrm{Im}\ \frac{X_e(1+X_i)}{1+X_e+X_i}$ and we have neglected temporal initial values. If absolute instability is to occur, we must ensure that $\alpha_1(x,p)$ is bounded for $|x| \to \infty$. For $x \to -\infty$, this condition is obviously satisfied but for $x \to +\infty$, we must require

$$\int dx' \frac{k_2^2 v_o^2}{8c^2} \frac{X_e\,(1+X_i)}{1+X_e+X_i} = \int dx' \frac{k_2^2(x')}{8} \frac{v_o^2}{c^2}\ \mathrm{Im}\ \frac{X_e}{1+X_e} \to \infty$$

where we set $X_i \overset{\sim}{\sim} 0$, the case when $\omega_2 \sim k_2 v_e$.

As can be seen from figure 14, this condition is obviously not satisfied in a finite plasma and so we conclude that absolute instability is not possible.

We need only now consider convective gain. Correspondingly, our equation is

$$\frac{d\alpha_1}{dx} = -\frac{k_2^2 v_o^2}{8k_1 c^2}\ \mathrm{Im}\ \left[\frac{X_e}{1+X_e}\right]\ \alpha_1$$

i.e. $$\alpha_1(x) = \alpha_1(0)\ \exp[\Gamma(x)] \qquad \ldots \text{(IV-9)}$$

where $$\Gamma(x) = \int dx' \frac{k_2^2 v_o^2}{8k_1 c^2}\ \mathrm{Im}\left[\frac{X_e}{1+X_e}\right], \quad X_e = X_e(a, k_1)$$

Let us now consider the properties of these solutions for the parameters:- 10.6 μm CO_2 -laser light, slab width 0.5 mm (or $L = 300\ K_o^{-1}$ as in Chapter III). A typical spatial gain is shown as a function of distance in figure 15.

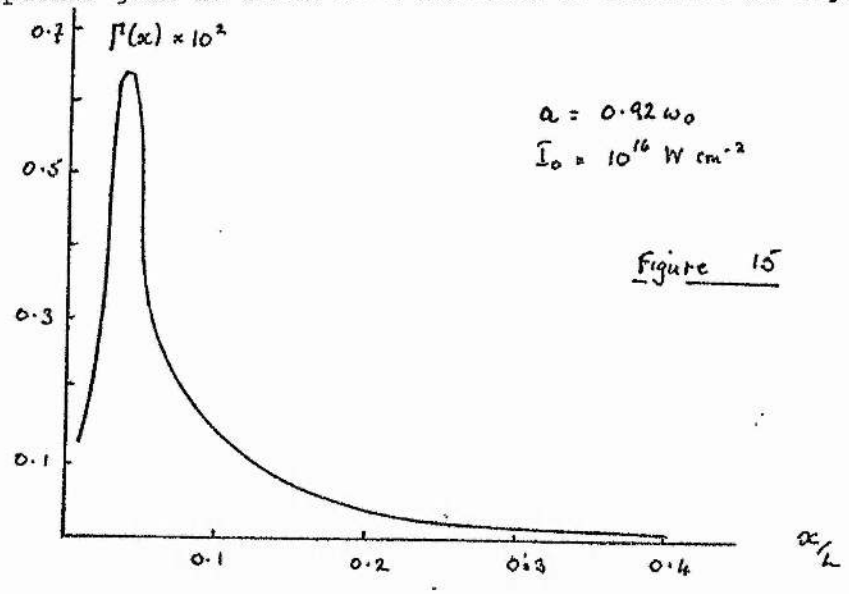

Figure 15

We note the very localised region of intense gain. This corresponds to the region where $k\lambda_D >> 1$ and $v_{ph} \equiv \omega_{2/k_2} \sim v_e$, the interacting particles then lying on the steepest slope of f_{e_o}; as x increases $k\lambda_D$ decreases and v_p moves off this steepest slope, the interaction then becoming weaker, as explained earlier. By the time, $x \sim L$ the interaction is negligible. Bearing in mind that while only convective gain occurs, we still have a frequency dependence on $a = \mathrm{Re}\ (\omega_1)$ through (IV-9) and this is shown in figure 16, approximating to the backscattered spectrum anticipated in an experiment. The fractional wavelength shift is

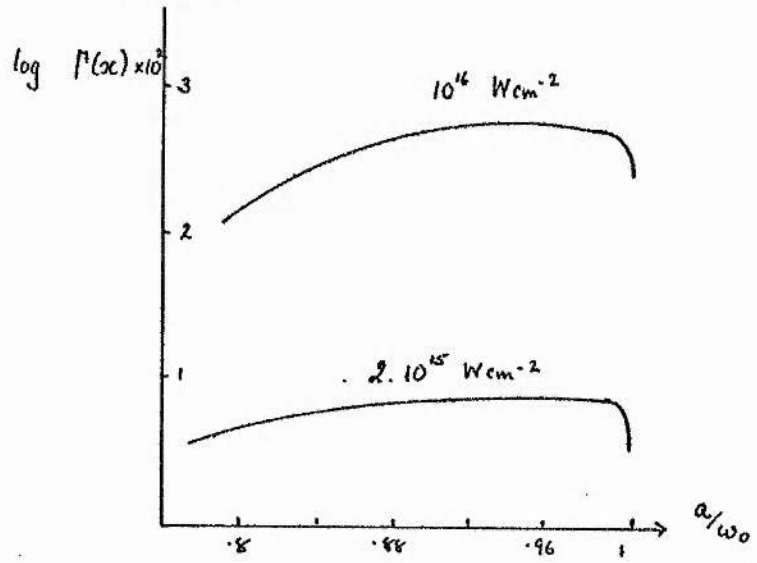

Figure 16 Frequency spread of spatial gain

$\sim 0.69 \times 10^{-5}$ which compares with that of Offenberger and Burnett (112) although we point out that the conditions are very different. Table I shows the gain expected as a function of input power, with $a = 0.96\ \omega_o$. The last column gives the amplification from a slab of width $L = 300\ K_o^{-1}$.

Table I

Power W cm^{-2}	gain factor,	Amplification over thermal level
10^{15}	0.4389×10^{-2}	3.732
5×10^{15}	0.16845×10^{-1}	0.157×10^{3}
10^{16}	0.2796×10^{-1}	0.439×10^{4}

Substantial gain occurs only for high pump powers, limiting this effect to the maximum pulse energy. In figure 17 we plot the effect of slab width on the gain. Obviously, the longer the slab the larger is the observed reflectance.

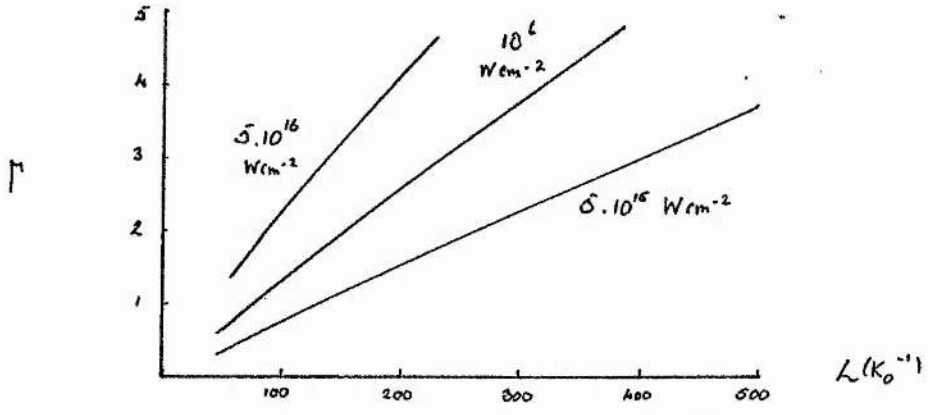

Figure 17 Gain against slab width

In as far as we concern ourselves with the effect on the pump of the gain in backscatter, we may derive equations similar to (III-7) for $k_j^{\frac{1}{2}} E_j = \alpha_j$, $j = 0,1$. In a completely analogous way, we find the solutions

$$\alpha_o^2(x) = c_1^2 \left[1 - \frac{\alpha_o^2(0) - c_1^2}{\alpha_o^2(0)} \exp\left(-c_1^2 \int^x dx' \, \Gamma(x')\right) \right]^{-1}$$

$$\alpha_1^2 = \alpha_o^2 - c_1^2$$

and these are plotted in figure 18 showing a minimal reduction in pump amplitude, consequently, a more reduced effect on the pump energy.

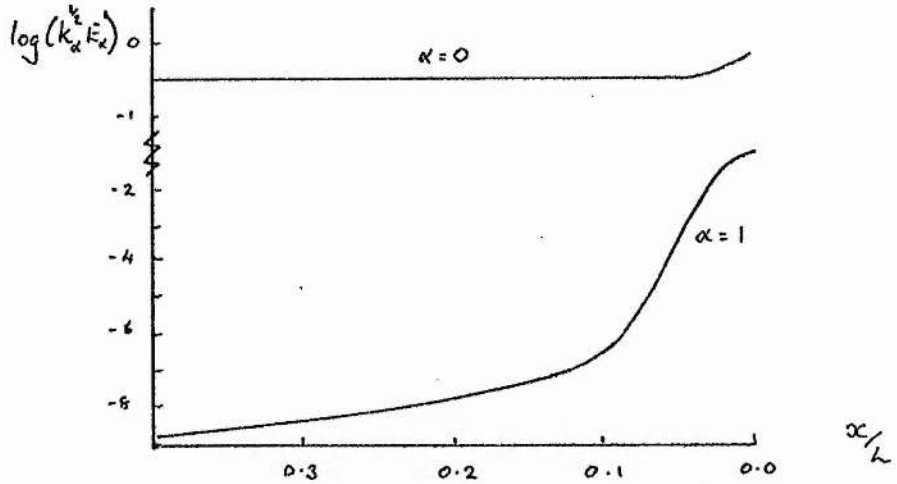

Figure 18 : Reflectance from slab

Even though there is such a small effect on the pump energy, the sizeable levels of the backscattered radiation imply that enhanced levels of electron density fluctuations will also result. We would expect, therefore, a perturbation to the background distribution function, f_{e_o}, through these energetic particles. Let us now examine the results of this process.

From (IV-9) the backscattered electric field is given by

$$E_{r/E_{r(o)}} = \frac{k_r^{\frac{1}{2}}(o)}{k_r^{\frac{1}{2}}(x)} \quad \exp \quad (\Gamma(x))$$

and the associated electron density fluctuation

$$\delta n_e = - \frac{k_2^2 \, v_o^2}{8\pi \, ea} \; E_r \; \mathrm{Im} \left[\frac{X_e}{1 + X_e}\right]$$

which governs the self-consistent space-charge field through Poisson's equation (with $n_i = o$)

$$\text{i.e.} \qquad E_s = \frac{4\pi e}{ik_2} \quad \delta n_e \qquad \ldots\ldots \text{(IV-10)}$$

In quasi-linear theory, the background electron distribution evolves according to

$$v \frac{\partial f_o}{\partial x} = \pi \left(\frac{e}{m}\right)^2 \frac{\partial}{\partial v} \sum_k \frac{|E_s|^2}{k} R\left(v - \frac{\omega}{k}\right) \frac{\partial f_o}{\partial v} \qquad \ldots\ldots \text{(IV-11)}$$

where we use the resonance function, $R(v - \frac{\omega}{k})$ of Dupree (123) and Cairns (102) to simulate the non-linear broadening of the quasi-linear resonance. This function is chosen to be zero outside the trapping width of the 'wave' (ω_2, k_2) given by

$$\Delta v = \left(\frac{2eE_s}{mk_2}\right)^{\frac{1}{2}}$$

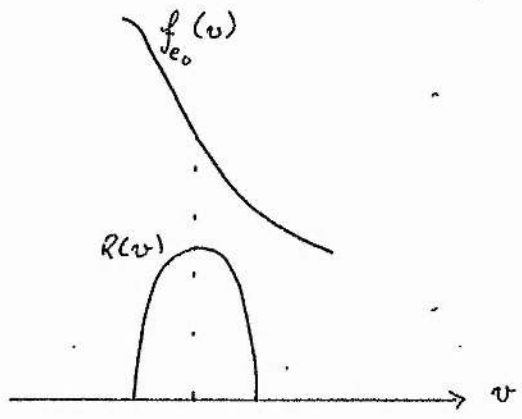

Figure 19

As shown in figure 19, this resonance function is zero for $|v-vp|<\Delta V$ and continuously varying between these limits. It is assumed to have the form (102),

$$R(v-\frac{\omega}{k}) = \frac{1}{2\,V}\left(1+\cos\left\{\frac{\pi\left(v-\frac{\omega}{k}\right)}{\Delta v}\right\}\right) \qquad , \left|v-\frac{\omega}{k}\right|<\Delta\ V$$

$$= 0 \qquad \left|v-\frac{\omega}{k}\right|\geq\Delta\ V$$

We solve (IV-10) and (IV-11) with this function and trapping width by a finite difference scheme (124). Rewriting (IV-10) as

$$\frac{v\,df}{\partial x} = \frac{\partial}{\partial v}\ D\ \frac{\partial f}{\partial v}$$

we approximate this as

$$v_j\ \frac{f_j^{n+1}-f_j^{n}}{\Delta x} = \frac{\theta[\,\delta(D\delta f)\,]_j^{n+1} + (1-\theta)[\delta(D\delta f)]_j^{n}}{(\Delta v)^2} \qquad \ldots\ (IV\text{-}12)$$

where $(\delta f)^n_j = f^n_{j+\frac{1}{2}} - f^n_{j-\frac{1}{2}}$, $[\delta(Du)]^n_j = D^n_{j+\frac{1}{2}}u^n_{j+\frac{1}{2}} - D^n_{j-\frac{1}{2}}\,u^n_{j-\frac{1}{2}}$,

$$f^n_j = f(v_j, L^n)\ ,\ v_j = v_o + j\Delta v\ (j=0,1,\ldots,J)\ ,\ x^n = x_o + n\Delta x\quad (n=0,1,\ldots,N)$$

and the system is always stable for $\frac{1}{2} \leq \theta \leq 1$.

This generates at each time-step, rearranging (IV-12),

$$-A_j f_{j+1} + B_j f_j - C_j f_{j-1} = D_j$$

where we have dropped the superscript n, $A_j = \theta \frac{\Delta x}{(\Delta v)^2} D_{j+\frac{1}{2}}$, $C_j = \theta \frac{\Delta x}{(\Delta v)^2} D_{j-\frac{1}{2}}$, $B_j = 1 + A_j + C_j$ and D_j depends on values of f at the previous time-step i.e. is known. We next write the solution as

$$f_j = E_j f_{j-1} + F_j \qquad \ldots. \text{ (IV-13)}$$

with boundary conditions $E_o = 0$ and $F_o = u_o$ where

$$E_j = \frac{A_j}{B_j - C_j E_{j-1}} \quad , \quad F_j = \frac{D_j + C_j F_{j-1}}{B_j - C_j E_{j-1}}$$

We calculate E_j and F_j for increasing $j (j=0,1,\ldots,J-1)$, under the condition that f_J be given initially. The values f_j are then computed for decreasing j from (IV-13). The advantage of choosing the resonance function $R(v - \frac{\omega}{k})$ in the above fashion is that $D_o = D_J = 0$, the boundary conditions on f_j are automatically set to zero and, hence, the calculation easily completed.

The results of these calculations are shown in figure 20. We have taken a small range of backscattered modes of frequencies $a/\omega_o \varepsilon [0.8, 0.98)$ to simulate the sum over k in (IV-11). As might be expected there is a substantial flattening of f_{e_o} in the region in velocity space where greatest interaction occurs.

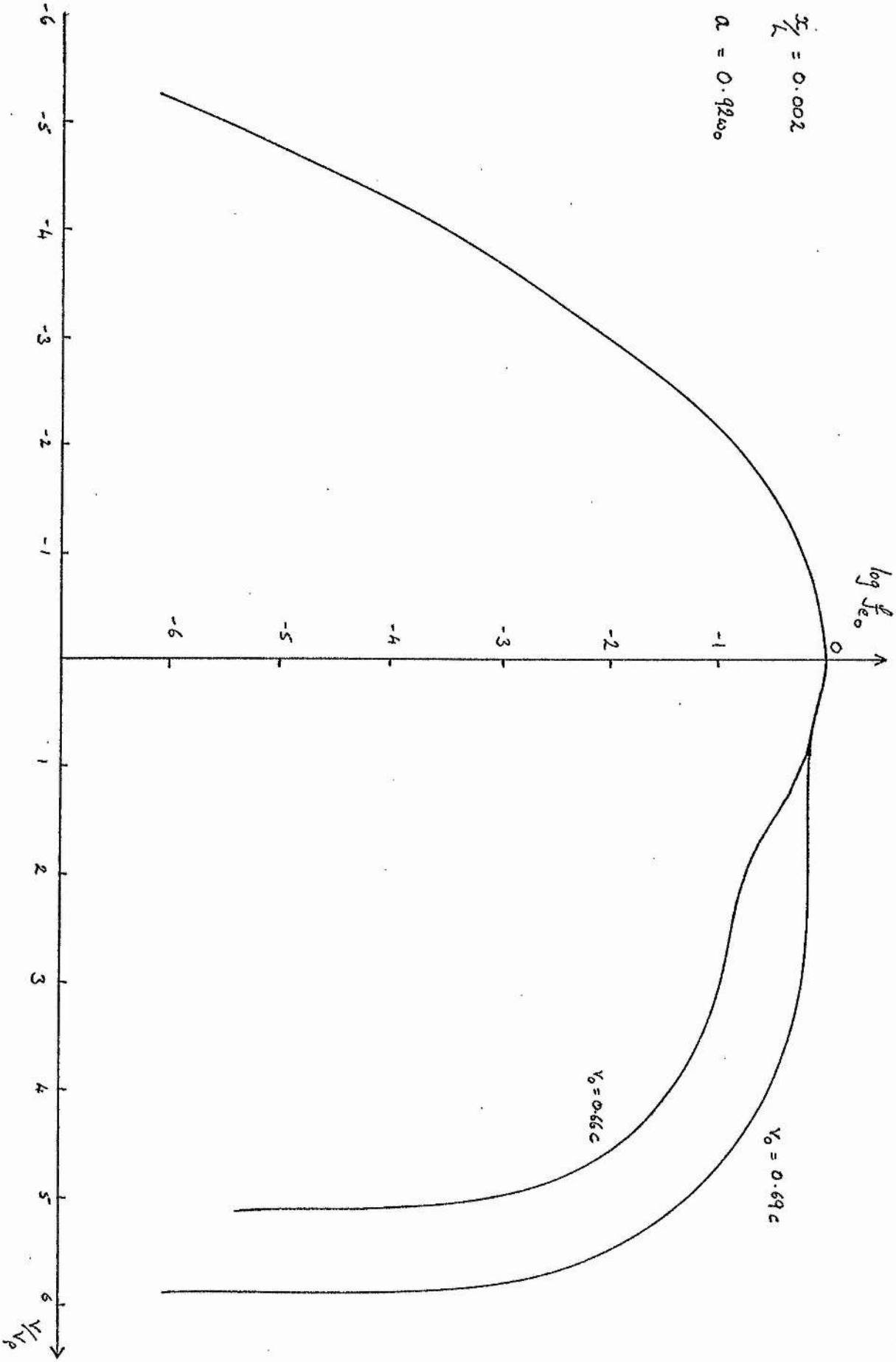

Figure 20 : Perturbation of background electron distribution function

These results seem to agree, at least qualitatively, with the fuller simulation studies of Lin and Dawson (44), who expect the dominant saturation mechanism for this instability would be just this flattening process. Physically, the strength of the instability depends on the beat velocity lying on the steepest slope of f_{e_o}. If we flatten this gradient, the instability is reduced. This is exactly what happens - the distribution flattens out, the gain reduces and the instability saturates. Arguably, the interaction could occur at higher velocities in figure 20 where the slope is again large. However, the small numbers of particles at these speeds, effectively, controls the scatter. An interesting set of results comes from Manheimer et al (122) who, by considering Compton sidescatter, find that diffusion occurs predominantly in the main part of f_{e_o}. They use a 4^{th} order diffusion equation to compute the variation in thermal velocity of the particles, consistent with their previous weak turbulence approach (also 123). As explained before, these different effects fit, physically, the differences in the direction of scatter. We should also add that they deal with a homogeneous plasma.

It has been suggested (e.g. Thomson et al (100)) that the introduction of a finite bandwidth pump mode would lead to a reduction in the growth rate of the stimulated scattering growth rate and, hence, the energy lost to the scattered and plasma modes. Because of the main feature of Compton scattering, that of no spatial resonance region, one might expect that this effect would be reduced in this case (125). Let us examine this hypothesis.

Assume a pump whose power has the frequency distribution

$$P(\omega) = P_o \mathcal{P}(\omega-\omega_o)$$

where P_o is the power of the monochromatic pump wave of frequency ω_o. Now, the amplitudes, wavenumber and non-linear beat force are all functions of ω. We may follow through the same analysis, again for one backscattered mode,

with the result that we replace (IV-9) by

$$k_1 c^2 \frac{\partial \alpha_1}{\partial x} = - C(x)\ \alpha_1$$

where $C(x) = \int d\omega\ k_2^2(\omega)\ v_o^2(\omega)\ \frac{}{8}\ \mathrm{Im}\ \frac{X_e(\omega)}{1 + X_e(\omega)}$ ..... (IV-14)

and $v_o^2(\omega) = V_o^2\ P\ (\omega - \omega_o)\ \frac{\omega_o^2}{\omega^2}$

We evaluate this expression numerically over the whole range of frequency space, using the same techniques as before. For simplicity, we represent $P(\omega-\omega_o)$ by a series of δ-functions, ensuring that the width of the pump, $\Delta\omega_o$, is such that $\Delta\omega_o < \omega_2$. We take a frequency spacing of 0.01 ω_o and a total of 21 frequencies to make up the pump. This gives a substantial bandwidth. We shall, for definiteness, adopt a Lorentzian frequency distribution for $P(\omega - \omega_o)$. (We could take any other distribution but Thomson and Karush (88) indicate the exact model is unimportant for sufficiently large bandwidths).

i.e. $$P(\omega - \omega_o) = \frac{D}{D^2 + (\omega - \omega_o)^2}$$

Converting the integral in (IV-14) to a series over the bands, m, we plot the total spatial gain, normalised to the gain with a monochromatic pump,

$$\Gamma_D(L) = \tfrac{1}{2} \int dx \sum_m \frac{(k_1^m\ v_o^m)^2}{8 k_r^m}\ \mathrm{Im}\ \left[\frac{X_e^m}{1 + X_e^m}\right]$$

as a function of D

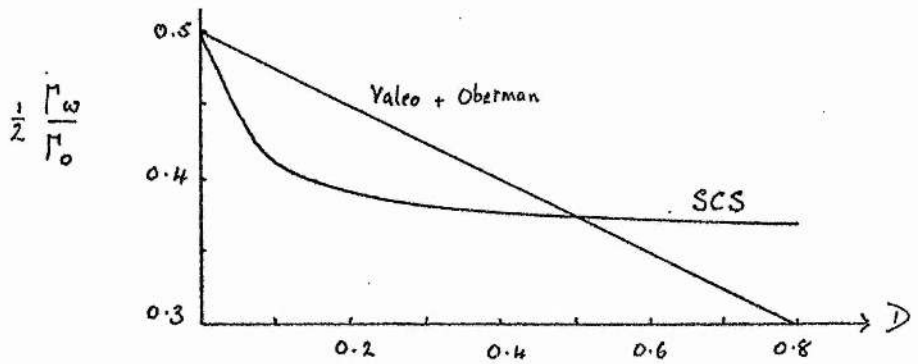

Figure 21 : Bandwidth effect on spatial gain

As can be seen the gain, in fact, decreases as the bandwidth becomes larger. In addition, as a rough guide, we plot results obtained for the general parametric decay case by Valeo and Oberman. For small $D < 1$, the averaged growth rate goes as $\frac{1}{2}(1 - \frac{D}{2})$. We note that there is a slightly more pronounced reduction in the Compton scattering case. Obviously, strict comparison is not possible, the latter analysis being for the temporal problem. Nevertheless, there are noticeable differences which we feel to be qualitatively true. However, these findings are in obvious contradiction to our earlier hypothesis that bandwidth effects would have little effect on this stability due to its effective lack of resonance region.

In fact, there is a resonance region but in velocity space not in x-space. As we indicated earlier, the greatest interaction occurs at wave-number k_2 such that $v_p = {}^{\omega}2/k_2\ v_e$ lies on the steepest slope of f_{e_o}. Consider the blow-up of this region in velocity space (figure 22).

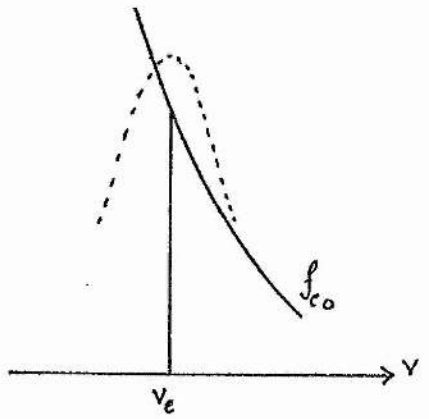

Figure 22 Blow-up of f_{e_o} around $v = v_e$

The monochromatic pump interacts with particles with velocities v_p. The finite bandwidth pump, however, interacts with a spectrum of modes whose phase velocities are spread around v_e, less energy going into each individual interaction. The energy lost from interaction at $v_p = v_e$ is not made up on either side. For $v_p < v_e$, whilst there are more interacting particles the

growth rate falls off very rapidly as we move away from $v_p = v_e$ (i.e. figure 15 for $x/L \lesssim x_m$) and so interaction is reduced. For $v_p > v_e$, the growth rate falls off much less abruptly but here there are fewer particles to interact in the resonance. Consequently, predominant scattering occurs for $v = v_p$ but with reduced intensity.

We mention one other property of this scattering which could be of considerable disadvantage to fusion schemes. Anticipating the following chapter, we note the possibility of modulation of the pump wave along the direction of propagation. This can enhance considerably the effect of this rather weak instability. Suppose there is a perturbation periodic such that the power input varies as

$$P(x) = P\,[1 + \lambda \sin \mu x]$$

where P is a constant. We further suppose the normalisation condition $\frac{1}{L}\int dx\, P(x) = P_o$, the power without any perturbation. The results are shown in figure 22. Values of the gain are shown for both amplitude and

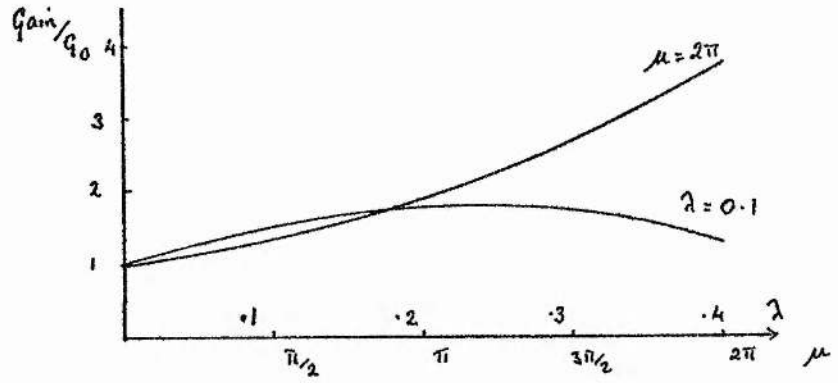

Figure 22 : Effective of a modulated pump wave

period variations. Since the modulations are long-wavelength (1,126), we need only consider period variations up to $\sim 2\pi$. There is enhancement of the effect since points of weaker interaction are now driven by a stronger pump field. We feel this could be a non-negligible effect.

Finally, we mention induced scattering off ions in inhomogeneous plasmas. In an analogous fashion to the discussion for stimulated Compton scattering, we would expect this process to be dominant when collective excitations of the ions i.e. ion acoustic waves are heavily damped. This occurs preferentially for $T_e \lesssim T_i$. We would, thus, expect resonance with plasma 'waves' of frequency $\omega_2 \sim k_2 v_i$ to occur in this situation. Because of the relative sizes of the decay frequencies we would expect $\omega_1 \sim \omega_o$. In fact, solving the resonance conditions (III-1), in a linear density gradient $n(x) = n_o x/L$, for x/L, gives

$$x/L = \tfrac{1}{2}\left[1 + \Omega_r^2 - \frac{1 + \Omega_r^4 - 2\Omega_r^2 + c^4/v_i^4 (1 - \Omega_r)^4}{2\, c^2/v_i^2 (1 - \Omega_r)^2}\right]$$

where $\Omega_r = \omega_1/\omega_o$. Since $v_i/c \sim O(10^{-3})$, we require, for any sensible result, that $1-\Omega_r \sim v_i/c$, in which case $x/L \sim 0.73$. We shall examine this effect only in the case $\Omega_r = v_i/c$. As a guide, Drake et al (46) quote that, in a homogeneous plasma, the growth rate can be comparable to that for stimulated Brillouin scattering, when $k\lambda_D << 1$. This region corresponds to the major part of the underdense plasma up to and around the critical surface. By the above, this is just the region of greatest interaction in an inhomogeneous plasma and so in plasmas of equal electron-ion temperatures, there should be a sizeable effect for this scattering.

The mathematical treatment follows the same lines as we pursued earlier and will not be repeated here, save to note the differences. Provided the pump power is not sufficiently strong as to have any relativistic effect on the electrons (i.e. $P_o \lesssim 10^{18}$ W cm^{-2}) we may neglect the ion motion entirely and so the non-linear beat force has the same form as (IV-3). Replace δn_e^* in (IV-5) by $\delta n_i^* = \frac{F_{NL}}{4\pi e_i} \frac{X_i X_e}{1 + X_i + X_e}$ with the result that we now have a gain term (cf. IV-9)

$$\Gamma_i(x) = \int dx' \frac{k_2^2 v_o^2}{8 k_1 c^2} \operatorname{Im}\left[\frac{X_i X_e}{1 + X_i + X_e}\right]$$

where we cannot, now, set $X_e = 0$. By analogy, we have, also, assumed that no absolute instability exists. We shall, therefore, consider the amplification due to a finite slab (figure 23)

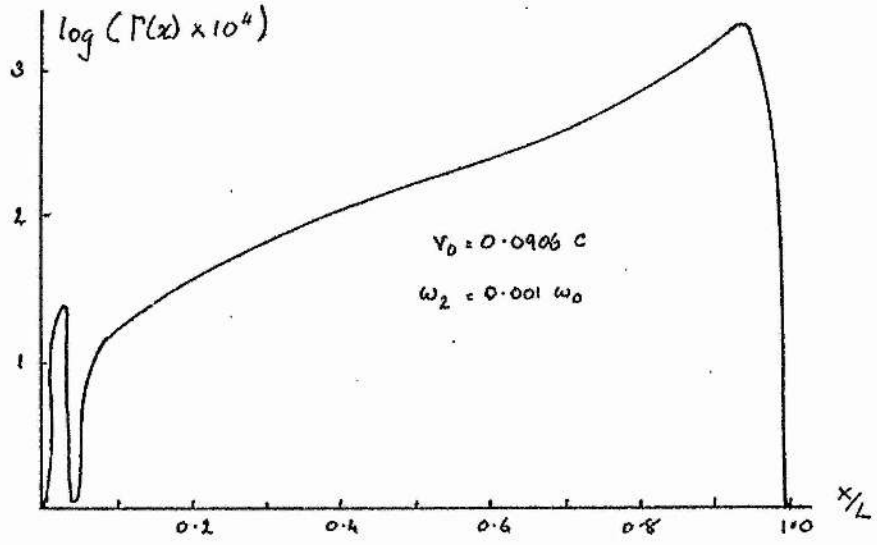

Figure 23 Gain due to a finite slab with density, $n(x)=n_o x/L$

We note there are two peaks - the smaller being due to electron scattering and the larger to the induced ion scattering. We also note that the ion scattering occurs at much lower powers than its electron counterpart. (Table II)

Table II

Power - 10^{14} W cm^{-2}	Amplification, L = 300
0.1	2.473
0.5	92.08
0.7	1.253×10^3
1.0	9.405×10^3

We can thus anticipate substantial effects in this case. However, only when $T_e \lesssim T_i$ can this occur, predominantly; a situation which, at least, in fusion situations is wanted but proving elusive to obtain. For this reason, we do not pursue this scattering more thoroughly save to point out, again, its relevance in applications where temperature equilibration is more easily attainable.

CHAPTER V

THE EFFECT OF A FILAMENTED CRITICAL SURFACE ON THE DECAY INSTABILITY

It has been noted by several works (126-30) that light waves in a plasma are unstable to filamentation and formation of bubbles, or cavities (131). The filaments can appear parallel and perpendicular to the direction of light propagation (126). Basically, the filamental instability is just one form of the modulational instability (38, 45) with the associated, purely growing envelope perturbation perpendicular to the direction of light propagation. It results in the formation of density striations which cause focussing of the laser, a process which we shall describe in detail below. It is possible in this way to generate regions of trapped electric field which are expected to affect light absorbtion, leading to an uneven absorbtion at the critic al surface which could, conceivably, give rise to imperfect implosion. Simulations of self-focussing show generation of hot and cold spots, of size $5\text{-}10\lambda_o$, near the critical surface. If the temperature gradient is perpendicular to the spontaneously generated magnetic field (132), asymmetries may affect the implosion (through a term $\nabla n \sim \nabla T \times \underline{B}$ (c.f. Tidman and Shanny (133) where magnetic field generation occurs via a $\nabla n \times \nabla T$ term) Langdon and Lasinski (131) have performed simulations in 2- and 3-D on the Raman and 2-plasmon instabilities. In the latter instance, filamentation caused trapping of the decay waves which then grow to large amplitude, enhancing the heating - something which does not occur in 3-D for plane polarised light. A Raman-like instability does occur with low trapping, due to the high wave phase velocity. The transverse electric field is trapped maintaining filaments but has no other effect. In the limit, the same decay is observed, filamentation perpendicular to $\underline{E}_o$ with $\underline{k} = \underline{k}_o$, together with a long wave-

length modulation parallel to $\underline{E}_o$. What is noticeable is that this process occurred over a wide range of densities, with some heating, the exact amount being slightly debatable from their results.

Recently, Max (127) cleared up a slightly embarassing theoretical problem. It was thought; in the weak limit, assuming that the ratio of light to plasma energy densities was of order unity, that the resulting filamentation occurred only for one pump value, that it was irreversible and that it, eventually, gave rise to a catastrophe as the intensity became infinite. By considering the effect, on the density, of the pondermotive force, she has managed to show that, for a cylindrical beam, there exists a radius at which propagation (of $\underline{E}_o$) occurs without dispersion or focussing and that the process is, otherwise, reversible. Basically, the filaments form then begin to oscillate in time. It is, however, only a linear theory and does not account for the main saturation process which occurs when the pondermotive force balances the excess plasma pressure due to the filament.

Finally, the filamentation of (128) and bubble formation and corrugation at (133) the critical surface have been examined in simul ation studies. The linear and non linear regimes are shown below. Strong filamentation can be seen to occur along the critical surface and it is this result which provides the basis for the rest of the chapter. The directions of propagation of the ion sound

Figure 24

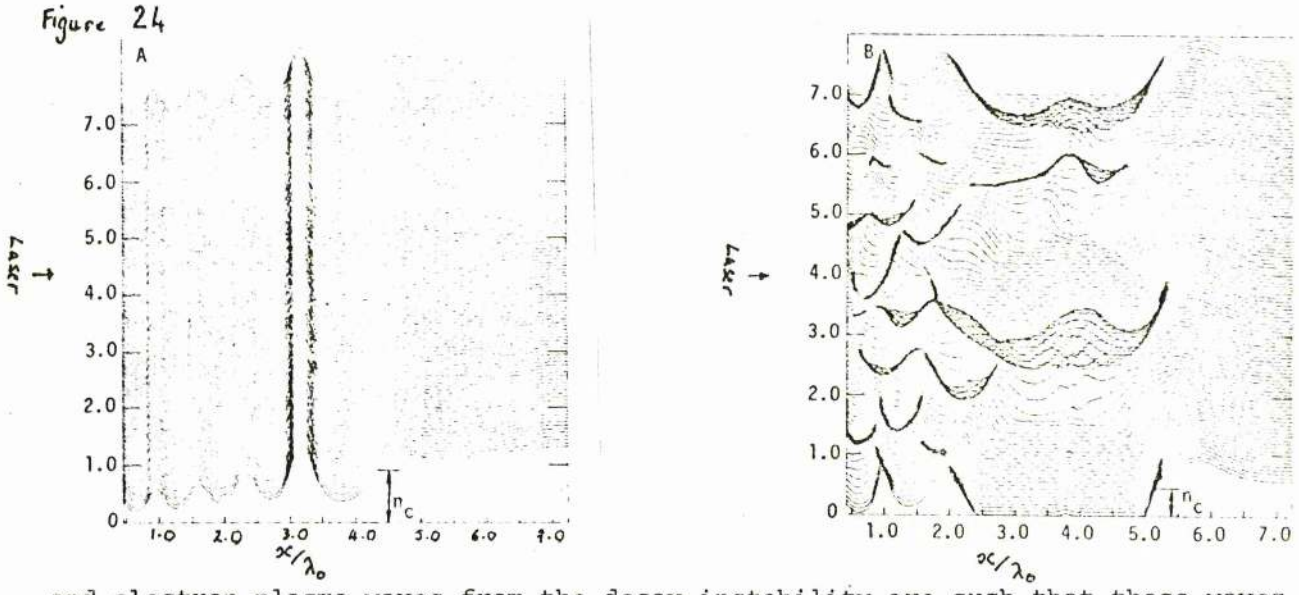

and electron plasma waves from the decay instability are such that these waves

must now propagate through the perturbation. As can be seen the high density regions are often greater than n_e. This is expected to cause a limitation in the decay instability and to affect light absorption. We shall now examine the former effect but first let us discuss the question of filamentation and its description in terms of the pondermotive force.

Suppose there is some initial density striation in the plasma and the light propagates parallel to this striation as shown in figure 25, then the

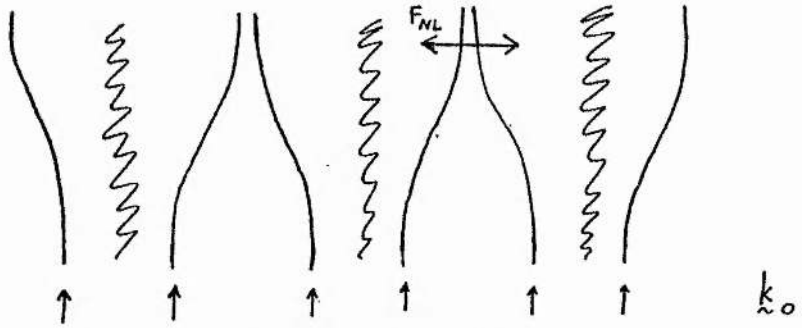

Figure 25 ; Radiation incident along density striations

refraction due to the density perturbation of wavenumber k_1 causes the light wave to be channelled into the region of lower density. This bunching in E causes an increase in the 'so-called' pondermotive force,

$$F_{NL} = -\frac{\omega_p^2}{\omega_o^2} \nabla \left\langle \frac{E^2}{8\pi} \right\rangle$$

which acts in the directions shown in figure 26 to push more particles

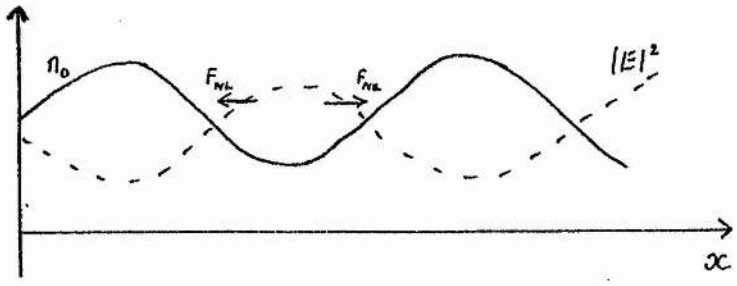

Figure 26 ; Action of the pondermotive force

out of the low density regions. The incident light is thus unstable to this type of perturbation.

In the steady-state, F_{NL} will balance the electron pressure difference across the filament, $\nabla(n\kappa T_e)$, thus giving rise to the form, independent of density scale length

$$n = n_o \exp\left[-\frac{\omega_p^2}{\omega_o^2} \frac{\langle E^2 \rangle}{8\pi n_o \kappa T_e} \right]$$

If the light waves are undamped and there were perfect Debye shielding then one would expect this equilibrium to be established at any intensity. However, from strict neutrality due to finite Debye length means that F_{NL} must overcome a small electric field, proportional to $k_1^2 \lambda_D^2$. The threshold for filamentation is then (129)

$$\frac{\gamma_o^2}{c^2} > 4 \left(1 + \frac{T_i}{T_e}\right) k_1^2 \lambda_D^2$$

This threshold is lower than that for most absolute parametric instabilities but, on the other-hand, the growth rate $\gamma \sim \frac{1}{2}\omega_{pi} v_o/c$ is smaller (cf. Stimulated Brillouin scattering a factor $(2c/c_s)^{\frac{1}{2}}$ greater). We also note that the scale length for electromagnetic field variation is (126)

$$\Gamma^2 = \frac{\omega_{po}^2}{c^2} E_o^2$$

where E_o is the constant pump amplitude and ω_{po} the plasma frequency in the region where no field is present. The fastest growing mode has wavenumber

$$k_y^2 = \frac{\omega}{c} \frac{\sqrt{3}}{8} \frac{\omega_{po}}{c} \frac{v_e}{v_o} \exp\left[-\frac{3}{8} \left(\frac{v_e}{v_o}\right)^2 \right]$$

A pondermotive force approach illustrates well the essential physics and, indeed, this particular problem was its first application. To maintain an almost two-pronged attack on the topic, we shall briefly describe the mode coupling approach.

The phenomenon may be viewed as the interaction of the pump mode, k_o, with an ion wave k_1 at right angles. Since k_1 is small, the anti-Stokes process, $k_2 = k_o + k_1$, figure 27(a) must be included as well as the usual Stokes one, $k_2 = k_o - k_1$, figure 27(b)

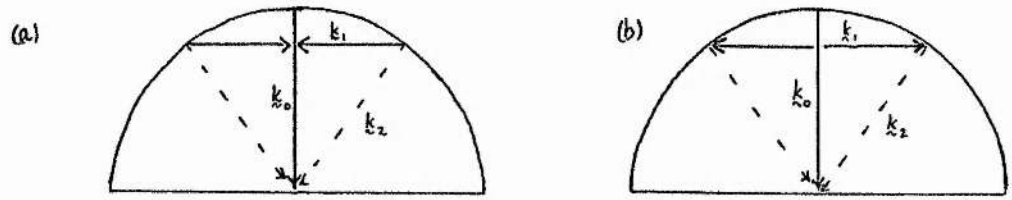

Figure 27 : The anti-Stokes (a) and Stokes (b) processes

This suggests the process must now be a 4 -wave interaction. Thus, we have forward scattering of the k_2 mode which will then interact with the pump wave to produce the refraction and self-focussing which we have already mentioned. We note that the geometry of this instability is identical with that of the OTSI which has already been discussed. Both instabilities are non-convective.

In view of the complex structure of the filaments and density perturbations resulting from the striation of the critical surface, to solve the problem of the decay instability in such a physical geometry would be inordinately complex not least however because of the form of E_o in such a case. We, therefore, propose to examine a simplified problem which illustrates, with obvious restrictions, the underlying effect of this filamentary instability upon the decay instability. The application to laser fusion is one of importance, the decay instability being one of the processes by which energy is absorbed and any reduction of the absorbtive mechanism being of concern.

We shall make the following simplifying assumptions. Firstly, we shall consider only a 2-D model, the pump being incident along the x-axis and the decay modes propagating along the y-axis (in opposite directions). Geometrically, we have a slab structure in x but essentially 'infinite' extension in y. Secondly, we idealise the density striations to a square wave with unequal perturbations about the critical density, as shown in figure 28.

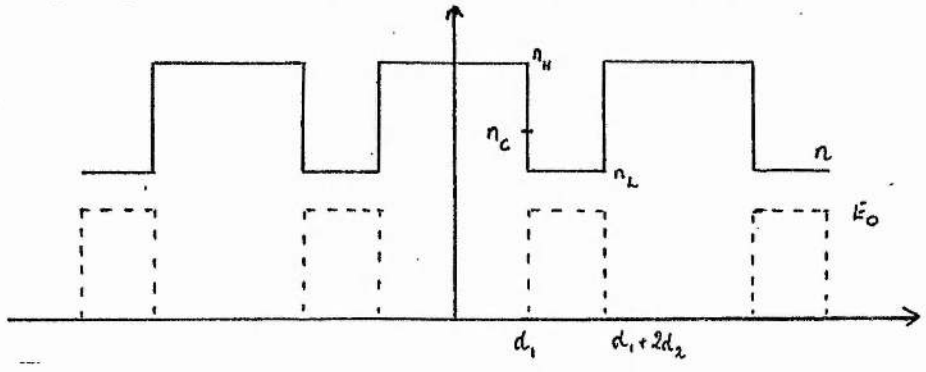

Figure 28 ; The Idealised Density Striations

We define the relative densities by

$$h_o = \frac{n_c - n_L}{n_c} \quad , \qquad h = \frac{n_H - n_c}{n_c}$$

The widths d_1, d_2, are chosen so that $d_1 < d_2$, and $d_2 \lesssim 10 d_1$, which would seem reasonable in the light of figure (24). Following this, we make our third assumption concerning E_o (shown in dotted lines in figure 28). We set E=0 in the overdense region, the decay instability no longer being driven there, and $E=E_o$ in the underdense parts where the decay waves are assumed to propagate.

We, therefore, have a model in which the density perturbation is square-wave like but in which the peak regions have been compressed with respect to the (larger) valley regions, where the decay instability is driven. The electron plasma and ion accoustic decay modes are generated in each valley and are forced to travel through the overdense region before being able to interact constructively with modes in the next valley (cf. the absence of filamentation when modes do interact everywhere and propagate outwards, unimpeded, being reinforced as they propagate).

The decay instability generates wave propagating along the y-axis. Because no preferred direction exists, we shall have two sets of decay modes, $(a_1,b_1,)$ and (a_2,b_2), such that $a_1 - a_2 = b_1 - b_2 = -1$ i.e. the two sets propagate in opposite directions. We assume that these two sets are independent as shown in figure 29.

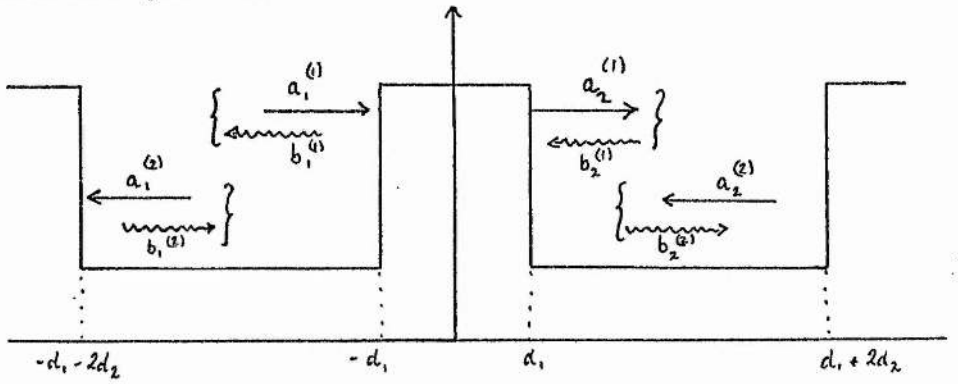

Figure 29

Intuitively, one would expect this situation to affect the absorption considerably as the decay waves are essentially trapped in the valley regions, setting up standing wave patterns of growing amplitude. There would be little propagation, and hence absorption, in the 'hill' regions. A non-uniform energy is, thus, expected. Due to this type of constraint the threshold for decay will rise and the growth rate would fall. We shall, now, examine the problem analytically to determine these effects. Let us represent by a column vector $\underset{\sim}{\Psi}$, the decay wave amplitudes

$$\underset{\sim}{\Psi}_i = (a_1^{(i)}, b_1^{(i)}, a_2^{(i)}, b_2^{(i)})^T$$

and consider the set-up in figure 29. We wish to determine the effect on ψ of one cycle of n, E i.e. to determine $\underset{\sim}{\Psi}_3(d_1)$ as a function of $\underset{\sim}{\Psi}_1(-d_1-2d_2)$. If they are connected by a matrix C such that

$$\underset{\sim}{\Psi}_3(d_1) = \underset{\sim}{\underset{\sim}{C}} \cdot \underset{\sim}{\Psi}_1(-d_1-2d_2)$$

then, for a physically real solution, the eigenvalues of C are all of modulus 1. This means the solution neither grows nor diminishes as we move long the filaments.

The matrix C is determined in two parts. Firstly, in the low density region, the equations for the decay instability give us,

$$\underset{\sim}{\Psi}_1(-d_1) = \underset{\approx}{R} \cdot \underset{\sim}{\Psi}_1(-d_1-2d_2)$$

Then, by considering the propagation of waves through the hills (cf. quantum mechanical tunnelling), we obtain

$$\underset{\sim}{\Psi}_3(d_1) = \underset{\approx}{S} \cdot \underset{\sim}{\Psi}_1(-d_1)$$

upon applying the appropriate boundary conditions. Thus, by substitution and comparison,

$$\underset{\approx}{C} = \underset{\approx}{S} \cdot \underset{\approx}{R}$$

Our task is to find the matrices S and R.

The analysis follows that of Nishikawa (30) and Nishikawa and Liu (1). The decay of a pump of frequency ω_o into plasma (A) and sound (B) waves generates perturbations of the forms

$$A \sim \underset{\sim}{A}_+ \, e^{i\omega t} + \text{c.c.} \qquad B \sim \underset{\sim}{B}_+ \, e^{i(\omega_o - \omega)t} + \text{c.c.}$$

which, in turn, may be written

$$\underset{\sim}{A}_+ \sim \underset{\sim}{a}_+ (x,t) \, e^{pt \mp ikx} \quad , \quad \underset{\sim}{B}_+ \sim \underset{\sim}{b}_+(x,t) e^{pt \pm ikx}$$

where the amplitudes $(\underset{\sim}{a}_+, \underset{\sim}{b}_+)$ are related by

$$\nu_1 a_{\pm} + \left(\frac{\partial}{\partial t} + V_1 \frac{\partial}{\partial x}\right) a_{\pm} = \gamma_o b_{\pm} \quad \ldots\ (V\text{-}1)$$

$$\nu_2 b_{\pm} + \left(\frac{\partial}{\partial t} - V_2 \frac{\partial}{\partial x}\right) b_{\pm} = \gamma_o a_{\pm} \quad \ldots\ (V\text{-}2)$$

where γ_o is the growth rate for a homogeneous plasma, in the absence of damping, V_1 and V_2 are group velocities and ν_1 and ν_2 damping rates.

Consider only the + modes and drop the subscript. If we take the Laplace Transform of these equations, writing $\tilde{a}(p) = \int dt\ e^{-pt}\ a(t)$, etc. and eliminate $\tilde{b}$, we obtain

$$\frac{\partial^2 a^2}{\partial X^2} + \left(\frac{p+\nu_1}{V_1} - \frac{p+\nu_2}{V_2}\right) \frac{\partial \tilde{a}}{\partial X} + \left[\gamma_o^2 - \frac{(p+\nu_1)(p+\nu_2)}{V_1 V_2}\right] \tilde{a}$$

$$= \frac{\gamma_o}{V_1} \frac{\partial}{\partial x} \gamma_o \tilde{b} + \text{initial value terms}$$

Setting RHS = 0 and eliminating $\frac{\partial a}{\partial y}$ by writing

$$\psi = \tilde{a} \exp\left[\frac{X}{2}\left(\frac{p+\nu_1}{V_1} - \frac{p+\nu_2}{V_2}\right)\right] \quad \ldots\ (V\text{-}3)$$

we find

$$\frac{d^2\psi}{dX^2} - \left[\tfrac{1}{4}\left(\frac{p+\nu_1}{V_1}\right) + \frac{p+\nu_2}{V_2}\right)^2 - \frac{\gamma_o^2}{V_1 V_2}\right]\psi = 0 \quad \ldots\ (V\text{-}4)$$

This equation determines the variation of the effect amplitudes (i.e. without phase differences) of <u>both</u> waves. It has solution

$$\psi = A \cos \mu X + B \sin \mu X$$

where $\mu^2 = \frac{\gamma_o^2}{V_1 V_2} - \tfrac{1}{4}\left(\frac{p+\nu_1}{V_1} + \frac{p+\nu_2}{V_2}\right)^2 > 0$, which generates

$$a = A_1(x) \cos \mu x + B_1(x) \sin \mu x$$

by (V-3) and, finally, $\tilde{b}$ through (V-1).

We shall take the growth rate to be proportional to E_o^2.

The form of $\gamma_o(x)$ is

$$\gamma_o(x) = \begin{cases} \gamma_o & -d_1-2d_2 < x < -d_1 \\ 0 & -d_1 < x < d_2 \\ \gamma_o & d_1 < x < d_1+2d_2 \end{cases}$$

The important simplification which we shall make is to neglect the phase differences between the waves and apply boundary conditions to the amplitudes. or ψ's. This is justifiable on the grounds that we are really only interested in the growth of the unstable modes, not in their phases.

(a) Determination of $\tilde{R}$

If we define $\tilde{k}^2 = \frac{\gamma_o^2}{V_1 V_2} - \frac{1}{4}\left(\frac{p+\nu_1}{V_1} + \frac{p+\nu_2}{V_2}\right)^2 > 0$

then the solution to (V-3) in the region of parametric growth i.e. $\gamma_o(x) = \gamma_o$, is

$$\psi_1 = A \cos kx + B \sin kx$$

Further, if we set $\pm\lambda = \frac{p+\nu_1}{V_1} - \frac{p+\nu_2}{V_2}$,

$$\tilde{a}_1 = A e^{\frac{-\lambda x}{2}} \cos kx + B e^{\frac{-\lambda x}{2}} \sin kx \qquad \ldots\ (V-5)$$

Recalling that the ion sound amplitude is given by (V-2)

We have

$$\tilde{b}_1 = \frac{V_1}{\gamma_o}\left(\frac{\lambda'}{2} \cos kx - k \sin kx\right) e^{\frac{-\lambda x}{2}} A + \frac{V_1}{\gamma_o}\left(\frac{\lambda'}{2} \sin kx + k \cos kx\right) e^{\frac{-\lambda x}{2}} B$$

where

$$\lambda' = \frac{p+\nu_1}{v_1} + \frac{p+\nu_2}{v_2}$$

Thus,

$$\begin{pmatrix} \tilde{a}_1 \\ \tilde{b}_1 \end{pmatrix} = \begin{pmatrix} e^{\frac{-\lambda y}{2}} \cos ky & e^{\frac{-\lambda y}{2}} \sin ky \\ e^{\frac{-\lambda y}{2}} \frac{v_1}{\gamma_o}\left(\frac{\lambda'}{2}\cos ky - k\sin ky\right) & e^{\frac{-\lambda y}{2}} \frac{v_1}{\gamma_o}\left(\frac{\lambda'}{2}\sin ky + k\cos ky\right) \end{pmatrix} \begin{pmatrix} A \\ B \end{pmatrix}$$

i.e.

$$\begin{pmatrix} \tilde{a}_1 \\ \tilde{b}_1 \end{pmatrix}_{y=-d_1-2d_2} = e^{(d_1+2d_2)} \times$$

$$\begin{pmatrix} \cos k(d_1+2d_2) & -\sin k(d_1+2d_2) \\ \frac{v_1}{\gamma_o}\ \frac{\lambda'}{2}\cos k(d+2d_2)+k\sin k(d+2d_2) & \frac{v_1}{\gamma_o}\ k\cos k\ (d_1+2d_2)\ -\frac{\lambda'}{2}\sin k\ (d_1+2d_2) \end{pmatrix} \begin{pmatrix} A \\ B \end{pmatrix}$$

and

$$\begin{pmatrix} \tilde{a}_1 \\ \tilde{b}_1 \end{pmatrix}_{y=-d_1} e^{d_2\lambda/2} \begin{pmatrix} \cos kd_1 & -\sin kd_1 \\ \frac{v_1}{\gamma_o}\left[\frac{\lambda'}{2}\cos kd_1 + k\sin kd_1\right] & \frac{v_1}{\gamma_o}\left[k\cos kd_1 - \frac{\lambda'}{2}\sin kd_1\right] \end{pmatrix} \begin{pmatrix} A \\ B \end{pmatrix}$$

Eliminating $(A\ B)^T$ we find a relation connecting the values $(a_1\ b_1)^T$ at either end of the decay instability interaction region :-

$$\begin{pmatrix} \tilde{a}_1 \\ \tilde{b}_1 \end{pmatrix}_{x=-d_1} = e^{-\lambda d_2} \begin{pmatrix} \cos 2kd_2 - \frac{\lambda'}{2k}\sin 2kd_2 & \frac{\gamma_o}{kV_1}\sin 2kd_2 \\ \frac{V_1}{\gamma_o}\left[-\frac{\lambda'^2}{4k}\sin 2kd_2 - k\sin 2kd_2\right] & \cos 2kd_2 + \frac{\lambda'}{2k}\sin 2kd_2 \end{pmatrix} \begin{pmatrix} \tilde{a}_1 \\ \tilde{b}_1 \end{pmatrix}_{x=-d_1-2d_2} \quad \ldots\ldots(V\text{-}6)$$

$$= \underset{\sim}{R}_1 \begin{pmatrix} \tilde{a}_1 \\ \tilde{b}_1 \end{pmatrix}_{x=d_1-2d_2}$$

The corresponding expression for $(a_2\ \ b_2)^T$ can be derived in a similar fashion. However, a simple derivation comes from the symmetry of the decay, that there is no preferred direction for the propagation and that the path of decay in one direction is just the path of growth in the other. Hence, the connecting matrix is just the inverse of the one in (V-6) which is

$$\underset{\sim}{R}_2 = e^{\lambda d_2} \begin{pmatrix} \cos 2kd_2 + \frac{\lambda'}{2k}\sin 2kd_2 & -\frac{\gamma_o'}{kV_1}\sin 2kd_2 \\ \frac{V_1}{\gamma_o}\left[k\sin 2kd_2 + \frac{\lambda'^2}{4k}\sin 2kd_2\right] & \cos 2kd_2 - \frac{\lambda'}{2k}\sin 2kd_2 \end{pmatrix}$$

Because we have treated the two sets of decay modes as essentially independent, there are no cross terms between $(\tilde{a}_1\ ,\ \tilde{b}_1)$ and $(\tilde{a}_2\ ,\ \tilde{b}_2)$ and the matrix $\underset{\sim}{R}$ is given by

$$\underset{\sim}{R} = \begin{pmatrix} \underset{\sim}{R}_1 & 0 \\ 0 & \underset{\sim}{R}_2 \end{pmatrix}$$

(b) Determination of $\underset{\sim}{S}_{\nu}$

In the region of peak intensity, not only is $\gamma_o=0$ but also $\omega_{pe} > \omega_o$. The latter constraint will alter the plasma wave solution but will leave the ion sound solutions unchanged, provided there are no temperature jumps across the hill-valley boundaries. Consequently, they will be affected solely by $\gamma_o=0$. i.e. $\underset{\sim}{b}$ will be continuous across the boundaries. The electron plasma waves will be partially reflected by the density hump and so we must resort to their original wave equation to examine this effect. The 2^{nd} order wave equation for this propagation is

$$\frac{\partial^2 A}{\partial t^2} - v_1^2 \frac{\partial^2 A}{\partial x^2} + \omega_{pe}^2 A = 0$$

writing $A=\alpha e^{iwt + pt}$ gives

$$[-(w-ip)^2 - v_1^2 \partial^2/\partial x^2 + \omega_{pe}^2]\alpha = 0$$

If now, we assume $\alpha \sim e^{\delta x}$,

$$\delta^2 v_1^2 = \omega_{pe}^2 - (\omega-ip)^2 \approx (\omega_{pe}^2 - \omega^2) + 2ip\omega$$

or

$$\delta = \pm \frac{1}{v_1}[\eta + i\mu]$$

where $\eta^2-\mu^2 = \omega_{pe}^2-\omega_o^2$ and $\eta\mu = p\omega$, provided $p < \omega$

It is an interesting observation that, for $\gamma_o=0$, propagation in the region $\omega_{pe} > \omega_o$ imparts a wobble (through $i\mu/v_1$) to the evanescence whilst in the case of $\omega_{pe} < \omega_o$ there is merely a larger oscillation.

We now recall (V-3) and define

$$k^2 = \frac{\gamma_o^2}{V_1 V_2} - \tfrac{1}{4}\left(\frac{p+\nu_1}{V_1} + \frac{p+\nu_2}{V_2}\right)^2 > 0$$

$$\lambda'^2 = \tfrac{1}{4}\left(\frac{p+\nu_1}{V_1} + \frac{p+\nu_2}{V_2}\right)^2 > 0$$

Then, the solution Ψ for $-d_1 < y < +d_1$ is of the form

$$C\, e^{\lambda' x} + D\, e^{-\lambda' x}$$

However, by the above, we must modify this solution by a term $e^{-\delta y}$ (for evanescence) where $\delta = \frac{(\omega_{pe}^2 - \omega^2)^{\frac{1}{2}}}{V_1}$, the limiting form, providing $p \ll \omega_o$. Writing $K_o = \lambda' - \delta$ and $K_1 = \lambda' + \delta$, the full solution for Ψ is,

$$\Psi = \begin{cases} A\, e^{ikx} + B\, e^{-ikx} & x < -d_1 \\ C\, e^{K_o x} + D\, e^{-Kx} & -d_1 < x < d_1 \\ F\, e^{ikx} + G\, e^{-ikx} & x > d_1 \end{cases}$$

The boundary conditions are that (1) E be continuous, (2) pressure be continuous, across the boundaries. Taking in our fluid model the ratio of the specific heats to be 3 we have,

$$p/n^3 = p_o/n_o^3$$

i.e. for perturbations p_1 and n_1

$$\frac{p_o + p_1}{n_o^3 (1+3n_1'/n_o)} = p_o/n_o^3$$

or $$p_1 = 3p_o \cdot n_1/n_o$$

Assuming constant temperature, the boundary condition becomes the continuity of density, or, by Poisson's equation, $\nabla \cdot \underline{E} = {}^{\partial E}/_{\partial y}$ be continuous across the boundary. These conditions, at $x = -a = d_1$ are sufficient to determine the relation between (A,B) and (C,D) to be

$$\begin{pmatrix} A \\ B \end{pmatrix} = \tfrac{1}{2} \begin{pmatrix} (1 - \frac{iK_o}{k}) e^{-K_o a + ika} & (1 + \frac{iK}{k}) e^{Ka + ika} \\ (1 + \frac{iK_o}{k}) e^{-K_o a + ika} & (1 - \frac{iK}{k}) e^{Ka + ika} \end{pmatrix} \begin{pmatrix} C \\ D \end{pmatrix}$$

Similarly, at $x = a = d_1$,

$$\begin{pmatrix} C \\ D \end{pmatrix} = \frac{1}{K+K_o} \begin{pmatrix} (K+ik) e^{ika - K_o a} & (K-ik) e^{-ika - K_o a} \\ (K_o - ik) e^{ika + Ka} & (K_o + ik) e^{-ika + Ka} \end{pmatrix} \begin{pmatrix} F \\ G \end{pmatrix}$$

and by substitution we obtain

$$\begin{pmatrix} A \\ B \end{pmatrix} = \tfrac{1}{2} \begin{pmatrix} (1+i\zeta) e^{2ika - 2K_o a} + (1-i\zeta) e^{2ika + 2Ka} & (\eta - i\varepsilon) e^{-2K_o a} + (\eta + i\varepsilon) e^{2Ka} \\ (\eta + i\varepsilon) e^{-2K_o a} + (\eta - i\varepsilon) e^{2Ka} & (1-i\zeta) e^{-2ika - 2K_o a} + (1+i\zeta) e^{-2ika + 2Ka} \end{pmatrix} \begin{pmatrix} F \\ G \end{pmatrix}$$

where we used the abbreviated notation

$$\zeta = \frac{k^2 - KK_o}{k(K + K_o)} \quad , \quad \eta = \frac{K - K_o}{K + K_o} \quad , \quad \varepsilon = \frac{k^2 + KK_o}{k(K + K_o)}$$

The case of interest to us is when G = 0, representing a travelling wave of amplitude A, incident from the left, generating a transmitted wave of amplitude F and reflected wave of amplitude B. We have, then,

$$\frac{F}{A} = \frac{2e^{-2ika}}{(e^{-2K_o a} + e^{2Ka}) + i\zeta(e^{-2K_o a} - e^{2Ka})}$$

and the transmission coefficient is seen to be

$$T = \left|\frac{F}{A}\right|^2$$

i.e.

$$T = 4/[(e^{-2K_o a} + e^{2Ka})^2 + \zeta^2(e^{-2K_o a} - e^{2Ka})^2]$$

The reflection coefficient, R $\left(= \left|\frac{B}{A}\right|^2\right)$ is then

$$R = 1 - T$$

We now use these results and the fact that our decay waves are treated as independent to derive connection formulae for $\Psi(-a)$ and $\Psi(a)$, i.e. the matrix $\underset{\approx}{S}$.

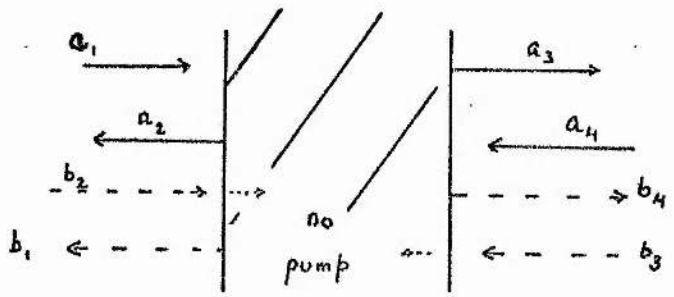

Figure 30

Consider the situation in Figure (30), the a_i representing plasma wave i and b_i ion acoustic wave i. Treating a_1 and a_4 as independent waves impinging on the shaded region the resulting waves a_2 and a_3 will have

components due to <u>both</u> the incoming waves (since a_2 is part reflection of a_1 and part transmission of a_4). Thus,

$$a_3 = T^{\frac{1}{2}} a_1 + R_1^{\frac{1}{2}} a_4$$

$$a_2 = R^{\frac{1}{2}} a_1 + T^{\frac{1}{2}} a_4$$

or rewriting a_3, a_4 as functions of a_1 , a_2 ,

$$a_3 = (T^{\frac{1}{2}} + {}^{R}/_{T^{\frac{1}{2}}}) a_1 + \frac{R^{\frac{1}{2}}}{T^{\frac{1}{2}}} a_2$$

$$a_4 = -\frac{R^{\frac{1}{2}}}{T^{\frac{1}{2}}} a_1 + \frac{1}{T^{\frac{1}{2}}} a_2$$

The form of the ion sound waves in the shaded (dense) region is

$$\underset{\sim}{b} = e^{\pm(\lambda' y - \lambda y/2)} = \exp\left(\pm\frac{(p - \nu_2)}{v_2} \; y/2\right)$$

The conditions that $b_i = b_i'$, i = 1, 4 then imply the following connection formulae

$$b_3 = e^{\frac{(p+\nu_2)a}{v_2}} \; b_1$$

$$b_4 = e^{-\frac{(p+\nu_2)a}{v_2}} \; b_2$$

Thus, utilising all these results and $d_1 \equiv a$

$$\underset{\sim}{\Psi}_3(+d_1) = \underset{\sim}{S} \; \underset{\sim}{\Psi}(-d_1)$$

where

$$\underset{\sim}{S} = \begin{pmatrix} T^{\frac{1}{2}} - {}^{R}/_{T^{\frac{1}{2}}} & 0 & {}^{R^{\frac{1}{2}}}/_{T^{\frac{1}{2}}} & 0 \\ 0 & e^{\frac{p+\nu_2}{v2} a} & 0 & 0 \\ -{}^{R^{\frac{1}{2}}}/_{T^{\frac{1}{2}}} & 0 & {}^{1}/_{T^{\frac{1}{2}}} & 0 \\ 0 & 0 & 0 & e^{-\frac{p+\nu_2}{v_2} a} \end{pmatrix}$$

Finally, if we now recall our required matrix $\underset{\sim}{C}$, defined by

$$\underset{\sim}{C} = \underset{\sim}{S} \cdot \underset{\sim}{R}$$

we have

$$\underset{\sim}{C} = \begin{pmatrix} c_{11} & c_{12} & c_{13} & c_{14} \\ c_{21} & c_{22} & 0 & 0 \\ c_{31} & c_{32} & c_{33} & c_{34} \\ 0 & 0 & c_{43} & c_{44} \end{pmatrix},$$

where $c_{11} = e^{-\lambda b} \left(T^{\frac{1}{2}} - R/T^{\frac{1}{2}}\right) \left(\cos 2kb - \frac{\lambda'}{2k} \sin 2kb\right)$ note $b = d_2$, $b > 0$

$$c_{12} = e^{-\lambda b} \left(T^{\frac{1}{2}} - R/T^{\frac{1}{2}}\right) \left(+\frac{\gamma_o}{kV_1} \sin 2kb\right)$$

$$c_{13} = -e^{-\lambda b} \frac{R^{\frac{1}{2}}}{T^{\frac{1}{2}}} \frac{V_1}{\gamma_o} \left(k \sin 2kb + \frac{\lambda'^2}{4k} \sin 2kb\right)$$

$$c_{14} = e^{-\lambda b} \frac{R^{\frac{1}{2}}}{T^{\frac{1}{2}}} \left(\cos 2kb + \frac{\lambda'}{2k} \sin 2kb\right)$$

$$c_{21} = e^{\frac{(p+\nu_1)}{V_2} a - \lambda b} \frac{V_1}{o} \left(-\frac{\lambda'^2}{4k} - k\right) \sin 2kb$$

$$c_{22} = e^{\frac{(p+\nu_2)}{V_2} a - \lambda b} \left(\cos 2kb + \frac{\lambda'}{2k} \sin 2kb\right)$$

$$c_{31} = -e^{-\lambda b} \frac{R^{\frac{1}{2}}}{T^{\frac{1}{2}}} \left(\cos 2kb - \frac{\lambda'}{2k} \sin 2kb\right)$$

$$c_{32} = -e^{-\lambda b} \frac{R^{\frac{1}{2}}}{T^{\frac{1}{2}}} \frac{\gamma_o}{kV_1} \sin 2kb$$

$$C_{33} = e^{\lambda b} \frac{1}{T^{\frac{1}{2}}} \left(\cos 2kb + \frac{\lambda'}{2k} \sin 2kb\right)$$

$$C_{34} = -e^{\lambda b} \frac{1}{T^{\frac{1}{2}}} \frac{\gamma_o}{kV_1} \sin 2kb$$

$$C_{43} = e^{\lambda b - (\frac{p+\nu_2}{V_2})a} \frac{V_1}{\gamma_o} \left(k \sin 2kb + \frac{\lambda^{12}}{4k} \sin 2kb\right)$$

$$C_{44} = e^{\lambda b - (\frac{p+\nu_2}{V_2})a} \left(\cos 2kb - \frac{\lambda'}{2k} \sin 2kb\right)$$

The eigenvalues of C are determined by

$$\det [\underset{\sim}{C} - q \underset{\sim}{I}] = 0$$

which generates the quartic in q :-

$$q^4 - q^3(C_{11}+C_{22}+C_{33}+C_{44}) + q^2(C_{11}C_{22}+C_{11}C_{33}+C_{11}C_{44}+C_{22}C_{33}+C_{22}C_{44}+C_{33}C_{44}-C_{12}C_{21}-C_{13}C$$

$$-q(C_{11}C_{22}C_{33}+C_{11}C_{22}C_{44}+C_{11}C_{33}C_{44}+C_{22}C_{33}C_{44}+C_{13}C_{21}C_{32}+C_{14}C_{31}C_{43}$$

$$-C_{11}C_{34}C_{43}-C_{12}C_{21}C_{33}-C_{12}C_{21}C_{44}-C_{13}C_{31}C_{22}-C_{13}C_{31}C_{44}-C_{22}C_{34}C_{43}) + 1 = 0 \qquad (V-7)$$

We recall that there is a condition on these eigenvalues; that they should all have modulus one (thus ensuring that the vectors Ψ do not tend to ∞ as $x \to \pm \infty$) where we have used the condition $\det \underset{\sim}{C} = 1$)

(i.e. we may set the constant term in the quartic for q to unity).

The problem now reduces to finding values of the growth rate, p (which is now a parameter such that the roots of (V-7) have unit modulus and the product of the roots is unity. Let us rewrite the quartic in the following form -

$$q^4 + 4aq^3 + 6bq^2 + 4cq + 1 = 0 \qquad \ldots\ldots (V-7)$$

From the above considerations there are three possible combinations, i.e. roots can be

I	$1, 1-, \alpha, \alpha^*$
II	$-1, -1, \alpha, \alpha^*$
III	$\alpha, \alpha^*, \beta, \beta^*$

where * represents the complex conjugate. Following Du rell and Robson (134), we reduce this quartic to the simpler quartic

$$y^4 + 6H y^2 + 4 G y + (I - 3H^2) = 0 \qquad \ldots\ldots (V-8)$$

by the substitution $y = q + a$

where $H = b - a^2$, $q = c - 3ab + 2a^3$

$I = 1 - 4ac + 3b^2$

Defining $J = \begin{vmatrix} 1 & a & b \\ a & b & c \\ b & c & 1 \end{vmatrix}$ and $\Delta = I^3 - 27 J^2$,

the conditions that we should have roots which are

(1) 2 equal real, complex conjugate pair is $\Delta = 0$, ($H<0$ and $12H^2-I>0$) is false

(2) 2 pairs of complex conjugate is $\Delta > 0$, ($H<0$ and $12H^2-I>0$) is false

The condition that the roots have unit modulus is most easily shown from Ferrari's Solution of the quartic (Du rell and Robson) (134), where for a suitable choice of λ, η, ζ we may write, using (V-7) this time,

$$(q^2 + 2ax + b + 2\lambda)^2 = (2\eta q + \zeta)^2$$

This reduces the two quadratic equations

$$q^2 + 2(a \pm \zeta) + (b + 2\lambda \pm \zeta) = 0$$

where λ is a root of

$$4\lambda^3 - I\lambda + J = 0$$

$$\eta = (\lambda + a^2 - b)^{\frac{1}{2}}$$

$$\zeta = (2a\lambda + ab - c)/\eta$$

and I, J are as defined above

If the roots then have modulus one,

$$b + 2\lambda \pm \zeta = 1$$

i.e. $b + 2\lambda = 1$ and $\zeta = 0$

i.e. $a = c$

We thus search for values of p s.t. $a - c = 0$

The possibility of this test allowing the real roots γ and $\frac{1}{\gamma}$ is excluded by searching, initially, for cases I, II, or III above i.e. by the time we come to apply this test we have roots $(\delta, \delta, \alpha, \alpha^*)$ or $(\alpha, \alpha^*, \beta, \beta^*)$, with $\delta = \pm 1$. The search is done numerically by varying p continuously such that $a - c$ is less than some error bound and then the largest resulting value of p is taken. Thus, in the results to follow, we show the effects of this filamentation on the fastest growing mode.

We have assumed, implicitly, till now that the filamentation instability had saturated, merely leaving a stationary perturbation of the critical surface. In this situation, the pondermotive force due to the bunching of the electric field in the low density regions will be balanced by the excess force from the increased pressure of the high density regions. In

other words,

$$-\frac{\omega_p^2}{\omega_o^2}\quad\frac{\langle E^2\rangle}{8\pi} = \nabla\,(n_H \kappa T - n_L \kappa T)$$

which in our formation, recalling our definitions of n_H and n_L, and $\omega_{pe}^2 = (1-h_o)\,\omega_o^2$, gives

$$\langle E_o^2\rangle = \frac{\delta\pi\,(h+h_o)}{(1-h_o)}\quad n_c\,\kappa T$$

or, using the fact that $V_o^2 = \dfrac{c^2 E_o^2}{m\omega_o^2}$,

$$V_o^2 = \frac{2(h+h_o)}{1-h_o}\quad V_e^2$$

Similarly,

$$\delta = 4.8876\quad\frac{h^{\frac{1}{2}}}{(1-h_o)^{\frac{1}{2}}}\,k\quad,\quad\frac{\gamma_o^2}{V_1 V_2} = 0.5554\quad\frac{h+h_o}{(1-h_o)^2}\quad k^2$$

This procedure was followed through, numerically, with mixed results. The value of h_o was selected such that perfect matching occurred in the valley regions. For $T_e = 10^7\ ^oK$, $T_i = T_e/10$, we took $h_o = 0.1$. The problem arose that there existed bands of solutions rather than continuous variation of growth rate over any particular parameter range, as can be seen in Table III. One noticeable feature was that the reflection coefficients

TABLE III

h	d_1	d_2	$p/_o$	R
0.1	20	1	0.075	0.84
0.2	20	1	no result	
0.1	50	1	0.058	0.89
0.1	60	1	0.104	0.84

were of order, at least, 0.84. This leads us to consider a simplified problem which, we feel, gives more realistic results with considerably less effort.

Consider the situation of figure 31. We assume that the density filament is of sufficient height and size to preclude any transmission of the electron plasma wave i.e. the wave is trapped by the filament. Since wave propagation occurs in each direction and there is 100% reflection, the amplitudes must be the same at both 0 and L_1. A standing wave is thus produced.

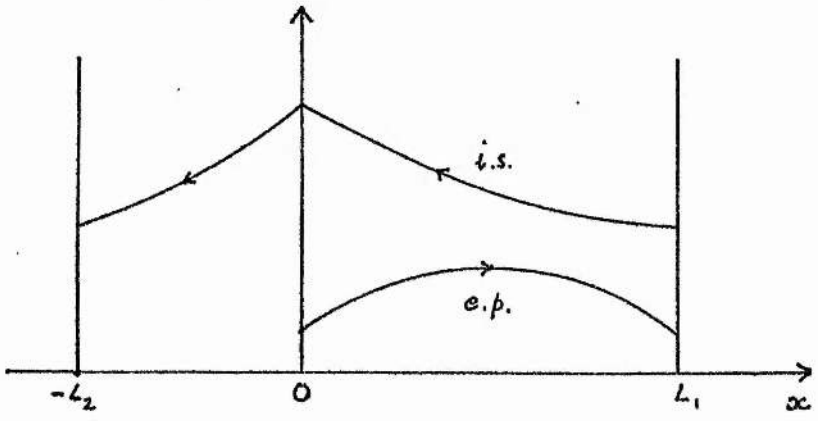

Figure 31

The ion sound wave is assumed unaffected by this filament except in as far as no pump wave exists in $(-L_2, 0)$ and so the wave attentuates. To ensure the cyclical nature of the problem and that no energy flows from $x < -L_2$ to $x > L_1$ we set the ion sound amplitudes equal at these two extremities.

From (V-5), the plasma wave amplitude is

$$a_p = e^{\frac{-\lambda y}{2}} \quad A \cos ky + B \sin ky$$

where k, λ are defined as before. Since the problem is linear, we may set, without loss of generality,

$$a_p(0) = 1 \qquad \text{i.e.} \quad A = 1$$

Imposing the condition $a_p(L_1) = a_p(0)$,

$$B = \frac{e^{\lambda/2 L_1} - \cos KL_1}{\sin k\, h_1}$$

Now, for $0 < y << L$, the ion-sound wave varies as (V-1)

$$a_i = \frac{V_1}{\gamma_o}\left[\lambda' \cos ky - k \sin ky + B\left(\frac{\lambda'}{2} \sin ky + k \cos ky\right)\right] e^{-dy/2}$$

and, for $-L_2 < y < 0$, through

$$(p + \nu_2) a_i - V_2 \frac{\partial a_i}{\partial y} = 0$$

i.e. as

$$a_i = a_i(0) \exp\left(\frac{p+\nu_2}{V_2}\right) y$$

Assuming a_i to be continuous at $y = 0$, we have

$$a_i(-L_2) = a_i(0) \exp - \frac{(p+\omega_2)}{V_2} L_2$$

where

$$a_i(0) = \frac{V_1}{\gamma_o}\left(\frac{\lambda'}{2} + Bk\right)$$

Finally, imposing the condition that the whole process be periodic, $a_i(-L_2) = a_i(L_1')$ we obtain the following condition on the growth rate p,

$$\frac{\lambda'}{2} \sin kL_1 - k \cos kL_1 + k e^{\frac{\lambda L_1}{2}} = e^{-\frac{\lambda L_1}{2}}\left(\frac{\lambda'}{2} \sin kL_1 + k \cos kL_1\right) - k\, e^{\frac{\lambda L_1}{2} + \frac{p+\omega_2}{V_2} L_2}$$

From our definition, $\lambda < 0$, for $V_1 > V_2$ and we have that the limiting value of p, as $L_2 \to \infty$, is determined by the square brackets tending to zero i.e. $k \to 0$ or

$$p \to \frac{2\gamma_o \sqrt{V_1 V_2}}{V_1 + V_2} - \left(\frac{\nu_1}{V_1} + \frac{\nu_2}{V_2}\right) \frac{V_1 V_2}{V_1 + V_2}$$

which is just the maximum growth rate for a pump of finite extent. As $L_1 \to 0$, we return to the homogeneous growth rate.

However, in the finite L_1, L_2 case, we expect the following restrictions on p. Since $V_1 \neq V_2$, there will be convection of any pulse as it grows in time, figure 32.

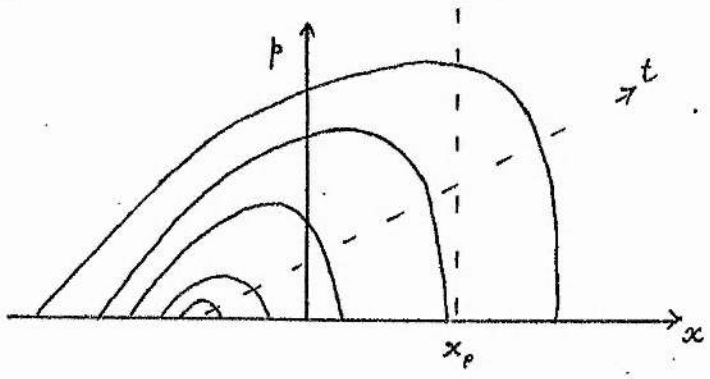

Figure 32 : Growth of pulse for $V_1 \neq V_2$

The peak grows with growth rate γ_o. However, at any other point, there will be a smaller growth rate (basically, the physical meaning of the term in $k^2 = \frac{\gamma_o^2}{V_1 V_2} - \frac{1}{4}\left(\frac{p+\nu_1}{V_1} + \frac{p+\nu_2}{V_2}\right)^2$ in the solutions). Hence, for a pump of finite extent, to x_p, the maximum growth will be reduced to the growth rate at x_p rather than γ_o. If at x_p, there is reflection growth will be impeded still further.

To examine the results, we measure p in units of the infinite, homogeneous growth rate, γ_o, and velocities in units of $\sqrt{|V_1 V_2|}$. Distance is then in units of $\gamma_o / \sqrt{|V_1 V_2|}$. The results, figure 33, show decreasing growth rates as a function of L_1. Also shown is the growth in the infinite homogeneous case with average growth rate of the filamented case.

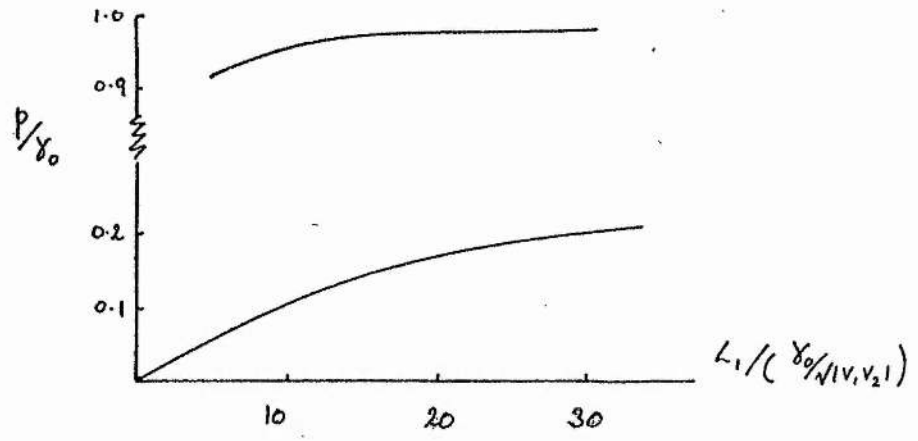

Figure 32 : Reduction of growth rate by filamentation, $\nu_2=0=\nu_1$

The dependence of L_2 is not too noticeable in the region of interest ($L_1 \sim 10\, L_2$), the value of λL_1 being so large it tends to swamp the smaller $\frac{p+\nu_2}{\nu_2}\, L_2$.

We can thus see the effect of this type of behaviour. Our model essentially included electron wave trapping so we would anticipate the results having a substantial range of validity. The growth rate is reduced by this filamentation. Whether absorption is radically affected is another question. From purely geometric grounds, the effect of a saw-tooth variation on the surface of sphere is reduced considerably as the sphere contracts. Hence, an uneven absorption shock would tend to homogeneity as it propagated inwards. Rapid electron thermal conduction would also reduce this effect. By an analogous argument, the enhanced fluctuations in limited regions giving rise to enhanced local absorption would also tend to iron itself out. Nevertheless, only by more substantial computation will the overall behaviour be seen in relation to the many other instabilities and motions present in these environments.

CHAPTER VI

In the preceding chapters, we have attempted to lay the groundwork and examine some problems of interest in the area of parametric instabilities in inhomogeneous plasmas. Special attention has been paid to their application in laser fusion research. Because of the vast amount of literature on the subject we have been forced to be selective in our discussions, indicating only generally the digressions to other fields. It was our aim to explain the physical basis of the work, the mathematical techniques involved in their solution and the practical impetus for their study. As we indicated, the solutions, let alone the real situation, were complicated and a suitable pathway has, hopefully, been cut through the resulting morasse.

Of the problems we discussed in detail, it would be advantageous to indicate the main results and pointers, once more. Firstly, we found that, by considering the whole interaction in the laboratory frame of reference, in which the plasma streams outwards, substantially enhanced levels of reflection (and pump depletion) were found to occur due to stimulated Brillouin scattering. Since this enhancement was fairly insensitive to 'off-resonance' situations, we felt that a severe barrier had been erected to fusion applications, especially as the powers involved were likely to be, practically, the most useful. Secondly, we discussed stimulated Compton scattering in the inhomogeneous geometry. Whilst the reflection was very small, it was found that substantial perturbations of the background distribution function resulted (135). Of more worry, was the finding that,

were the pump to develop a modulation along its direction of propagation, then, here, there was cause for alarm. Such a situation could easily arise if the laser were being pumped consistently at its maximum output. Thirdly, we discussed the effects on the decay instability of a filamented critical surface. The growth rate was found to be substantially reduced but whether this would result in an overall reduction in the absorption efficiency is not clear.

Finally, as this is very much an on-going subject, it would seem appropriate to indicate hopes for future research. Obviously, much more experimental work, at the high pump powers, needs to be done, and the results published. On the theoretical side, the linear theory is well covered, although, for completeness, we would like to see the solution of the decay problem in a finite, turbulent plasma. A possible extension to other space dimensions would also be welcomed (although, one must mention that experimenters do find agreement with the present linear theory). Much work, however, still remains in the saturation of instabilities, in the amalgamation of hydrodynamic and instability studies, in heating mechanisms and in the role of fast ions. Simulations will, doubtless, continue to provide food for thought but it is encouraging to find more tractable and more physical methods producing the same results (102). On all levels, the problems are there, what we have to do is solve them.

REFERENCES

(1) K. Nishikawa and C.S. Lin, Advances in Plasma Physics 6, 3 (Interscience NY) (1976).

(2) Lord Rayleigh, Phil. Mag. 15, 229 (1883)

(3) I. Huntley and R. Smith, J. Fl. Mech. 61, 401 (1974)

(4) R.E. Franklin, M. Price and D.C. Williams, ibid 57, 257 (1973).

(5) I. Huntley, 1975 - St. Andrews University Seminar.

(6) O.M. Phillips, Ann. Rev. Fl. Mech. 6, 93-110 (1974)

(7) O.M. Phillips, Dynamics of the Upper Ocean', London (1974)

(8) G.B. Whitham, 'Linear and non-linear waves', NY (1974)

(10) A.D.D. Craik, ibid 34, 531 (1968).

(11) J. Usher and A.D.D. Craik, ibid 66, 209 (1974) and ibid 70, 437 (1975).

(12) W.F. Simmons, Proc. Roy. Soc. A 309, 551 (1969).

(13) V.N. Oraevsky and R.Z. Sagdeev - Sov. Tech. Phys. 32, 1291 (1962).

(14) B.B. Kadomtsev, 'Plasma Turbulence', London. (1964).

(15) R.N. Franklin, S.M. Hamberger, G. Lampis and G.J. Smith, Phys. Rev. Lett. 27, 1119 (1971)

(16) V.N. Oraevsky, Nucl. Fusion 4, 263 (1964).

(17) A.A. Galeev and R.Z. Sagdeev, Nucl. Fusion 13, 603 (1972).

(18) D.F. Dubois and M.V. Goldman, Phys. Rev. Lett. 14, 544 (1965).

(19) V.P. Silin, Sov. Phys.JETP 21, 1127 (1965)

(20) N.E. Andreev, A. Yu Kiryi and N.P. Silin, Sov. Phys. JETP 30, 559 (1970)

(21) J. Drake, Y.C. Lee, P.K. Kaw, C.S. Liu, G. Schmidt and M.N. Rosenbluth, Phys. Fluids 17, 778 (1974).

(22) R.Z. Sagdeev and A.A. Galeev, 'Nonlinear Plasma Theory', Benjamin (1969).

(23) V.N. Tsytovich, 'Nonlinear Effects in Plasmas', Plenum (1970).

(24) R.C. Davidson, 'Methods in Non-linear Plasma Theory', Academic (1972).

(25) D.F. Dubois and H.V. Goldman, Phys. Rev. Lett 28, 218 (1972).

(26) E.J. Valeo, C. Oberman and F.W. Perkins, ibid, 340 (1972).

(27) D.F. Dubois and M.V. Goldman, Phys. Fluids 15, 919 (1972).

(28) W.L. Kruer and E.J. Valeo, ibid 16, 675 (1973).

(29) J.J. Thomson, R.J. Fae hl W.L. Kruer and S.E. Bodner, Phys. Fluids 17, 973 (1974).

(30) K. Nishikawa, J. Phys. Soc. Japan 24,916 and 1152 (1968).

(31) P.A. Sturrock, Phys. Rev. 112, 1488 (1958).

(32) R.J. Briggs, 'Electron Stream Interaction with Plasmas',MIT Press (1964).

(33) C.L. Tang, J. Appl. Phys. 37, 2945 (1966).

(34) W.F. Utlaut and R. Cohen, Science, 174, 245 (1971).

(35) R.J. Bickerton and B.E. Keen, Plasma Physics,IOP (1974).

(36) R.W. Perkins and P.K. Kaw, J. Geophys. Res. 76, 282 (1971).

(37) K. Dysthe, 3rd Plasma Physics Conference, IOP, Swansea (1976).

(38) J. Nuckolls, L. Wood, A. Thiessen and G. Zimmerman, Nature 239, 139 (1972

(39) J.L. Emmett, J. Nuckolls and L. Wood, Sc. Am. June(1974.)

(40) K.A. Brueckner and S. Jorna, Rev. Mod. Phys. 45, 325 (1974).

(41) M.N. Rosenbluth and R.Z. Sagdeev, Comm. Plasma Phys. and Nucl. Fusion, 1, 129 (1973).

(42) P.K. Kaw and J.M. Dawson, Phys. Fluids, 12, 2586 (1969).

(43) J.S. Degroot and J.I. Katz, Phys. Fluids 16, 401 (1973).

(44) A.T. Lin and J.M. Dawson, Phys. Fluids 12, 201 (1975).

(45) C.S. Lin, Advances in Plasma Physics, 6, 120 (1976)

(46) N.M. Manheimer and E. Ott, Phys. Fluids, 17, 1413 (1974).

(47) R.A. Stern and N. Tzoar, Phys. Rev. Lett. 17, 903 (1966).

(48) I.E. Gekker and D.V. Sizukhin, Sov. Phys. JETP 28, 1220 (1969).

(49) H.P. Eubank, Phys. Fluids 14, 2551 (1971).

(50) D. Phelps, N. Rynn and G. Van Hoven, Phys. Rev. Litt. 26, 688 (1971).

(51) H. Dreicer, D.B. Henderson and J.C. Ingraham, Phys. Rev. Lett 26, 1618 (1971).

(52) T.K. Chu, H.W. Hendel and J.H. Dawson, Comments in Plasma Phys. and Contra Nucl. Fusion 1, 11 (1972).

(53) T.P. Hughes, 'Plasmas and Laser Light', Bristol (1976).

(54) C.T. Yamanska, T. Yamanaka, T. Sasaki, K. Yoshida, M. Waki and H.B. Kang, Phys. Rev. A6, 2335 (1972).

(55) J.L. Bobin, M. Decroisette, B. Meyer and Y. Vitel, Phys. Rev. Litt. 30, 594 (1973).

(56) J.L. Bobin, 'Laser Interaction and Related Plasma Phenomena' Vol 3B, Plenum (1974).

(57) J. Soures, L.M. Goldman and M. Lubin, ibid.

(58) C. Yamanaka, T. Yamanaka and H.B. Kang, ibid.

(59) K. Eidmann and R. Sigel, ibid

(60) E.A. McLean, and J.M. McMahon, B.Am.Phys.Soc 18, 1256 (1973).

(61) B.H. Rippin, J.M. McMahon, E.A. McLean, N.H. Manheimer, J.A. Stamper Phys. Rev. Lett. 33, 634 (1973).

(62) A. Saleres and H. Decroisette, VIIth European Conf. on Controlled Fusion and Plasma Physics, Lausanne (1975).

(63) K.A. Brueckner, in 'Laser Interaction' ed Schwarz and Hora, Vol 3A Plenum (1976)

(64) D.B. Henderson (private communication).

(65) J.L. Emmet, J.H. Nuckolls, H.G. Ahtstrom, C.D. Hendricks, L.W. Coleman, J.A. Glaze, J.H. Holzrichter and G.H. Dahlbacka, as in (62).

(66) B.R. Guscott, G. Charatis, J.S. Hildum, R.R. Johnson, F.J. Mayer, D.E. Solomon and C.E. Thomas, ibid.

(67) A. Galeev, V. Oraevsky, R. Sagdeev, Sov. Phys. JETP Lett. (1972).

(68) J. Katz, J. De Groot, W. Kruer, J. Dawson. B. Am. Phys. Soc 17, 2045 (1972

(69) W.L. Kruer, Advances in Plasma Physics 6 (1976) and 'Laser Interaction' 3A (ed. Schwarz and Hora) Plenum (1976).

(70) S.E. Bodner, G.F. Chapline, J. De Groot, Plasma Phys. 15, 21 (1973).

(71) W.L. Kruer, E.J. Valeo and K.G. Estabrook, Phys. Rev. Lett 35, 1076 (1975

(72) C.S. Lui and P.K. Kaw, Advances in Plasma Physics 6, 83 (1976).

(73) L.A. Zhekulin, Sov Phys. JETP 4, 76 (1938).

(74) A.D. Piliyn, Sov. Phys. Tech. Phys 11, 609 (1966).

(75) J.P. Friedberg, R.W. Mitchell, R.L. Morse and L.R. Rudinskii, Phys. Rev Lett. 28, 795 (1971).

(76) D.W. Forslund, J.M. Kindel, K. Lee and E.L. Lindman, Phys. Rev. Lett. 34, 193 (1975); Phys. Rev. Lett. 36, 35 (1976); + R.L. Morse, Phys. Rev. A11, 679 (1975).

(77) J.P. Dougherty, J. Plasma Phys. 4, 761 (1967);ibid 11, 331 (1974).

(78) T.J.M. Boyd and J.G. Turner, J. Phys A5, 881 (1972); ibid A 6, 272 (1973)

(79) B. Coppi, M.N. Rosenbluth and R.N Sudan, Ann. Phys. 50, 207 (1969).

(80) E.A. Jackson, J. Math. Phys. B, 1189 (1972).

(81) R.W. Harvey and G. Schmidt, Phys. Fluids 18, 1395 (1975).

(82) V. Fuchs and G. Beaudry, J. Math. Phys. 17, 208 (1976).

(83) D.J. Kaup, Studies in Applied Maths LV, 9 (1976).

(84) R. White, P. Kaw, D. Pesme, M.N. Rosenbluth, G. Laval, R. Huff and R. Varma Nucl. Fusion, 14, 45 (1974).

(85) G. Laval, R. Pellet and D. Pesme, Phys. Rev. Lett., 36, 192 (1976).

(86) M.Y. Yu, P.K. Shukla and K.H. Spatschek, Phys. Rev. A 12, 656 (1976).

(87) E.J. Valeo and C. Oberman, Phys. Rev. Lett., 30, 1035 (1973).

(88) J.J. Thomson and I. Karush, Phys. Fluids, 17, 1608 (1974)

(89) W.L. Kruer and K.G. Estabrook, in 'Laser Interaction and Related Plasma Phenomena', 3A (Plenum) (1976).

(90) M.N. Rosenbluth, Phys. Rev. Lett, 29, 595 (1972).

(91) A.D. Piliya, in 'Proc Tenth Int. Conf. on Phenomena in Ionised Gases', ed. R.N. Franklin, Oxford (1971).

(92) M.N. Rosenbluth, R.B. White and C.S. Lui, Phys. Rev. Lett. 31, 1190 (1973).

(93) R.A. Cairns, J. Plasma. Phys 12, 169 (1974).

b. R.A. Cairns, ibid 14, 327 (1975).

(94) D. Pesme, G. Laval and R. Pellat, Phys. Rev. Lett. 31, 203 (1973).

(95) D. Dubois, D.W. Forslund and E. Williams, Phys. Rev. Lett. 33, 1013 (1973).

(96) D.W. Forslund, J.M. Kindel and E.L. Lindman, (a) Phys. Fluids 18, 1002 (1975) (b) ibid , 1017 (1975).

(97) D.R. Nicholson and A.N. Kaufman, Phys. Rev. Lett. 33, 1207 (1974).

(98) A.N. Kauffman and B.I. Cohen, Phys. Rev. Lett. 30, 1306 (1973).

(99) D.F. Dubois, M.V. Goldman and D. McKinnis, Phys Fluids 16, 2257 (1973).

(100) J.J. Thomson, R.J. Faehl and W.L. Kruer, Phys. Rev. Lett. 31, 918 (1972).

(101) The analogously derived situation in linear theory is treated by C.S. Liu, M.N. Rosenbluth and R.B. White, Phys. Fluids, 17, 1211 (1974).

(102) R.A. Cairns, (1976) to be published.

(103) A.A. Galeev, G. Laval, T. O'Neil, M.N. Rosenbluth and R.J. Sagdeev, Sov. Phys. JETP Lett. 17, 35 (1973).

(104) M.N. Rosenbluth, R.B. White and C.S. Lui, Phys, Rev. Lett. 31, 697 (1973).

(105) I.M. Begg and R.A. Cairns, VIIth European Conf. on Controlled Fusion and plasma Physics, Lausanne (1975); J. Phys. D 9, 2341 (1976).

(106) B.D. Fried and R.W. Gould, Phys. Fluids 4, 139 (1961).

(107) J. Peyrand, J. Physique, 30, 307 and 460 (1969).

(108) F.V. Bunkin and A.E. Kazakov, Sov. Phys. JETP 32, 1208 (1971).

(109) J. Martineau and H. Pépin, J. App. Phys., 43, 917 (1972).

(110) I.K. Kraysuk, P.P. Paskinin and A.M. Prokhorov, Sov. Phys. JETP. Lett. 12 305 (1970).

(111) a. M. Decroisette, G. Piar and F. Floux, Phys. Lett. 32A, 249 (1970).
b. M. Decroisette, J. Peyrand and G. Piar, Phys. Rev. A4, 1391 (1972).

(112) N.H. Burnett, R.D. Kerr and A.A. Offenberger, Opt. Comm. 6, 372 (1972) and others therein.

(113) J.P. Babuel-Peyrissac, Phys. Lett. 41A, 143 (1972).

(114) A.A. Offenberger and N.H. Burnett, Phys. Lett 42A, 527 (1973).

(115) M.N. Rosenbluth and C.S. Lui, Phys. Rev. Lett. 29, 701 (1972).

(116) A.E. Kazakov, I.K. Kraysuk, P.P. Pashinin and A.M. Prokhorov. Sov. Phys. JETP Lett. 14, 280 (1971).

(117) I.K. Kraysuk, P.P. Pashinin and A.M. Prokhorov, Sov. Phys. JETP Lett. 17, 92 (1973).

(118) A.L. Vinogradov, B. 7a. Zel'dorich and I.I. Sobel'man, Sov. Phys. JETP Lett. 17, 130 (1972).

(119) J.R. Albritton, Phys. Fluids 18, 51 (1975).

(120) H. Dreicer, Phys. Fluids 7, 735 (1964).

(121) E. Ott, W.M. Manheimer and H.H. Klein, Phys. Fluids 17, 1757 (1974).

(122) W.M. Manheimer, D. Coloumbant and R. Flynn, Phys. Fluids 19, 1354 (1976)

(123) T.H. Dupree, Phys. Fluids 9, 1773 (1966).

(124) R.D. Richtmeyer and K.W. Morton, (1967), Difference Methods for Initial Value Problems', Wiley, NY.

(125) T.P. Hughes, (private communication).

(126) P.K. Kaw, G. Schmidt, and T. Wilcox, Phys. Fluids 16, 1522 (1973) and refs. 4-7 therein.

(127) C.E. Max, Phys. Fluids 19, 74 (1976).

(128) E.J. Valeo and K.G. Estabrook, Phys. Rev. Lett. 34, 1008 (1975).

(129) F.F. Chen, in 'Laser Interaction' ed. Schwarz and Hora, 3A, 291 Plenum. (1976)

(130) B. Langdon and B. Lasinski, Phys. Rev. Lett. 34, 934 (1975).

(131) K.G. Estabrook, Phys. Fluids 19, 1733 (1976).

(132) J.A. Stamper, K. Papadopoulos, R.N. Sudan, S.O. Dean, E.A. McLean and J.M. Dawson, Phys. Rev. Lett. 26, 1012 (1971).

(133) D.A. Tidman and R.A. Shanny, Phys. Fluids 17, 1207 (1974).

(134) C.V. Durrell and A. Robson, 'Advanced Algebra Vol II' London (1962).

(135) Substantial anomalous absorbtion can be obtained through the mechanism Manheimer et al (122) obtain, by studying the analagous sidescatter process, that absorbtions of order 20% may be achieved, albeit for very large slab lengths. One could thus envisage this weaker type of instability having most effect long cylindrical plasma with londitudinall incident light.

(136) J.J. Thomson, W.L. Kruer, S.E. Bodner and J.S. De Groot, Phys. Fluids, 17, 849 (1974).

(137) R.A. Cairns (private communication).